Universidad Autónoma de Madrid

FACULTAD DE CIENCIAS

DEPARTAMENTO DE BIOLOGÍA MOLECULAR

PROGRAMA DE DOCTORADO EN BIOCIENCIAS MOLECULARES

STUDY OF MEMBRANE PROTEOME OF DGKζ-DEFICIENT CYTOTOXIC T LYMPHOCYTES

TESIS DOCTORAL

GONZALO MARTÍNEZ MARTÍNEZ

MADRID, 2019

Universidad Autónoma
de Madrid

FACULTAD DE CIENCIAS

DEPARTAMENTO DE BIOLOGÍA MOLECULAR

PROGRAMA DE DOCTORADO EN BIOCIENCIAS MOLECULARES

STUDY OF MEMBRANE PROTEOME OF DGKζ-DEFICIENT CYTOTOXIC T LYMPHOCYTES

Gonzalo Martínez Martínez
Licenciado en Biología
Directoras de tesis: Isabel Mérida de San Román y
Severine Isabelle Gharbi
Centro Nacional de Biotecnología (CSIC)
Madrid, 2019

El trabajo presentado en esta memoria ha sido realizado por Gonzalo Martínez Martínez, en el Centro Nacional de Biotecnología (CSIC), bajo la dirección de la Dra. Isabel Mérida de San Román y de la Dra. Severine Isabelle Gharbi.

La realización de esta tesis ha sido posible gracias a una beca de Formación del Profesorado Universitario (FPU) del Ministerio de Educación, Cultura y Deporte.

A mis padres

In memoriam Juan Pablo Albar

«The Pole. Yes, but under very different circumstances from those expected».

Captain Robert F. Scott

INDEX

Index

ABSTRACT

Abstract

T cells are key cells in the coordination and implementation of the adaptive immune response. Specifically, cytotoxic T lymphocytes are responsible for eliminating cells presenting antigens on their surface either viral or tumor type. After antigen presentation, these cells must undergo a series of changes in the pattern of protein expression to reinforce the signaling capability and allow movement to the site of action. In case of membrane proteins, there are changes in expression of surface receptors in order to receive chemical signals in the form of cytokines and other molecules, and also in adhesion molecules to allow the exit of the secondary lymphoid organs towards periphery. However, tumor cells can avoid CTL action in some cases, using escape mechanisms which limit their cytotoxic activity.

Signaling by diacylglycerol (DAG) plays an essential role in antigen presentation. Diacylglycerol kinase (DGK) enzymes family negatively regulates this response by phosphorylation of DAG into phosphatidic acid (PA). ζ isoform (DGKζ) deficient mice CTL show increased activation and better response to tumors. Furthermore, DGKζ deficiency has been associated with changes in protein expression on the cell surface related to cell adhesion. Determining the role of DGKζ deficiency in cell surface protein expression pattern can help to understand key aspects like its effects in tumor elimination.

In order to better understand the role of the DAG in CTL response, a proteomic study was designed to analyze the expression of proteins of these cells, with special interest in plasma membrane proteins. Firstly, a method of protein enrichment of the plasma membrane by biotinylation was optimized in Jurkat T cells, while other strategies such as subcellular fractionations were also tested to obtain better results. This method was then used with CTL, and changes in the expression pattern of membrane proteins dependent of DAG were studied by adding a phorbol ester (PMA) or by analyzing CTL obtained from DGKζ-deficient mice. To complete this study, a quantitative proteomics analysis was performed by SILAC labeling to determine significant quantitative changes in protein expression from DGKζ-deficient CTL. The results showed a higher expression of cytotoxic components such as granzyme B in the membrane fraction of DGKζ$^{-/-}$ CTL.

RESUMEN

Resumen

Los linfocitos T son células fundamentales en la coordinación y ejecución de la respuesta inmune adaptativa. En concreto, los linfocitos T citotóxicos (CTL) se encargan de la eliminación de células infectadas por patógenos intracelulares o células tumorales que presentan en su superficie antígenos específicos. Tras la activación, los CTL experimentan una serie de cambios en el patrón de expresión de proteínas que les permiten aumentar su capacidad de señalización y su desplazamiento hacia los sitios de acción. En el caso de las proteínas de membrana presentan cambios en la expresión de receptores de citocinas y moléculas de adhesión. Sin embargo, las células diana tumorales en algunos casos son capaces de eludir la acción de los CTL mediante mecanismos de evasión que limitan su capacidad efectora.

La señalización del diacilglicerol (DAG) juega un papel esencial durante la activación de los linfocitos T. La familia de enzimas de las diacilglicerol quinasas (DGK) regula negativamente esta respuesta mediante la fosforilación del DAG y su conversión en ácido fosfatídico (PA). Los CTL de ratones deficientes en la isoforma DGKζ muestran una mayor activación y una mejor respuesta frente a tumores. Además, la deficiencia en DGKζ se ha asociado a cambios en la expresión de proteínas de la superficie celular relacionadas con la adhesión celular. Determinar cómo la deficiencia de DGKζ afecta al patrón de expresión de proteínas de superficie puede ayudar a entender fenómenos como su mayor eficiencia en la eliminación de tumores.

Para comprender mejor el papel de DGKζ en la respuesta de las CTL, diseñamos una aproximación proteómica para caracterizar las proteínas expresadas en su superficie celular. En primer lugar se optimizó en células T Jurkat un método de enriquecimiento de proteínas de la membrana plasmática mediante biotinilación, a la vez que se ensayaron otras estrategias como fraccionamientos subcelulares para obtener mejores rendimientos. Después se empleó este método con CTL, y se estudiaron los cambios en el patrón de expresión de proteínas de membrana dependientes del DAG mediante la adición de un éster de forbol (PMA) o el análisis de CTL obtenidos a partir de ratones deficientes en DGKζ. Para completar el estudio se realizó un análisis de proteómica cuantitativa mediante marcaje SILAC para determinar cambios cuantitativos significativos en proteínas expresadas en CTL de ratones deficientes en DGKζ. Los resultados arrojaron una mayor expresión de componentes citotóxicos como granzima B en la fracción de membranas de CTL DGKζ$^{-/-}$.

ABBREVIATIONS

Abbreviations

1D/2D PAGE	One-dimensional/two-dimensional polyacrylamide gel electrophoresis
ACN	Acetonitrile
AICD	Activation-induced cell death
Akt	Protein kinase B
AMP	Adenosine monophosphate
AP-1	Activator protein 1
APC	Antigen-presenting cell
ATP	Adenosine triphosphate
BID	BH3 interacting-domain death agonist
BSA	Bovine serum albumin
CAR	Chimeric antigen receptor
CD	Cluster of differentiation
CE	Collision energy
CID	Collision-induced dissociation
CSF1R	Macrophage colony-stimulating receptor factor
CTLA-4	Cytotoxic T-lymphocyte protein 4
CUR	Curtain gas
Cy5	Cyanine
DAG	Diacylglycerol
DD	Death domain
DDA	Data-dependent acquisition
DDR1	Epithelial discoidin domain-containing receptor 1
DGK	Diacylglycerol kinase
DIA	Data-independent acquisition
DIGE	Difference gel electrophoresis
DMEM	Dulbecco's Modified Eagle Medium
DMSO	Dimethyl sulfoxide
DP	Declustering Potential
DTT	Dithiothreitol
ECL	Enhanced chemiluminescence
EDTA	Ethylene diamine tetraacetic acid
ERK	Extracellular signal regulated kinase
ESI	Electrospray ionization
FA	Formic acid
FADD	Fas-associated protein with death domain
FasL	Fas ligand

FBS	Fetal bovine serum
FDR	False discovery rate
Foxp3	Forkhead box P3
GEF	Guanine nucleotide exchange factor
GO	Gene ontology
GS1	Ion Source Gas 1
HPLC	High-performance liquid chromatography
HRP	Horseradish peroxidase
IAM	2-Iodoacetamide
ICAD	Inhibitor of caspase-activated DNase
IDA	Information Dependent Acquisition
IDO	Indoleamine 2,3-dioxygenase
IFNγ	Interferon gamma
IGF	Insulin-like growth factor
IGF1R	Insulin-like growth factor-1 receptor
IHT	Interface heater temperature
IL	Interleukin
IP3	Inositol 1,4,5-trisphosphate
ISVF	Ionspray voltage floating
iTreg	Induced regulatory T cell
ITAM	Immunoreceptor tyrosine-based activation motif
ITIM	Immunoreceptor tyrosine-based inhibitory motif
ITSM	Immunoreceptor tyrosine-based switch motif
LC-MS/MS	Liquid chromatography tandem-mass spectrometry
LTG	Lysotracker green
m/z	Mass-to-charge ratio
MALDI	Matrix-assisted laser desorption/ionization
MDSC	Myeloid-derived suppressor cells
MFI	Mean fluorescence intensity
MHC	Major histocompatibility complex
MRM	Multiple reaction monitoring
MS	Mass spectrometry
MS/MS	Tandem mass spectrometry
MTOC	Microtubule organizing center
mTOR	Mammalian target of rapamycin
Munc13	Mammalian uncoordinated homology 13
NFAT	Nuclear factor of activated T-cells
NF-κB	Nuclear factor of kappa B
NK	Natural killer
NKG2D	NK cell receptor D
NKT	Natural killer T cell

nTreg	Natural regulatory T cell
OVA	Ovalbumin
PA	Phosphatidic acid
PBS	Phosphate-buffered saline
PD1	Programmed cell death protein 1
PD-L1	Programmed cell death 1 ligand 1
PD-L2	Programmed cell death 1 ligand 2
PE	Phycoerythrin
PECy7	Phycoerythrin-cyanine conjugate
PFA	Paraformaldehyde
PI3K	Phosphatidylinositol-3-kinase
PIP2	Phosphatidylinositol 4,5-bisphosphate
PKC	Protein kinase C
PKD	Protein kinase D
PLC	Phospholipase C
PMA	Phorbol 12-myristate 13-acetate
PMSF	Phenylmethylsulfonyl fluoride
PNGaseF	Peptide-N-Glycosidase F
PRM	Parallel reaction monitoring
PTPN23	Tyrosine-protein phosphatase non-receptor type 23
PVDF	Polyvinylidene fluoride
QTOF	Quadrupole time-of-flight
RasGRP	Ras guanyl-releasing protein
RIPA	Radioimmunoprecipitation assay buffer
RP-HPLC	Reversed phase HPLC
RPMI	Roswell Park Memorial Institute
SDS-PAGE	Sodium dodecyl sulfate polyacrylamide gel electrophoresis
SEM	Standard error of the mean
SHP	Src homology region 2 domain-containing phosphatase
SILAC	Stable isotope labeling by amino acids in cell culture
SMAC	Supramolecular activation cluster
SNX27	Sorting nexin 27
SREBP	Sterol regulatory element-binding protein
STAT	Signal transducer and activator of transcription
Sulfo-NHS-Biotin	Sulfosuccinimidyl biotin
Sulfo-NHS-SS-Biotin	Sulfosuccinimidyl-2-[biotinamido]ethyl-1,3-dithiopropionate
TAA	Tumor-associated antigen
TACE/ADAM17	Tumor necrosis factor-alpha-converting enzyme
TCL	Total cell lysate
TCR	T cell receptor

TFA	Trifluoroacetic acid
TFE	Trifluoroethanol
TfR	Transferrin receptor
TGF	Transforming growth factor
TIL	Tumor-infiltrating lymphocyte
TNF	Tumor necrosis factor
TNFR	Tumor necrosis factor receptor
TOF	Time-of-flight
TRAIL	TNF-related apoptosis-inducing ligand
TRAIL-R	TRAIL receptor
TRANCE	TNF-related activation-induced cytokine
Treg	Regulatory T cell
TSA	Tumor-specific antigen
VEGF	Vascular endothelial growth factor
VLA-2	Very Late Antigen 2 (integrin $\alpha 2\beta 1$)
WB	Western blot
WT	Wild type

INTRODUCTION

Introduction

1. Inmune system and cancer

1.1. Global vision of immune system

The immune system is in charge of protecting the host against pathogens and harmful substances like toxins that invade the organism. It consists of specialized organs and tissues, as well as a series of effector cells and molecules that are responsible for carrying out coordinated action against external threats. The immune response comprises two main components: the innate and the adaptive response. While the first has no specific target, the second is accurately directed against a target pathogen unleashing powerful, specific responses.

The cells of the innate immune system carry out the most immediate response as soon as pathogens cross the body's natural barriers. These include macrophages, mast cells, dendritic cells and γδ T cells that are present in the tissues, or cells recruited from the bloodstream, such as monocytes, granulocytes and NK cells. These cells fight the infection and are also able to alert the components of adaptive immunity, which initiate a slower but specific response to pathogens.

The cells responsible for this adaptive immunity are T and B lymphocytes. The adaptive immune response initiates when antigen-presenting cells (APC) present in their surface antigens to T lymphocytes, which act as effective executors and regulatory components of the immune system. The CD4 T lymphocytes collaborate in the differentiation of B lymphocytes to plasma cells for the production of specific antibodies (humoral response). They also help in the elimination of intracellular pathogens by stimulating and differentiating other cellular components by chemical signals known as cytokines. These include CD8 T lymphocytes or cytotoxic T lymphocytes (CTL), capable of killing infected cells which present antigens on their surface (cellular response) (Murphy & Weaver, 2016).

1.2. Cytotoxic T lymphocytes

The cellular response through cellular cytotoxicity mechanisms is carried out by NK cells in the case of the innate immune system, and by CD8 T lymphocytes in the case of the adaptive immune system. There are two different mechanisms, the induction of apoptosis

by ligands of the tumor necrosis factor (TNF) family and the release of cytolytic granules. In the first case, cell surface-expressed proteins such as Fas ligand (FasL), TNF or TNF-related apoptosis-inducing ligand (TRAIL) bind to their respective receptors in target cells: Fas, tumor necrosis factor receptor (TNFR)-1, TRAIL receptor (TRAIL-R)-1 and TRAIL-R2. These receptors contain cytosolic death domains (DD) that bind to adapter proteins through the Fas associated death domain (FADD), triggering the activation of caspases 8 and 10 involved in programmed cell death (Krammer et al., 2007). This mechanism is responsible for the death of activated cells in a process known as activation-induced cell death (AICD), one of the mechanisms that regulate the immune response. Patients with mutations in the Fas or FasL genes have a lymphoproliferative syndrome with T and B cells accumulation and autoimmune symptoms (Rieux-Laucat et al., 1995).

In the second mechanism, CTL release, in a polarized manner, lytic granules with cytolytic proteins that penetrate the target cell and cause its programmed cell death. In the case of CTL, the process begins with the recognition of the target cell by the CTL. The nucleated cells of the organism express in the plasma membrane the major histocompatibility complex (MHC)-I molecules attached to fragments of proteins generated in the cell. CTL express in their surface the multimeric T cell receptor (TCR) capable of binding to these complexes. There are a large number of T cell clones with a different TCR generated from somatic recombination of the genes encoding the chains of this receptor. During an education process in the thymus, T cell clones with TCRs capable of binding only to MHC-I:non-self peptides complexes are selected. Thus, when a cell presents foreign peptides from viral or tumor origin, CTL circulating in the body will be able to recognize them and trigger a cytotoxic response (Germain, 1994).

This recognition establishes a signaling structure called the immunological synapse (Lee et al., 2002), in which the CTL and the target cell come into contact, align and reorganize the molecules related to antigen recognition. This is known as supramolecular activation cluster (SMAC). After the antigenic recognition, a central region (cSMAC) is formed enriched with the molecules most involved in signaling such as TCR, CD8, CD28 and other co-receptors, and a peripheral region (pSMAC) that contains integrins and talin that promotes adhesion between the two cells. Finally, there is a distal region (dSMAC) where the CD45 phosphatase is accumulated (Monks et al., 1998). At the same time, there is a polarization towards the contact zone of the entire secretory machinery, which includes the Golgi apparatus and the microtubule organizing center (MTOC). The reorientation of the CTL microtubule network towards the synapse facilitates the migration and exocytosis of lytic granules to the target cell through the cSMAC (Stinchcombe et al., 2006), in what is known as secretory domain (Stinchcombe et al., 2001). This polarization allows cytolytic actions to

be confined in the synaptic cleft and to avoid damage to neighboring cells. The process from the formation of the immunological synapse to the secretion of granules responsible for the death of the target cell in a few minutes, and after the CTL cell can repeat the process with another target cell (Bossi et al., 2002; Huppa & Davis, 2003) (Figure 1).

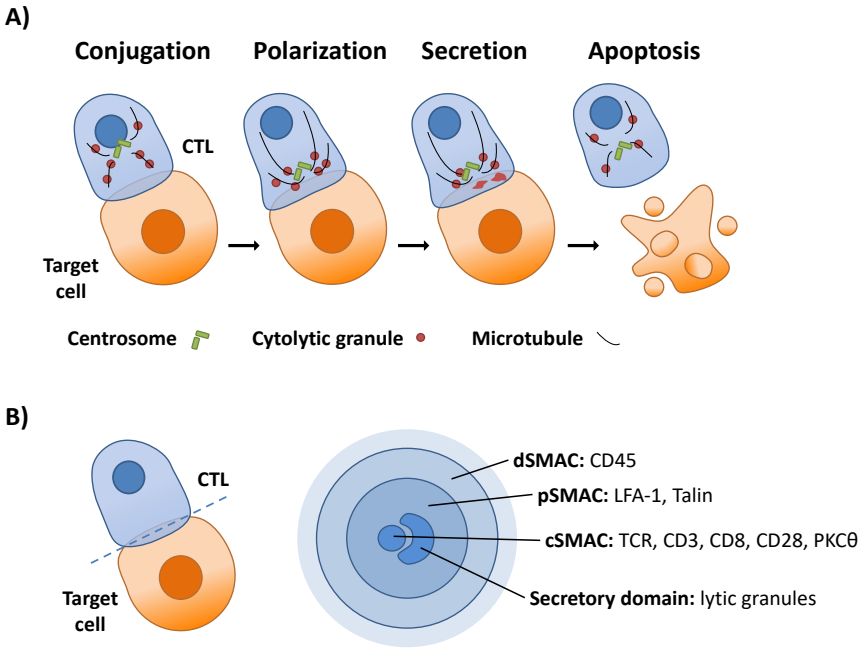

Figure 1: Immune synapse
A) Scheme showing the different phases of the cytolytic action carried out by the CTL. After recognizing the specific peptides presented by the MHC-I of the target cell, the CTL begins to reorient its cytolytic machinery, and the release of lytic granules will initiate apoptosis. B) Diagram of the immune synapse, with molecules that can be located in each SMAC. Adapted from (Dieckmann et al., 2016).

1.2.1. Lytic granules

The release of lytic granules is the main mechanism of action of CTL cells. These granules are modified lysosomes, known as secretory lysosomes, which contain lysosomal enzymes hydrolases. In CTL, NK cells, mast cells and eosinophils, these granules also display lysosomal functions, at different of non-hematopoietic cells such as melanocytes and endothelial cells that contain both specialized granules and lysosomes that share biogenesis. In a CTL the number of lytic granules is approximately between 15-25, with a thickness of 700nm that in mouse can reach more than 5µm, and with one or more of electron-dense content core (Peters et al., 1991). This electron-dense core is formed by the proteins that will be released to the synaptic cleft. As the secretory lysosomes mature, they accumulate

proteins that arrive from the Golgi or other vesicles, so that these structures become more evident. This process takes several days since the activation of the CTL, and requires the gene expression and synthesis of the protein components (de Saint Basile et al., 2010).

Cytotoxic proteins are stored inside lytic granules under conditions such as acid pH or interaction with other proteins that prevent them from exerting their action. One of the main components of lytic granules is perforin, a protein with homology with members of the complement (Tschopp et al., 1986), which has the ability to form pores in the plasma membrane. Mice lacking perforin have impaired cytotoxic capacity in their CTL (Kägi et al., 1994). At first it was thought that the mechanism of perforin action was to open pores in the target cell membrane causing its death. More recent studies have shown that perforin function facilitates the passage of a family of serin esterases, called granzymes, capable of activating caspase proteins in the target cell, which then initiate the apoptotic process. The presence of granzymes alone is not sufficient for the cytolytic action of CTL (L. Shi et al., 1992), and they require the presence of perforin (Nakajima et al., 1995). Granzymes and perforin are found in the lytic granules forming complexes with the proteoglycan serglycin, which would act as scaffold. The entry of calcium into the CTL allows the exocytosis of the granules and the release of these complexes to the synaptic cleft. The mechanism by which perforin allows granzymes to enter into the target cell is controversial. It is thought that perforin, through the formation of pores or even incomplete pore structures, could temporarily permeabilize the membrane and allow the passage of granzymes (Lopez et al., 2013). Some studies suggest that granzymes would be endocytosed through the mannose-6-phosphate receptor (Motyka et al., 2000), and perforin would facilitate their exit from the endosome towards the cytosol, allowing its cytolytic action. However the content of the endosomes would lack the calcium concentration and the pH conditions necessary for the perforin to form pores (Gerasimenko et al., 1998).

Until now 5 isoforms of granzyme in human (A, B, H, K and M) and 10 in mouse (A-G, K, M and N) have been described (Bovenschen & Kummer, 2010). The most studied isoform in the induction of cell death is granzyme B. This protein has several targets, including BH3 interacting-domain death agonist (BID), whose proteolytic cleavage alters the permeability of the mitochondria and causes the release of cytochrome c to the cytosol, with a proapoptotic effect (Sutton et al., 2000). Another way of action of granzyme B is the cleavage and activation of pro-caspase 3 that, in its active form, degrades inhibitor of caspase-activated DNase (ICAD), a DNA inhibitor responsible for DNA degradation (Goping et al., 2003). The mouse isoform however does not efficiently process BID, so in the case of mice the caspase pathway represents the main mechanism of cell death (Cullen et al., 2007). In addition to those mentioned, additional nonapoptotic granzyme B substrates

have been discovered (N. J. Waterhouse et al., 2006).

In addition to perforin and granzyme, the granules contain other lytic components such as granulisin, which is expressed only in humans and has antimicrobial function (Krensky & Clayberger, 2009). Other components are involved in the protection against the effects of perforin and granzyme, so that the CTL are not affected by the content of their own granules. Calreticulin, for example, maintains perforin in its inactive conformation by sequestering Ca^{2+} ions (Andrin et al., 1998). Serpins are inhibitory proteases that can block the action of granzymes (Sun et al., 1996). Some cathepsins in addition to their lysosomal function are important in the context of lytic granules. Cathepsin C is responsible for the processing of granzymes, while cathepsin B can cleave and inactivate them (Balaji et al., 2002). Other proteins present in the granules are the before mentioned serglycine, and Fas ligand that collaborates in cell death (Lieberman, 2003).

1.3. The control of the immune response

The effector responses of the immune system are a powerful weapon that must be regulated by various mechanisms, to return to homeostasis once its function is finished and to avoid damages in the organism. In addition, mechanisms of tolerance are established so that the components of the immune system capable of recognizing their own antigens are eliminated or lose their effector function. In the case of T lymphocytes there are central tolerance processes (Hogquist et al., 2005), where the autoreactive T lymphocytes are eliminated after a process of education in the thymus. There is also a peripheral tolerance (Mueller, 2010), in which these cells are inactivated in the absence of an inflammatory context due to lack of co-stimulation, what is known as anergy (Schwartz, 2003), or due to the action of cellular components as regulatory T cells, by suppression mechanisms. On the other hand, chronic exposure to the antigen can lead to a state of exhaustion, in which the T cell undergoes functional changes and stops responding to antigen as a protective mechanism of the surrounding tissues (Pauken & Wherry, 2015). Both tolerance and exhaustion phenomena can lead to the onset of apoptosis (Krammer et al., 2007).

1.3.1. CTL activation

The activation of the CTL initiates a complex signaling network to allow differentiation to effector cells. This activation begins with TCR recognition of specific antigens presented by the MHC-I complex. The CD8 co-receptor binds to this complex, and allows the binding of tyrosine kinase Lck belonging to the Src family kinases (Artyomov et al., 2010). Together with another component of this family, Fyn, they phosphorylate immu-

noreceptor tyrosine-based activation motif (ITAM) domains of the CD3 complex chains, where the Zap70 protein is anchored. After being phosphorylated by Lck, Zap70 activates and phosphorylates scaffold LAT and SLP-76 (Jordan et al., 2003). Phospholipase C (PLC) γ binds to this complex, which will be activated by the Itk protein of the Tec family kinases (Schaeffer et al., 1999). Phospholipase activity will convert phosphatidylinositol 4,5-bisphosphate (PIP2), a membrane phosphoinostide, into diacylglycerol (DAG) and inositol 1,4,5-trisphosphate (IP3) (Smith-Garvin et al., 2009) (Figure 2).

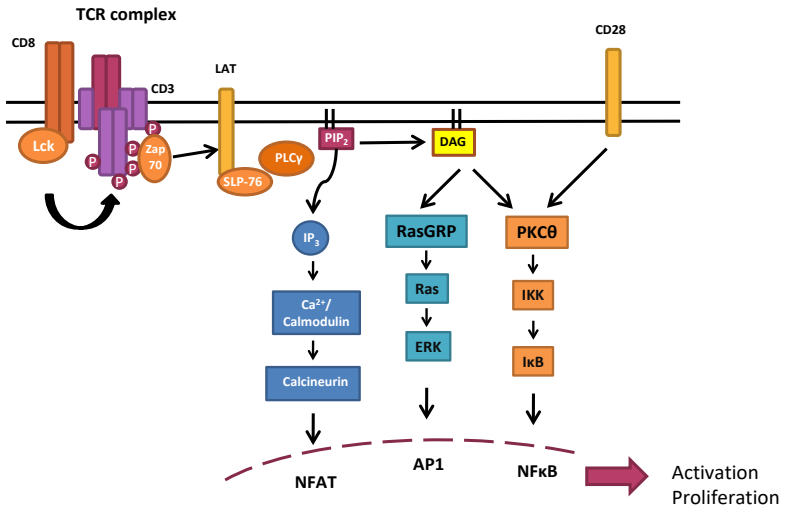

Figure 2: Main signaling pathways dependent on TCR activation
After the stimulation of TCR, a signaling cascade is triggered, activating PLCγ. The production of IP3 involves the activation of the transcription factor NFAT, while the production of DAG activates AP-1 and NF-κB. Adapted from (Zhong et al., 2008).

These second messengers initiate three signaling pathways. On the one hand, IP3 will open channels of Ca^{2+} from the endoplasmic reticulum and plasma membrane, producing an increase of Ca^{2+} concentration in the cytosol. After binding to calmodulin, it will activate the phosphatase calcineurin that will dephosphorylate the nuclear factor of activated T-cells (NFAT) transcription factor, allowing its nuclear translocation (Hogan et al., 2003). On the other hand, DAG will participate in two signaling pathways. The Ras guanyl-releasing protein (RasGRP) is able to bind to this second messenger, and acts as a guanine nucleotide exchange factor (GEF) of the Ras G protein, which is activated by binding to GTP. Ras initiates activation of the MAP kinases cascade, resulting in translocation to the nucleus of Fos, a component of the activator protein 1 (AP-1) transcription factor (Genot & Cantrell, 2000). The second DAG-dependent signaling pathway requires activation of co-stimulatory molecules like CD28 and involves protein kinase C (PKC) θ. The activation of this pathway allows the release of the NF-κB transcription factor from the inhibitory protein IκB and

its translocation into the nucleus (S. Paul & Schaefer, 2013).

For a complete T cell activation, all pathways need to be implemented. Transcription factors are involved in the expression of genes such as interleukin (IL)-2, a cytokine responsible for lymphocyte proliferation. Deficient signaling of DAG-dependent pathways versus Ca^{2+} dependent pathways may lead to a state of inactivation or anergy (Zheng et al., 2008).

1.3.2. Immune checkpoints

T lymphocytes express a series of activating or inhibiting receptors that help modulate the effector response. These are proteins, usually expressed in plasma membrane, which either limit co-stimulatory signals or help to the termination of the peripheral T cell responses. They have been called immune checkpoints, highlighting cytotoxic T-lymphocyte protein 4 (CTLA-4) and programmed cell death protein 1 (PD1), although there are a large number of receptors and ligands with similar functions that are less understood (Pardoll, 2012) (Figure 3).

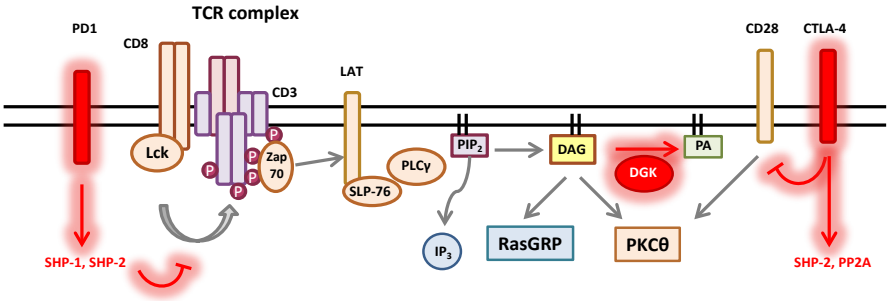

Figure 3: Negative regulation of TCR signaling
Different proteins participate in the negative regulation of TCR-dependent signaling. The CTLA-4 receptor binds to CD80 and CD86, competing with the CD28 co-receptor. In addition, it activates phosphatases which reverse the activation of TCR signaling cascade proteins. The PD1 receptor binds to its PD-L1 and PD-L2 ligands, and also activates inhibitory phosphatases through its cytoplasmic tail containing ITIM and ITSM domains, such as SHP-1 and SHP-2. DGK would participate converting the DAG into PA, attenuating the signaling dependent on this second messenger, such as the RasGRP and PKC pathways.

The CTLA-4 receptor is expressed on T lymphocytes at 24-48h after activation (Linsley et al., 1992). After recognition of the antigen presented by MHC-I by TCR, the lymphocyte needs a co-stimulatory signal to become activated, which is usually CD28. This receptor is able to bind to the CD80 and CD86 receptors of the antigen-presenting cell, and to initiate bidirectional signaling that culminates with the complete activation of the T

lymphocyte. CTLA-4 is able to bind to CD80 and CD86 in such a way that it is capable of preventing binding to CD28 by competition, and also generates inhibitory signals (Linsley et al., 1994). CTLA-4 signaling is subjected to controversy, since although domains of tyrosine phosphorylation in the cytoplasmic sequence that could serve as binding to phosphatases such as Src homology region 2 domain-containing phosphatase (SHP)-2 have been detected, it has been questioned whether they are really necessary and can fulfill this function (Walker & Sansom, 2015). In fact it is thought that the role of these domains could be involved in subcellular localization (Shiratori et al., 1997), since the CTLA-4 produced by the cell is initially stored in intracellular vesicles until its accumulation at the immune synapse (Egen & Allison, 2002). The importance of CTLA-4 in tolerance processes is observed in CTLA-4-deficient mice, which suffer from a lethal autoimmune and lymphoproliferative syndrome (P. Waterhouse et al., 1995).

The PD1 receptor is expressed in T cells after sustained activation in peripheral tissue (Agata et al., 1996). It binds to ligands programmed cell death 1 ligand (PD-L)1 and PD-L2, which in the first case is expressed in a large number of cells and in the second in antigen-presenting cells during inflammation (Keir et al., 2008). Thus, when a T lymphocyte is activated for a prolonged time it expresses the PD1 receptor, and the contact with self-cells and/or other activated T cells favors its exhaustion avoiding excessive response (Barber et al., 2006). The receptor contains two tyrosine phosphorylation immunoreceptor tyrosine-based inhibitory/switch motif (ITIM and ITSM) domains that bind SHP-1 and SHP-2 phosphatases that inhibit the TCR signaling cascade after ligand binding (Sheppard et al., 2004). In addition, the PD-L1 ligand can bind to the CD80 receptor expressed on T lymphocytes, and induce down-regulation (Butte et al., 2007). In contrast, in the case of regulatory T cells the binding of the PD1 receptor to its ligands causes activation (Francisco et al., 2009). Mice deficient in this receptor undergo autoimmunity, due to impaired tolerance but not as strong as in the case of CTLA-4 deficiency (Nishimura et al., 1998).

In addition to the previous membrane receptors, there are other less known immune checkpoints that also act diminishing the effector response. Among them is BTLA, which is activated by binding to HVEM. HVEM is a molecule that exerts a complex regulation, since it can also inhibit or activate T cells binding to CD160 and LIGHT receptor, respectively (Pasero & Olive, 2013). Another immune checkpoint is LAG3, with high expression in activated T cells, able to binding mainly to MHC-II, and that causes the inhibition of the effector response. It is also expressed in regulatory T cells, which can inactivate MHC-II-expressing cells as dendritic cells (Andrews et al., 2017). The TIM-3 receptor also inhibits the action of CD8 T cells on binding to galectin-9 (Zhu et al., 2005), as well as KIR receptors, capable of binding to MHC, which in addition to expressing NK cells have an inhibitory role

in T cells (Mingari et al., 2005).

1.3.3. Diacylglycerol kinases as negative regulators of immune response

The diacylglycerol kinases (DGK) constitute a family of enzymes conserved throughout the evolution. These lipid kinases catalyze the conversion of DAG into phosphatidic acid (PA), a reaction dependent on ATP consumption, and are involved in cell signaling processes dependent on these metabolites, and in the phosphoinositide cycle regulation (Figure 3). Ten isoforms are currently known in mammals with a specific distribution according to tissues, and remarkably functions like their role in the immune and nervous systems. They share a catalytic domain with a specific ATP-binding sequence, and atypical cysteine-rich zinc finger C1 domains that facilitate enzyme migration from the cytosol to the membrane. In addition, each isoform has its own regulatory domains that allow them to be grouped into 5 types, and which suggest a fine regulation for these enzymes (Mérida et al., 2008).

In the immune system the DGKα and DGKζ isoforms are highly expressed, especially in T cells (Sanjuán et al., 2001; Zhong et al., 2002). They play an important role in the regulation of T cell activation by reducing DAG levels and attenuating signaling cascades dependent on this molecule. In the basal state these enzymes remain in the cytosol in its inactive form. DGKα has at its N-terminus an inhibitory region (Sanjuán et al., 2001) with recoverin and EF hands domains, able to bind to Ca^{2+}. Thus, Ca^{2+} release promoted by TCR signaling facilitates a conformational change favoring DGKα activation. DGKα phosphorylation by Lck facilitates transient translocation to plasma membrane and complete activation (Merino et al., 2008). DGKζ, possesses at its C-terminus an inhibitory region containing ankyrin repeats and a PDZ binding domain. Through this domain DGKζ binds to proteins such as sorting nexin 27 (SNX27), a protein involved in vesicular trafficking (Rincon et al., 2007) that contributes to the localization of DGKζ in the immunological synapse (Rincon et al., 2011). DGKζ also contains a MARCKS-like domain, whose phosphorylation by PKCα (Luo et al., 2003) facilitates its sustained membrane binding and activation (Santos et al., 2002).

DGK activity limits DAG-dependent regulation of Ras activation. In T lymphocytes, the GEF of Ras RasGRP binds DAG, and activates the Ras/extracellular signal regulated kinase (Ras/ERK) pathway allowing the activation of Fos of the AP-1 transcription factor (Ebinu et al., 1998). Both DGKα and DGKζ limit the activation of this pathway by reducing DAG levels (Sanjuán et al., 2003; Zhong et al., 2002). In fact, mouse models deficient in these enzymes corroborated an increase in ERK activation (Olenchock et al., 2006; Zhong et al., 2003). In addition to this axis, the activation of the PKCθ-dependent transcription factor NF-κB is preferentially affected by DGKζ (Ávila-Flores et al., 2017). Both axes are required together with Ca^{2+}-dependent NFAT activation for complete gene expression during

T lymphocyte activation, and its attenuation leads these cells to a state of anergy (Macián et al., 2002). In agreement with this, DGKα and DGKζ deficient mice are anergy resistant.

DGK activity not only regulates transcription but also contributes to the regulation of immune synapse formation During the formation of the immunological synapse, the accumulation of DAG in the contact membrane region is essential to allow correct polarization of the secretory machinery (Quann et al., 2009), thanks to the action of several PKCs (Quann et al., 2011). DGKζ is able to translocate to the synapse, where it regulates DAG levels and production of PA predominantly unlike DGKα (Gharbi et al., 2011; Joshi et al., 2013), and participates in the polarization of MTOC to the immune synapse during the formation of the cytotoxic immune synapse (Andrada et al., 2016). It also limits translocation of PKCα, regulator of signaling by the Ras/ERK axis (Gharbi et al., 2013), and of PKCθ, associated with CD28-dependent signaling (Ávila-Flores et al., 2017). In CD4 T cells, DGKα participates in the formation of the DAG gradient by being preferentially located around the synapse (Chauveau et al., 2014). DGKα also plays a role in the secretion of exosomes expressing FasL (Alonso et al., 2011), another mechanism of CTL to induce cell death.

1.3.4. Regulatory T cells

Regulatory T cells (Treg) are CD4 T cells, which are involved in maintaining tolerance towards self antigens by suppressing immune responses. They are characterized by high expression of the α chain of the IL-2 receptor (CD25), and expression of the forkhead box P3 (Foxp3) transcription factor. In fact the mutation of these genes causes the lack of Treg, leading to lymphoproliferative autoimmune syndromes (Brunkow et al., 2001; Sadlack et al., 1995). Treg originate in the thymus, from CD4 cells whose TCR recognizes their own peptides. These cells are known as natural regulatory T cells (nTreg). Treg can also be generated from naïve CD4 T cells in the periphery by the action of cytokines such as transforming growth factor (TGF) β and are known as induced regulatory T cells (iTregs) (Chen et al., 2003). This occurs as a mechanism of tolerance when self-antigens are recognized in the absence of an innate immune response. The maintenance of Treg depends on the presence of IL-2, which also favors the expression of Foxp3 (Malek, 2003).

Treg affect both activation and effector functions of T cells by several mechanisms. One is the production of immunosuppressive cytokines such as TGFβ, IL-35 and IL-10. Another is the suppression of dendritic cells by the action of the CTLA-4 molecule constitutively expressed in the membrane. CTL-4, when bound to CD80, prevents proper activation and induces indoleamine 2,3-dioxygenase (IDO) expression, which depletes tryptophan and compromises the T-cell response (Grohmann et al., 2002). The IL-2 uptake by Treg can reduce its availability for other cells, and is another immunosuppression mechanism (Pan-

diyan et al., 2007). Mice deficient in DGKζ express higher percentages of Treg (Schmidt et al., 2013), unlike mice deficient in DGKα (Joshi et al., 2013).

1.4. Tumor immune evasion

The term cancer encompasses a group of diseases characterized by the uncontrolled growth of cells that escape the mechanisms of homeostasis that assure the balance in the cellular proliferation. This is because these cells undergo a series of progressive genetic modifications that make them acquire, when affecting oncogenes, or lose, for tumor suppressor genes, certain functions. Uncontrolled cell growth or neoplasia causes a tumor mass, which can lead to cancer if it acquires invasive characteristics. As this process of malignancy progresses, the cells end up colonizing other tissues, known as metastasis. The tumor is a complex structure, in which tumor cells are surrounded by other cell types, and where angiogenesis occurs and the infiltration of components of the immune system is detected (Hanahan & Weinberg, 2011).

Early theories supported a process of surveillance of the immune system against tumors, in which the cells of the immune system would patrol the body in search of tumors for its elimination. In fact, the existence of immunodeficiencies in mice increases the risk of the appearance of certain specific types of tumors (Dunn et al., 2002). Currently this concept has evolved towards that of immunoediting, which is divided into three phases. In the phase of elimination, the immune system reacts against tumor cells and can achieve tumor eradication. If this does not happen, an equilibrium phase is reached where mutations appear in the tumor cells and the most resistant cells are selected. In the escape phase some cellular variants finally evade the immune mechanisms and grow uncontrollably (Dunn et al., 2002).

Nonetheless, in many cases tumor cells are poorly immunogenic, and the immune system is not able to differentiate them from normal cells. When presentation occurs, antigens can be classified into two categories. Tumor specific antigens (TSA) comprise the product of genetic mutations, alterations of membrane glycolipids and/or viral antigens when the tumor is produced by a virus. Tumors may express antigens of other cell types (tumor-associated antigens, TAA), like antigens of fetal origin that are not expressed in adult, or characteristic of immune privileged niches like the melanocyte tyrosinase (Vigneron, 2015). Even in the case of antigenic recognition, tumors evade the immune response taking advantage of the mechanisms of peripheral tolerance that are used for healthy cells to avoid self-recognition and/or damage by sustained inflammatory conditions. The lack of appropriate co-stimulation and the immunosuppressive tumor environment favor tolerance induction of T cells. In some cases, tumor structure may prevent the correct access

of cells of the immune system, which precludes its antitumor action (Salmon et al., 2012).

1.4.1. Cellular components of tumor microenvironment

The analysis of solid tumor environment reveals in many cases the presence of infiltrated T lymphocytes. CTL represent the main population that fights against the tumor. The presence of tumor-infiltrating-lymphocytes (TIL) in the tumor is in fact considered a sign of good prognosis for cancer outcome (Galon et al., 2006; Gooden et al., 2011). T lymphocytes need to recognize tumor antigens presented in tumor cells to eliminate them. It is not well known how the tumor initially triggers this immune response. Dendritic cells are proposed to collaborate by presenting tumor antigens, captured for example from dead tumor cells. Another possibility is that of detection by dendritic cells of associated molecular patterns generated during tumor growth (Hernandez et al., 2016). Once these cells present the antigens to T cells these would be recruited to the tumor thanks to the production of chemoattractant molecules as several chemokines in the tumor environment (Harlin et al., 2009).

In addition to CTL, other cells of the immune system may help to eradicate the tumor. CD4 T helper cells foster the action of CTL by producing cytokines such as IFNγ and TNFα, which also increase the expression of MHC-I in tumor cells and stimulate the action of macrophages (Hadrup et al., 2013). Mice deficient in INFγ production have a higher frequency of tumors (Kaplan et al., 1998). The production of IFNγ has also been demonstrated in some populations of NKT cells (Moreno et al., 2008), as well as in γδ T cells (Silva-Santos et al., 2015). NK cells also represent another mechanism of antitumor action. These cells can act against tumor cells when, as a mechanism for T cell evasion, they lose the expression of MHC-I molecules. In addition, some tumors may express NKG2D ligands, a NK cell activating receptor, which trigger its action (Waldhauer & Steinle, 2008).

Macrophages present in tumor microenvironment may either promote or suppress tumor growth. M1 macrophages are activated by IFNγ and receptors of molecules containing damage-associated molecular patterns, and exert an antitumoral role. M2 macrophages on another hand produce molecules that induce angiogenesis such as vascular endothelial growth factor (VEGF), and TGF-β. TGF-β as well as the production of the IL-10 immunosuppressive cytokine can also reduce the T cell response (Chanmee et al., 2014). Other cells related to the macrophage lineage are the myeloid-derived suppressor cells (MDSC). These are hematopoietic precursors of myeloid cells such as macrophages, dendritic and granulocytes, which in the tumor environment differentiate towards an immunosuppressive phenotype. MDSC produce inhibitory IL-10 and also free radicals that can damage T lymphocytes. They also produce the enzyme IDO, what induces the development of Treg,

exerting an inhibitory action on T cells (Monu & Frey, 2012). Tumor can also recruit nTreg and/or favor the differentiation of iTregs (Deng, 2018).

1.4.2. Tumors trigger expression of negative regulators of immune response

The expression of immune checkpoints, whose function is to avoid self damage, also occurs in the tumor microenvironment and is used by cancer cells to evade the immune response. In the tumor microenvironment, due to low immunogenicity, the antigen-presenting cells express few CD80/CD86 molecules and CTLA-4 is competing with CD28 for the binding of CD80/CD86, inducing T cell inhibition. Treg constitutively express CTLA-4, and their signaling favors their own activation (Wing et al., 2008), inhibiting T cell functions. The development of antibodies that block CTLA-4-CD80/86 binding was the first treatment of immunotherapy applied to an immune checkpoint (Hodi et al., 2003). In the tumor microenvironment diverse cells, including tumor cells, can express the ligands PD-L1 and PD-L2. This expression may be innate, due to an oncogenic pathway such as phosphatidylinositol-3-kinase-protein kinase B (PI3K-Akt) (Parsa et al., 2007), or adaptive by the continued action of T cells, for example via IFNγ secretion (Taube et al., 2012). TIL over time express PD1 and undergo exhaustion due to their binding to the ligands. This has promoted the development of antibodies that block against the binding of PD1 with its ligands, with excellent clinical results of melanoma and other types of cancer (Balar & Weber, 2017).

The existence of a large number of checkpoints opens the door to a specific treatment according to cell surface protein expression pattern of tumor cells, in addition to the combined therapy to increase its efficiency (Sharma & Allison, 2015). These treatments can be combined with the application of other immunotherapy strategies such as vaccination with tumor antigens to increase the immunogenicity of tumors (Farkas & Finn, 2010), or adoptive cell therapy with transgenic T lymphocytes with chimeric antigen receptors (CAR) (Kalos & June, 2013) that potentiate the activation of these cells against the tumor. The study of the mechanisms that control the immune system therefore involves increasing the chances of achieving an effective treatment against cancer.

1.4.3. The role of diacylglycerol kinases in cancer

In addition to its important role as negative control of the immune response, DGK could also play an important role in the development of cancer. In some types of cancer DGKα is found overexpressed in tumor cells compared to surrounding tissue cells (Takeishi et al., 2012). The action of the protein Src tyrosine kinase on DGKα allows its activation and potentiates its invasiveness (Baldanzi et al., 2008), and in turn DGKα can enhance the

activation of Src, facilitating growth and survival (Torres-Ayuso et al., 2014). In the case of DGKζ, the production of PA by this isoform favors the activation of mTOR, a cell growth regulator (Ávila-Flores et al., 2005). In addition, the decrease in DAG levels favors the activation of the SREBP-1 transcription factor that favors the expression of lipid metabolism enzymes, necessary for tumor growth (Torres-Ayuso et al., 2015). In this way, both DGKα and DGKζ represent attractive therapeutic targets against cancer.

On the other hand, DGK also exert an important role in the immune system cells infiltrated in the tumor microenvironment. In fact, there is a greater expression of DGKα in TIL with respect to non-infiltrated lymphocytes as in the case of other immune checkpoints that facilitates tumor evasion mechanisms (Prinz et al., 2012). In the CAR transduced T cells an increase in the expression of DGKα and DGKζ has been observed, which limits the efficacy of this technique (Moon et al., 2014). When T cells obtained from DGKα and DGKζ deficient mice are used for CAR transduced T cells, there is an improvement in cytokine production and cytotoxic response, and tumor growth is limited (Riese et al., 2013). Xenograft models in DGK deficient mice show enhanced tumor rejection by DGKζ deficient CTL (Riese et al., 2011; Andrada et al., 2017). Furthermore, DGKζ deficiency also potentiates NK cells (Yang et al., 2016).

Therefore, this double effect of DGK favoring the development of tumor cells and the loss of T cell effector response could be counteracted with the use of specific DGK inhibitors. In fact, when evaluating the action of the specific inhibitor of DGKα CU-3, a higher antitumor response and cytokine production in T cells is observed (Liu et al., 2016). The search for new specific inhibitors for DGK isoforms will increase the chances of finding new immunotherapeutic drugs against cancer.

2. Proteomics

Proteomics is the science that studies the proteome. Proteome is known as the set of proteins, expression product of the genome (Wilkins, 2009), present in an organism, tissue or cell at a given time. Its expression is dynamic in time and space, and it is subject to different levels of regulation. In addition, due to phenomena such as alternative splicing, RNA editing and post-translational protein modification, there are a much larger number of protein species than genes (Gstaiger & Aebersold, 2009). The level of expression of these proteins is changing and it does not always correlate with transcriptional and translational regulation, so messenger RNA levels do not always correspond to protein levels (Schwanhäusser et al., 2011). Thus proteomic studies can provide more accurate information on protein expression and cellular function.

One of the objectives of proteomics is the identification of all or most proteins of a proteome, whose major paradigm is the human proteome project (Legrain et al., 2011). In addition, it is possible to quantitatively analyze the differences in expression between samples, as well as to detect post-translational modifications and interactions of a given protein. With all these possibilities proteomics can provide answers to biological problems such as the complete characterization of proteomes and clinical problems, such as the search for biomarkers that can provide information about the state of a disease or can serve as therapeutic targets (Aebersold & Mann, 2016).

2.1. Mass spectrometry-based proteomics

Although there are proteomic approaches such as the use of protein microarrays (Poetz et al., 2005), advances in the field of proteomics rely mainly on the development of mass spectrometry (MS) (Domon & Aebersold, 2006). A mass spectrometer is able to measure the mass-to-charge ratio (m/z) of ionized molecules, and in proteomics, we generally refer to the peptides obtained from enzymatic digestion of proteins. Selective mass and fragmentation profile of proteolysed peptides can be predicted *in silico* and used as a database to search experimental observations by mass spectrometry. From this information the proteins of a proteome can be identified. There are many types of mass spectrometers that should be employed according to the type of analyte to be measured, the complexity of the samples, their matrix or the requirement for quantification. Most proteomics-based methodologies are done using a bottom-up approach, although other alternative strategies are gaining much interest and becoming invaluable tools to gain in speed, quantitation and robustness, such as data-independent acquisition (DIA), multiple reaction monitoring (MRM) and parallel reaction monitoring (PRM) methods (T. Shi et al., 2016).

Mass spectrometers consist of an ion source where the sample is ionized and gains a charge which will enable it to enter the mass spectrometer, a mass analyzer that separates the ionized molecules according to their m/z, and a detector that captures and records the intensity of the ions. The generated information is analyzed and compared with databases with the help of bioinformatic software to elucidate the protein composition of the original sample. Mass spectrometry can achieve a high sensitivity and wide dynamic range, capable of detecting molecules with high order of magnitude up to femtomoles or attomoles. New instruments benefit from a high resolution and mass accuracy, as well as an increased speed, with differences in m/z of thousands of Da (Yates, 2013).

2.1.1. Ionizations methods

Among the sources of ionization used in proteomics are those that produce a soft ionization, which prevent the molecule from rupturing, and which do not require sample volatilization such as matrix-assisted laser desorption/ionization (MALDI) (Karas & Hillenkamp, 1988) and electrospray ionization (ESI) (Fenn et al., 1989). The latter is the ionization method most used in data-dependent acquisition (DDA) or global proteomics profiling, also known as shotgun proteomics. ESI allows positively or negatively charged ionization of peptides that have been separated in liquid phase. For this, the high-performance liquid chromatography (HPLC) flow is passed through a thin needle where a high electric potential difference of 0.5-4.5kV is applied (Glish & Vachet, 2003). This normally generates multiply charged ions. Metabolite charging allows a reduction in the m/z permitting large peptides to be within the mass range of the equipment. The electric field induces in the fluid the formation of a Taylor cone and the ejection of liquid which is dispersed, generating many droplets in a spray due to the repulsion of charges (Taylor, 1964). The result is the production of an aerosol, directed into the equipment due to the internal high vacuum.

2.1.2. Mass analyzers

After ionization, the ion m/z is evaluated by mass analyzers, such as time-of-flight (TOF), quadrupole, ion trap and cyclotron resonance (Yates et al., 2009). In the case of TOF (Weickhardt et al., 1996), the ions go through a vacuum tube and are detected by a time detector located at the end of the tube. The ions with higher m/z take longer to travel the same path. In the case of the quadrupole mass analyzer (W. Paul & Steinwedel, 1953), it consists of four elongated rod-shaped electrodes placed in parallel, delimiting a space through which the ions cross (Hoffmann & Stroobant, 2007). These electrodes are subjected to radiofrequency and direct current voltages, which allow to select a narrow range of mass of the ions that will cross the quadrupole to the detector, and to deflect out the unwanted ions. By changing the radiofrequency voltages, it is possible to select ions of different m/z that will reach the detector sequentially.

2.1.3. Tandem mass spectrometry (MS/MS)

In the classical proteomic approach, the proteins in the sample are digested by using a proteolytic enzyme that cleaves the protein into peptide fragments. Trypsin is one of the most commonly used digesting enzymes in proteomics since it is able to generate peptides of compatible mass range and with positive charge, resulting in good ionization and MS identification. The m/z values of the resulting peptides are analyzed and compared with the

theoretical values obtained by in silico digestion of the proteome of the species of interest. By means of a computer application, the most probable peptides are assigned to these m/z, and in turn are targeted to proteins containing these peptides (Pappin et al., 1993). When a complex protein mixture is analysed, it becomes impossible to identify a protein based on peptide mass. Therefore, in a shotgun analysis of complex proteomes, tandem mass spectrometry (MS/MS) is used, in addition to measuring the m/z of the precursor peptides or ions, to fragment and analyze the m/z of the ions product. This fragmentation spectrum is compared with *in silico* generated spectra from tryptic peptides, to find out the mass and sequence of the original peptide (Domon & Aebersold, 2006) (Figure 4).

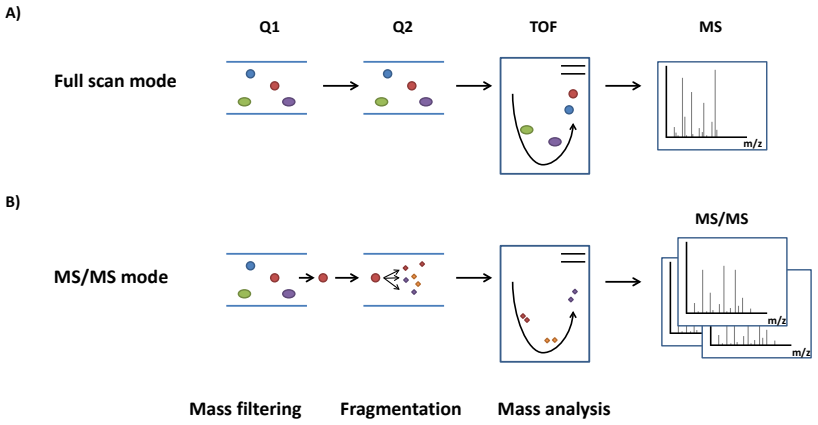

Figure 4: Tandem mass spectrometry
Simplified scheme of a MS/MS experiment in data-dependent acquisition configuration in a QTOF type spectrometer. A) In full scan mode all ionized peptides pass through the first quadrupole (Q1), and arrive without fragmentation to the TOF, where they are separated according to m/z and detected. B) In MS/MS mode the Q1 filters ionized peptides in a determined interval of m/z, which are fragmented in the second quadrupole (Q2) by means of CID, before passing to the TOF. Adapted from (Domon & Aebersold, 2006).

2.1.4. Sample preparation and separation of proteins

Although new mass spectrometers can deal with complex samples, best results are obtained and deeper coverage of the proteome is achieved when samples are sub fractionated using orthogonal approaches. Peptide fractionation may be employed to obtain smaller subproteomes than a total proteome (Dreger, 2003). This is critical to avoid ion suppression in the mass spectrometer. Sample separation can be done at protein or peptide level. Protein separation can be done based on its molecular weight or isoelectric point, such as electrophoresis in polyacrylamide gels in one or two dimensions (1D- and 2D-PAGE), which allow a separation by molecular mass. In the case of 2D-PAGE (O'Farrell, 1975) an isoelectric point separation is performed. In this manner a collection of spots in a gel is obtained. Another possibility is the prior separation by various types of HPLC chromatogra-

phy (Lescuyer et al., 2004). Protein separation can also be carried out based on its function or selective characteristics, such as immunoprecipitation, subcellular fractionation or pull-downs to enrich proteins based on protein-protein interactions. The method of separation will depend on the characteristics of the sample for a higher peak resolution. In addition, sample complexity can be reduced at peptide levels. Typically, peptides can be separated based on their biochemical characteristics such as mass, charge or hydrophobicity.

2.1.5. Quantitative Proteomics

One of the goals of proteomics is to find differences in protein expression or post-translational modifications between different study conditions. In this way, changes can be detected between proteomes of different cells lines, different stages of development or samples of patients against healthy individuals, among others (Bantscheff et al., 2012). Although strategies based on gels such as 2D-PAGE and 2D-difference gel electrophoresis (DIGE) (Ünlü et al., 1997) were initially used, the implementation of shotgun techniques has required the development of new quantification techniques based in mass spectrometry, including label-free (Neilson et al., 2011) and especially isotopic labeling methods. In techniques with differential isotopic labeling, the proteins or peptides are modified with the addition of different isotopes for each treatment or mass tags. The physicochemical properties of the peptides with or without labeling are identical, whereby the chromatography can be performed together. MS analysis will detect m/z differences between treatments and allows relative quantification (Gygi et al., 1999; Ross et al., 2004; Thompson et al., 2003).

Another approach is metabolic labeling, in which the incorporation of isotopic labeling occurs during the metabolism of the original sample, in the case of cells in culture or even in complex organisms (Gouw et al., 2010). Thus, technical variability during the sample processing can be reduced, since samples can be pooled from the initial steps of the preparation. One of most used techniques is stable isotope labeling by amino acids in cell culture (SILAC) (Ong et al., 2002). This labeling is usually performed by adding 13C-labeled lysine and arginine amino acids to the culture medium or diet. The choice of these amino acids is because they are the target of trypsin activity, so that all the peptides generated contain labeled amino acids. Quantification is carried out comparing peptide doublets in MS mode (Mortensen et al., 2010). The samples are divided into light and heavy depending on the medium used, although it is possible to compare more than two samples using amino acids with different labeling (Tzouros et al., 2013). The disadvantage of metabolic labeling methods is that they can be only used in proliferating samples to allow heavy amino acid incorporation. Therefore, samples that cannot proliferate properly in culture such as tissues or body fluids of patients will not be appropriate for this technique. To overcome

this limitation, the use of SILAC labeled cells as a spike-in standard can solve this problem, what is known as super-SILAC (Ishihama et al., 2005).

2.1.6. Membrane proteomics

Plasma membrane proteins contain hydrophobic regions that anchor or associate with the lipid bilayer, in many cases passing through the membrane one or several times, which causes a very stable interaction. These proteins also contain other hydrophilic regions that contact both external and internal side and allow interaction with cargoes, ligands and other proteins. Due to the presence of hydrophobic regions, membrane proteins are difficult to solubilize and possess few charged lysine and arginine for trypsin cleavage and they are often found at low abundance (Vit & Petrak, 2017). Traditional techniques for enrichment of these proteins rely on subfractionations to reduce the complexity of the proteome and to remove other more abundant proteins from other cellular compartments. These methods may include ultracentrifugations, density gradients or separation with different matrices to isolate hydrophobic proteins from total lysates (L. Zhang et al., 2005). In these cases, there may be problems in differentiating proteins from either plasma membrane or other endomembranes.

There are other approaches to specifically isolate proteins from the plasma membrane, mainly directed to the hydrophilic extracytosolic domains. One example is labeling with biotin derivatives of cell surface proteins (Peirce et al., 2004). These reagents have the ability to bind to the primary amino groups of the lysine and N-terminal side chains. After the cell lysate, the labeled molecules are isolated with streptavidin bound to different matrices, taking advantage of the great affinity it has with biotin, of the highest ones without being a covalent bond (Elia, 2008). Another strategy is the cell shaving, in which the intact cell is subjected to the action of a protease to cut out the protein fragments from the outer cell side, for example proteinase K (Speers et al., 2007) or phospholipase D (Elortza et al., 2006). The analysis of these fragments provides topological information about proteins. The disadvantage of this technique is that the protease can damage the cells and lead to cell lysing and release also cytosolic proteins.

Most of membrane proteins have on their outer side some type of glycosylation. One strategy for the purification of membrane proteins has focused on the isolation of N-linked glycoproteins by using lectins that bind to their glycogenic part as concanavalin A or wheat germ agglutinin, since the isolation of O-linked glycoproteins by lectins is less effective (Pan et al., 2011). Another approach is the use of hydrazide-derivatives of biotin, which react with the glucidic portion previously treated with an oxidizing agent. These studies also focus on N-linked glycoproteins, because the peptide-N-glycosidase F (PNGaseF) enzyme,

specific for this type of glycosylation, is used to release proteins from their carbohydrate part prior to analysis by mass spectrometry (Wollscheid et al., 2009).

2.1.7. Bioinformatic analysis proteins

Bioinformatics has facilitated the analysis of the large amount of data obtained in shotgun proteomic experiments, helping with their biological interpretation (Carnielli et al., 2015). In a first case where the detected proteins have not been characterized it is possible to use applications capable of extracting biological information from protein sequence (Juncker et al., 2009). Some applications analyze regions of hydrophobicity and can predict transmembrane domains using hidden Markov models (Krogh et al., 2001). The problem is that being a membrane protein does not always imply that it belongs to the cell surface. If the protein has been described in previous studies, the text mining applications can analyze the scientific literature written in natural language and try to search for information about proteins on their properties and interactions, and translate them into a structured language (Rebholz-Schuhmann et al., 2012).

In general, the interpretation of a shotgun proteomic experiment will require the use of a database where previously the biological information of the proteins has been cataloged in a standardized way and with a controlled vocabulary that uniquely identifies the properties of a protein (Calderón-González et al., 2016). One of the most important examples is UniProt, a database where researchers store the identified proteins (Apweiler et al., 2004). A further step is the use of hierarchical languages such as ontologies, like Gene Ontology (GO) (Ashburner et al., 2000). This project describes the proteins according to three categories: cellular component, molecular function and biological process. GO terms within each category are hierarchized at multiple levels, from the most general to the most specific, and the type of relationship between parent and child terms is specified.

There are a large number of computer applications capable of retrieving information from these databases to interpret biological information (Huang et al., 2009a). Enrichment analyzes look at a list of proteins those GO terms that are over- or underrepresented, as in the case of DAVID (Dennis et al., 2003). It also groups clusters of proteins belonging to similar categories. Another application used for these purposes is GSEA, focused on quantitative genomic analysis between samples (Subramanian et al., 2005). To facilitate the visualization of the results, applications such as Cytoscape allow representing the proteins in an interaction map (Shannon et al., 2003). In this Cytoscape framework, applications have been developed to analyze and represent enriched GO categories, including BinGO (Maere et al., 2005), EnrichmentMap (Merico et al., 2010), with ClueGO (Bindea et al., 2009) and CluePedia (Bindea et al., 2013), which allow to show the GO terms and proteins related.

OBJECTIVES

Objectives

CTL perform immunovigilance and develop a response against tumor cells. However, this response may be compromised due to the regulation of tumor microenvironmental factors or homeostatic mechanisms of the T lymphocyte itself. DGKζ is a member of the diacylglyerol kinase family that regulates the levels of DAG and PA. DGKζ has been shown to participate in the activation of T cells and particularly on the cytolytic response of CTL. The signaling pathways dependent on DGKζ have been well studied as well as their impact on the expression of some proteins involved in tumor recognition. However, a comprehensive and unbiased study characterizing the changes in the proteome of CTL in response to DGKζ activity has not yet been carried out.

Our main objective was the characterization of the proteome of CTL, with special interest in proteins expressed at cell surface, which are know to be critical for cell-cell communication. With this in mind, we focused on plasma membrane proteins for the search of specific markers of tumor response.

To achieve this goal, we set several specific objectives:

1. Develop methods of enrichment of plasma membrane proteins, and other cell compartments, to perform shotgun mass spectrometry analysis.
2. Determine the impact of DGKζ activity on protein expression changes in CTL:
    2.1. In response to phorbol esters
    2.2. Using DGKζ-deficient mice models (OTI-DGKζ$^{-/-}$)
3. Perform a quantitative proteomic analysis to quantify possible differences in protein expression.
4. Study of possible observed quantitative changes by other techniques and validate our findings.

MATERIALS AND METHODS

Materials and Methods

1. Reagents

Table 1: Reagents and their corresponding manufacters

Reagent	Supplier
Aprotinin	Roche
Concanavalin A	Sigma-Aldrich
IL-2	PeproTech
Leupeptin	Roche
Ovalbumin (OVA) (257-264)	AnaSpec
Phorbol 12-myristate 13-acetate (PMA)	Sigma-Aldrich
Phenylmethylsulfonyl fluoride (PMSF)	Sigma-Aldrich
Sodium fluoride (NaF)	Sigma-Aldrich
Sodium orthovanadate (Na3VO4)	Sigma-Aldrich
β-glycerophosphate	Sigma-Aldrich
Dimethyl sulfoxide (DMSO)	Sigma-Aldrich
Acrylamide/Bis Solution, 29:1 (30%)	Bio-Rad
Paraformaldehyde (PFA)	Sigma-Aldrich
poly-D,L-Lysine	Sigma-Aldrich
LysoTracker Green (LTG)	Life Technologies
Trypsin	Sigma-Aldrich

2. Antibodies

Table 2: Antibodies and their corresponding manufacters

Antibody	Supplier
ERK	Cell Signaling Technology
GM130	BD Biosciences
Histones	Millipore
p-AKT S473	Cell Signaling Technology
p-ERK Y202/T204	Cell Signaling Technology
PLCγ-1	Millipore
p-PKCα T638	Cell Signaling Technology
Streptavidin-peroxidase	Thermo-Scientific
Transferrin receptor	Zymed

Antibody	Supplier
β-actin	Sigma-Aldrich
anti-mouse IgG horseradish peroxidase (HRP)	Dako
anti-rabbit IgG horseradish peroxidase	Dako
CD4-APC	eBioscience
CD8-PECy7	BioLegend
CD28-PE	eBioscience
CD80-PE	Pharmingen
CD274-PE (PD-L1)	Pharmingen
CD279-APC-eFluor780 (PD1)	eBioscience
CD314-PE (NKG2D)	eBioscience

3. Cell culture

The Jurkat cell line (ATCC TIB-39, clone E6-1) was grown below $5 \cdot 10^5$ cells/mL in Dulbecco's Modified Eagle Medium (DMEM) (BioWhittaker) supplemented with 10% heat-inactivated fetal bovine serum (FBS) (Gibco) and 2mM of L-glutamine (Invitrogen). Primary mouse lymphocytes were cultured in Roswell Park Memorial Institute (RPMI) 1640 medium (BioWhittaker) supplemented with 10% FBS, 2mM glutamine and 50μM of β-mercaptoethanol (BioWhittaker). All cells were grown at 37°C and 5% CO2.

For the SILAC metabolic labeling of primary mouse lymphocytes, SILAC RPMI medium without arginine or lysine (Thermo Scientific) was used, supplemented with 10% dialyzed FBS (Gibco) heat-inactivated at 56°C for 30min, 2mM of L-glutamine (Invitrogen), 300mg/L of L-proline (Sigma-Aldrich), 50μM of β-mercaptoethanol (BioWhittaker) and 10mM HEPES. For the light condition 0.4mM L-arginine and 0.8mM L-lysine were added, while for the heavy condition 0.4mM $^{13}C_6$-L-arginine and 0.8mM $^{13}C_6$-L-lysine (Silantes) were used.

4. SILAC labeling

Two replicates with reverse labeling were performed, so that in one of them the primary wild type (WT) mouse lymphocytes were cultured in light condition and the DGKζ$^{-/-}$ in heavy condition, and in the other the WT cells were cultured in heavy condition and the DGKζ$^{-/-}$ cells in light condition. During the activation of the lymphocytes with OVA peptide, they were cultured in standard medium, while once in the proliferation phase with IL-2, they were transferred to SILAC medium for 5 days.

5. Mice

All the procedures used for the mouse work were approved by the CSIC Ethics Committee. DGKα-deficient mice were donated by Dr. Xiao-Ping Zhong of Duke University Medical Center (Durham NC), and DGKζ-deficient mice by Dr. Gary Koretzky of the University of Pennsylvania (Philadelphia PA). These mice were crossed with OT-I strains to get OT-I mice DGKα$^{-/-}$ and OT-I DGKζ$^{-/-}$ at the CNB animal facility.

6. Primary mouse lymphocytes isolation and activation

Six- to fourteen- week-old mice were used to obtain primary mouse lymphocytes. Lymph nodes or spleens were removed and homogenized in a cell strainer (Becton Dickinson). The cells were resuspended with phosphate-buffered saline (PBS) for counting. In the case of spleens, erythrocyte lysis buffer (0,154M NH_4Cl, 10 mM $KHCO_3$, 0.1 mM ethylene diamine tetraacetic acid (EDTA) pH 7.4) was additionally used. Finally, after washing with PBS, 10^5 cells/mL were plated in culture medium for stimulation. For OT-I mice, SIINFEKL 10nM peptide from ovalbumin (OVA257-264) (AnaSpec) was added, or 2µg/mL concanavalin A in the case of non OT-I mice. After 72h, cells were stimulated with IL-2 (100U/mL) during 4 days.

7. Western blot

Cell lysis was performed for 15min at 4°C with radioimmunoprecipitation assay (RIPA) buffer (10 mM Tris pH 7.4, 100 mM NaCl, 1 mM EDTA, 1% Triton X-100, 10% glycerol, 0.1% sodium dodecyl sulfate (SDS), 0.5% deoxycholate), containing protease inhibitors (20 µM leupeptin, 1.5 µM aprotinin, 1 mM PMSF) and phosphatases (1 mM Na_3VO_4, 40 mM β-glycerophosphate and 2 mM NaF). Then the lysate was centrifuged for 15min at 4°C at 12000g. Pierce Protein Assay 660nm (Thermo Scientific) reagent was used to quantify the samples. The same amount of protein from the different samples was denatured at 96°C in sample buffer (Laemmli, 1970) and then analyzed by SDS-PAGE. The proteins were transferred from the gel to a polyvinylidene fluoride (PVDF) membrane (BioRad). After incubation with the corresponding primary antibodies, it was incubated with a secondary antibody coupled to peroxidase, which was revealed by chemiluminescence of the ECL (Amersham) reagent collected by autoradiography.

8. Flow cytometry

Cells were transferred to a V-shape bottom 96-well plate. After washing, they were stained with the corresponding primary antibody bound to fluorochrome in PBS staining

(2% FBS and 0.02% sodium azide) for 30min at 4°C. They were then washed again in PBS staining and kept cold until analysis by a Cytomics FC500 (Beckman Coulter) flow cytometer. The analysis was performed using FlowJo v10 (Tree Star) software.

9. Confocal microscopy

To evaluate the permeability of the biotins, Jurkat cells are labeled with Sulfo-NHS-Biotin or Sulfo-NHS-SS-Biotin. The cells were plated in crystals coated with poly-D,L-Lysine and incubated for 15 minutes to allow adhesion. They were then washed with cold PBS and fixed with 2% PFA for 10min, room temperature. The cells were permeable (4min) with PBS 0.2% Triton X-100 and blocked in PBS 1% BSA. After washing with PBS incubation with Streptavidin-Cy5 secondary antibody diluted 1:2000 in PBS with 3%FBS 1h 37°C is performed. It was also incubated with rhodamine phalloidin 1:3000 for 10min 37°C. The samples were washed with PBS and mounted with Aqua Poly/Mount (Polysciences). The images were acquired with an Olympus Fluoview FV-1000 confocal microscope and processed using Image J software.

10. Lysotracker green staining

The lysosomes staining was done with LTG, always applied as the last stain. The cells were resuspended in tempered medium at 37°C with the probe, at 50, 70, 100 or 200nM depending on the treatment. Incubation time was 2 or 30 minutes. The cells were kept in RPMI or switched to PBS or HBSS and were immediately analyzed by flow cytometry or confocal microscopy. In the case of confocal microscopy, stained cells were incubated in chambers previously coated with poly-D,L-Lysine for 5 minutes before visualization.

11. Biotinylation

For the proteomics experiments, about $5{\cdot}10^7$ and 108 cells were collected for Jurkat and differentiated CTL experiments, respectively. For the study of the PMA effect, this molecule was added at 0.1µg/mL or DMSO for the control treatment for 4h, 37°C. The cells were washed twice with cold PBS and sulfo-NHS-biotin or sulfo-NHS-SS-biotin (Pierce) was added at 1mg/mL for 20min, 4°C in agitation. Afterwards, two washes were performed with cold PBS, and the action of biotin was blocked by incubation with medium with serum for 20min, 4°C in agitation. After another wash with cold PBS, the cells were collected for lysis with RIPA buffer with protease and phosphatase inhibitors for 15min 4°C in agitation, followed by centrifugation for 15min, 4°C, 12000g. We discarded the pellet and recovered the postnuclear supernatant for the pull-down assay. We saved an aliquot of the

total for later analysis by western blot. We performed a pre-clearing of 1h, 4°C in agitation with agarose beads (Thermo), and after recovering the supernatant we incubated 1h, 4°C in agitation with NeutrAvidin agarose (Thermo). The supernatant was discarded, and after repeated washing with RIPA buffer or high salt buffer (PBS with 1.2M NaCl, 1% Triton X-100) is prepared with sample buffer at 96°C for protein separation and denaturation. After filtering using empty Bio-Spin columns (BioRad), the eluates are processed for separation using SDS-PAGE, while reserving 1/10 of the volume for further analysis by western blot. Alternatively, in the case of sulfo-NHS-SS-biotin, proteins were eluted by reducing the disulfide bridges by the addition of 50µL and 150µL in two rounds of elution buffer (20mM Tris, 50mM DTT), 4°C overnight (Figure 5).

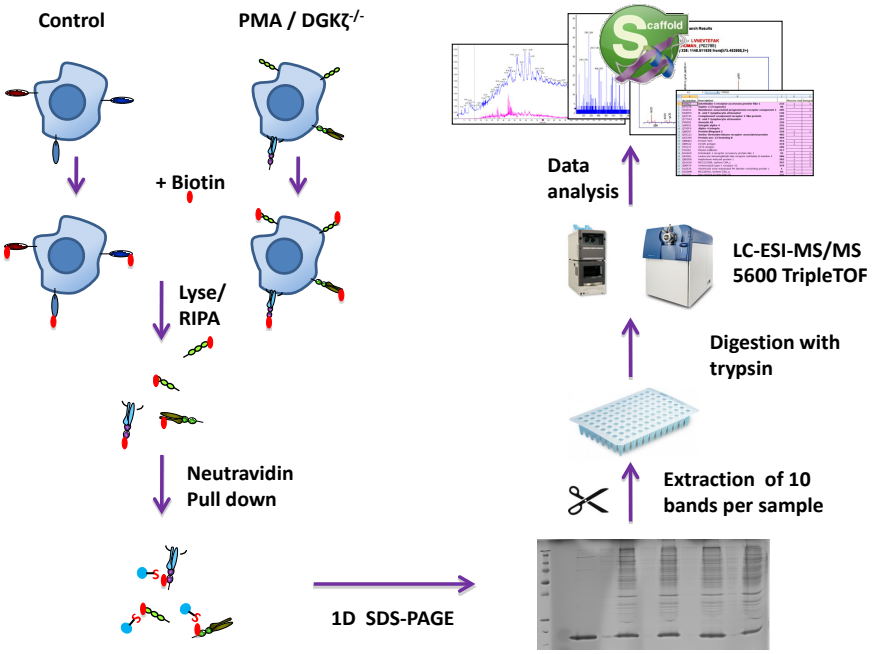

Figure 5: Biotinylation workflow
The cells of the different treatments were incubated with biotin, and then lysed to isolate the membrane proteins by pull-down with neutravidin. The lysate was separated by 1D SDS-PAGE, and bands were extracted for digestion with trypsin. The mixture of tryptic peptides was analysed by LC-ESI-MS/MS, and the data obtained were analysed to identify the corresponding proteins.

12. SUBCELLULAR FRACTIONATION

Subcellular fractionation was performed using the ProteoExtract kit (Calbiochem) following the manufacturer's instructions as described (Abdolzade-Bavil et al., 2004). Briefly, the cells were sequentially subjected to a series of lysis buffers and centrifugations to separate the cytosol, membrane, nucleus and cytoskeleton fractions. These fractions were prepared for separation by SDS-PAGE or RP-HPLC, as well as for western blot analysis.

13. PROTEOMIC WORKFLOW

13.1. Protein separation

13.1.1. SDS-PAGE

In the case of biotinylation, the proteins from the pull down with NeutrAvidin were eluted in sample buffer and separated by SDS-PAGE. In the case of subcellular fractionation, about 100µg of protein was loaded from each fraction in the gel. After electrophoresis, the gel was stained with coomassie brilliant blue (QuickCoomassie, Generon). Sixteen bands were cut and transferred to a 96-well plate for further automatic in-gel digestion using a Proteineer DP (Bruker Daltonics). The bands were washed with 50mM ammonium bicarbonate, and then washed and dried with 100% ACN. The bands were then reduced and alkylated adding 10mM DTT and 50mM IAM respectively, and were washed with 50mM ammonium bicarbonate and dried with N2 prior to digestion with trypsin 15ng/µL (4h, 37°C). The peptides obtained were extracted by the addition of 0.5% TFA / 50% ACN, and dried in SpeedVac (Eppendorf) to be kept at -20°C until analysis by LC-MS/MS.

13.1.2. RP-HPLC

From the subcellular fractions of cytosol, membranes and nucleus, a protein precipitation was carried out by sequentially adding methanol, chloroform and water (4:1:3). After centrifuging (15000g, 2min), the supernatant was discarded, and after washing with methanol the pellet was centrifuged again and recovered. It was then resuspended at TFE / 50mM ammonium bicarbonate 50% (v/v), reduced at 10mM DTT (30min, 56°C) and alkylated at 50mM IAM (30 min, room temperature). It was diluted with 50mM ammonium bicarbonate to reduce the concentration of TFE to 5%. Then trypsin 1:50 (w/w) was added and left incubated at 37°C overnight. After the digestion process the samples were dried in SpeedVac.

A reverse phase chromatographic separation was then performed on basic mobile phase, with a 4.6 mm x 150 mm column XBridge BEH C18 5µm (Waters). The samples were resuspended in buffer A (10mM NH_4OH, pH 9.4). During the chromatographic development, the proportion of buffer B (80% methanol at 10mM NH_4OH, pH 9.4) was increased. It remained in isocratic conditions at 2% in 5min, increased linearly to 25% in 10 minutes, to 70% in 40min, and to 100% in 5min. After 10 minutes in isocratic conditions, it returned to 2%. About 30 fractions were collected, which were neutralized with TFA, and were concatenated into 10 fractions, combining fractions 1, 11, 21; 2, 12, 22; and so on. The samples

were dried in SpeedVac and stored at -20°C until analysis by LC-MS/MS.

13.2. Mass spectrometry

13.2.1. LC-MS/MS analysis

The samples were resuspended in 2% ACN 0.1%FA, of which one-third was used in a volume of 5µL for LC-MS/MS analysis. The tryptic peptides were analysed using a nano-HPLC system (Eksigent Technologies nanoLC Ultra 1D plus, AB SCIEX) coupled online to a TripleTOF 5600 mass spectrometer (AB SCIEX) equipped with a nano-spray ionization source (NanoSpray III, AB SCIEX) with a fused-silica nano spray tip (10µm x 120mm PicoTip emitter, New Objective). An analytical nano-Acquity UPLC column (1.7 µm, BEH 130 C18; Waters), situated online after the trap nanoViper column Acclaim PepMap C18, 5 µm (Thermo), was used to separate the peptides. For the chromatographic gradient, a binary solvent system consisting of a mobile phase A (0.1% FA in water) and a mobile phase B (0.1% FA in ACN) was used. During 10 min the loading was carried out in the trap column with a flow of 2 µl/min of buffer A under isocratic conditions. Chromatography was then started on the analytical column with a flow rate of 250nL/min, at 40°C in 150min. During 1min it was kept in isocratic conditions of 98% buffer A and 2% buffer B. Afterwards, successive linear increases of buffer B were made, to 30% in 110min, to 40% in 10min, to 90% in 5min, and it remained under isocratic conditions in 90% of B during 5min. Finally, the initial conditions were restored to reequilibrate the column.

13.2.2. Data acquisition

The acquisition was performed in positive ionization mode using an IonSpray Voltage Floating (ISVF) of 2800 V, curtain gas pressure (CUR) of 20 psi, interface heater temperature (IHT) of 150°C, nebulizer ion source gas 1 pressure (GS1) of 30 psi, and declustering potential (DP) of 85 V. The data were acquired according to the information-dependent acquisition (IDA) mode, using the Analyst TF 1.5 (AB SCIEX) software. The acquisition cycles consisted of a 250ms MS survey scan within 350-1250 m/z range, followed by a maximum of 25 MS/MS scans of 100ms within 100-1500 m/z range. Only ions with a higher intensity greater than 90 counts and a charge between +2 and +5 were selected for further collision-induced dissociation (CID), whose collision energy (CE) was set as variable, determined in each case by the software. The selected ions were excluded for 20 seconds after being fragmented twice.

13.2.3. Data analysis

The raw files generated were processed with the Peak View software (v 1.1, AB SCIEX) to mascot general file (mgf) format and searched in an in-house Mascot Server v.2.5.1 (Matrix Science) against a protein database without isoforms concatenated to the corresponding decoy sequences using DBtoolkit (v4.1.4). The selected human and mouse databases, containing 40 470 and 33 604 entries, were released in January 2016 and July 2016 respectively (UniProtKB/SwissProt database). Search parameters were set as follows: parent ion tolerance was 25 ppm and fragment ion mass tolerance was 0.05 Da. Carbamidomethyl cysteine was specified in Mascot as fixed modification, while oxidation of methionine and acetylation of the N-terminus were specified in Mascot as variable ones. Additionally, for the bioninylation experiments, the biotin moiety conjugated to lysine residues and protein N-termini was added as a variable modification, and for SILAC experiments $^{13}C_6$-L-arginine and $^{13}C_6$-L-lysine were set as variable modification. Two tryptic digestion missed cleavages were allowed. Each dat file extracted from Mascot was then uploaded in the Scaffold bioinformatic tool v. 4.6.1 (Proteome Software), where different replicates were compared under the same conditions, and proteins were grouped using protein cluster analysis option. For statistical analysis, a false discovery rate (FDR) ≤ 1% at the protein level was applied to filter false positives.

The quantitative analysis was performed by Proteobotics. The signals of the peptides with and without labeling were detected, eliminating the noise and correcting the proportion between them. A fold change was calculated with the signal variations between pairs of peptides, while the proteins were filtered applying a FDR ≤1%.

13.3. Bioinformatic analysis

To classify proteins according to their location within the cell, the information contained in the cellular component ontology of GeneOntology has been used. Access to this information for each protein from the UniProt database and the clustering of the analyzed proteins in different categories was facilitated by the Protein Information and Knowledge Extractor (PIKE) application (Medina-Aunon et al., 2010). Twelve categories were created to cover the main cell locations, with special interest in plasma membrane and cell surface for this study (Table 3).

For the functional analysis of proteins, EnrichmentMap, a plug-in of Cytoscape (version 3.2.1) was used. Proteins were grouped in Gene Ontology categories, where node size was related to number of genes within that category, and color intensity was related to statistical significance of enrichment analysis. The thickness of the edges represented the

protein overlap between Gene Ontology categories. For the Venn diagrams, BioVinci (version 1.1.3) was used.

Table 3: Cluster names and their corresponding cellular component GO terms

Cluster name	GO term
NUCLEAR	GO:0005634
CYTOPLASM	GO:0005737
PLASMA MEMBRANE	GO:0005886
CELL SURFACE	GO:0009986
PERINUCLEAR	GO:0034399
GOLGI COMPLEX	GO:0005794
ENDOPLASMIC RETICULUM	GO:0005783
ENDOSOME	GO:0005882
MITOCHONDRIAL	GO:0005739
PEROXISOME	GO:0005777
CYTOSKELETON	GO:0005856
EXTRACELLULAR	GO:0005576

13.4. Statistical analysis

The data were analyzed with the GraphPad Prism program, applying the one- or two-way ANOVA for multiple comparisons. Three replicates were performed in these experiments.

RESULTS

Results

1. Analysis of different methodologies for the study of T cell membrane proteome

To obtain a T cell surfaceome map as complete as possible, we employed two approaches to enrich cell surface proteins: biotin labeling and subcellular fractionations. From these cell surface protein enriched samples we performed shotgun proteomic analysis by mass spectrometry technology (LC-MS/MS) with the objective of identifying most of the membrane proteins we could. The optimization of these methodologies was carried out in Jurkat T cells, since this is a T cell line model for T-cell receptor signaling study (Abraham & Weiss, 2004).

1.1. Enrichment of membrane proteins by biotinylation

We first performed an enrichment of cell surface proteins using biotin labeling. This enrichment step coupled to mass spectrometry has been used previously (Peirce et al., 2004). This strategy consists of labeling primary amines of proteins in the outer face of the plasma membrane with a derivative of biotin in intact cells during cell culture. Biotinylated proteins are then purified based on their affinity for streptavidin (Elia, 2008). These enriched cell surface proteins or surfaceome are then identified by mass spectrometry using standard procedures.

We initially performed a titration in Jurkat T cells in order to estimate the optimal concentration of biotin to recover most membrane proteins as possible with minimal labeling (Figure 6). We chose different concentrations, and after carrying out the biotinylation and purification steps we verified protein labeling efficiency by western blot.First, we checked by HRP-conjugated streptavidin that proteins of pull-down were labeled with biotin. The higher the concentration of biotin employed, the greater the degree of labeling. Most biotin labeled proteins were detected in the bead-enriched fraction and not in the unbound fraction, suggesting that the stoichiometry of beads employed was correct and we could capture most of the biotinylated proteins (Figure 6A).

At the same time, we measured specific subcellular localization markers to evaluate the degree of enrichment of membrane proteins compared to known cytosolic markers (Figure 6B). The presence of transferrin receptor in the bead-bound fraction indicated en-

richment of transmembrane protein, whereas in the case of other markers such as GM130 (Golgi), pPKCα (cytosol) or actin (cytoskeleton) no apparent protein was detected. The presence of PLCγ suggested that some protein-protein interactions could be preserved and non-transmembrane proteins with clear membrane localization could also be enriched in these biotin-pull-down fractions, resulting in enrichment in proteins temporally associated to membrane. Nonetheless, for subsequent experiments we chose the concentration of 1mg/mL of biotin, as this allowed more robust labeling without increasing contamination of other non-plasma membrane proteins.

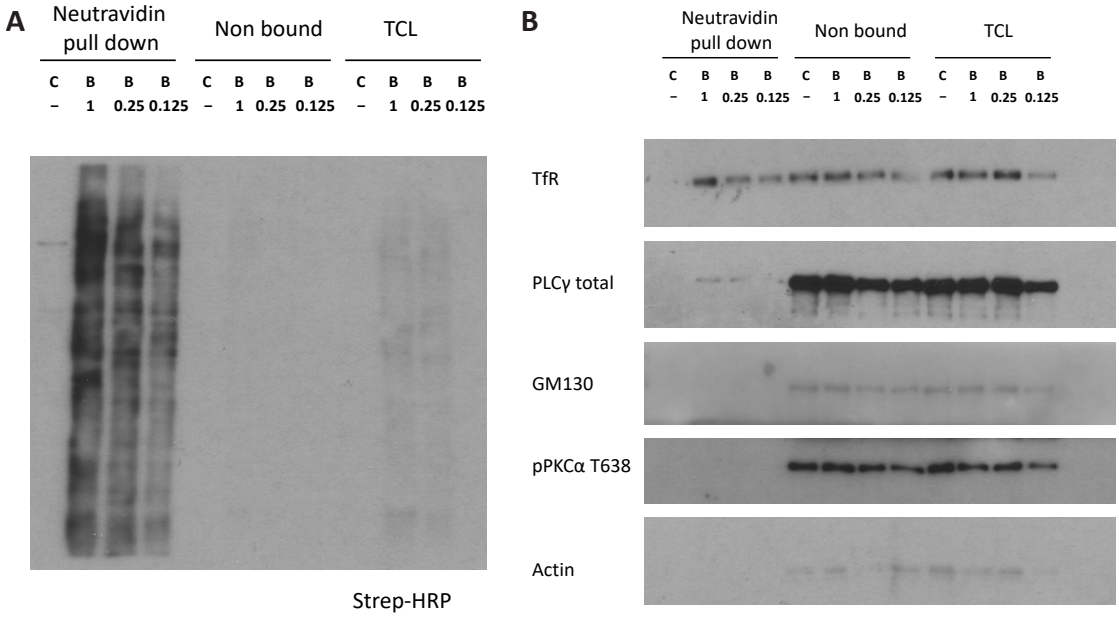

Figure 6: Biotin titration
Titration of the optimum concentration of biotin for correct labeling and precipitation of plasma membrane proteins. **(A)** The expression of different proteins which act as subcellular localization markers was checked in biotinylated proteins pull-down and in the total cell lysate by western blot. **(B)** The recovery of biotinylated proteins was assessed incubating with streptavidin-HRP.

Next we took advantage of this technology to see the effect of DAG metabolism on the cell surfaceome. We mimicked DGK loss or T cell activation by addition of the DAG analogue PMA, a phorbol ester that is frequently used to examine the effects of sustained DAG generation. This molecule simulates effects of shedding and changes the expression of membrane proteins (Ahram et al., 2005; Gharbi et al., 2013). We validated again by western blot the efficiency of biotinylation and the effect of PMA addition (Figure 7). Our western blot data confirmed that most of the biotinylated proteins were enriched in the biotin-bound fraction. Different markers were also used to check the efficiency of biotin enrichment. Again, we observed an enrichment of the transferrin receptor and PLCγ, but

not of other cytosolic proteins. ERK phosphorilation and reduction of PKCα levels in the total lysate were monitored to check for correct PMA activity (Ahnadi et al., 2000). Analysis of the pull-down showed a lower level of transferrin receptor in the PMA treated samples. This would be in agreement with internalization of the receptor in response to PMA treatment (Klausner et al., 1984; Meng et al., 2010).

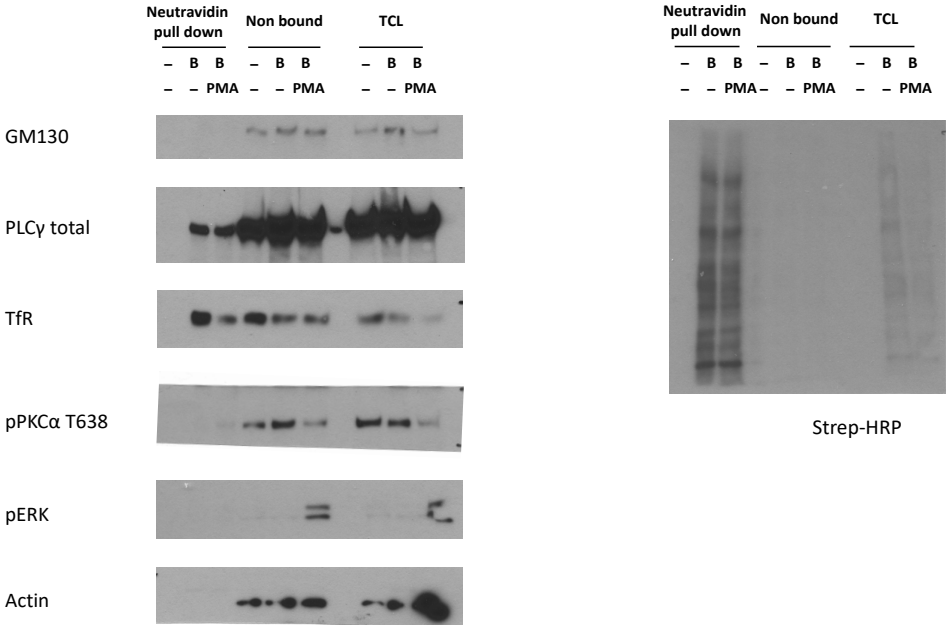

Figure 7: Cell surface protein enrichment in Jurkat T cells by biotinylation
A Jurkat T cell culture was treated with PMA for 4h. After this time period an enrichment of plasma membrane proteins was carried out by biotinylation. The membrane protein enrichment and PMA addition effects were assessed by western blot.

1.2. Shotgun proteomic analysis

Once we obtained a pull-down of enriched cell surface proteins by biotinylation, a shotgun proteomic analysis was performed. We did two replicates of Jurkat cell line that were analyzed together. In each replicate cells were treated with PMA or vehicle (DMSO). A control sample from Jurkat cells that were not treated with biotin was used in order to distinguish non-specific contaminant proteins that can interact with streptavidin beads.

The number of proteins identified by mass spectrometry was similar in PMA or in DMSO treated cells (Figure 8) (Supplemental table 1). Furthermore, the proteins identified in the different biological replicates was reproducible, with 65% of the proteins identified in all replicates. The comparison of the proteins detected in the absence or presence of PMA indicated they were mostly shared in both treatments, while less than 10% belonged

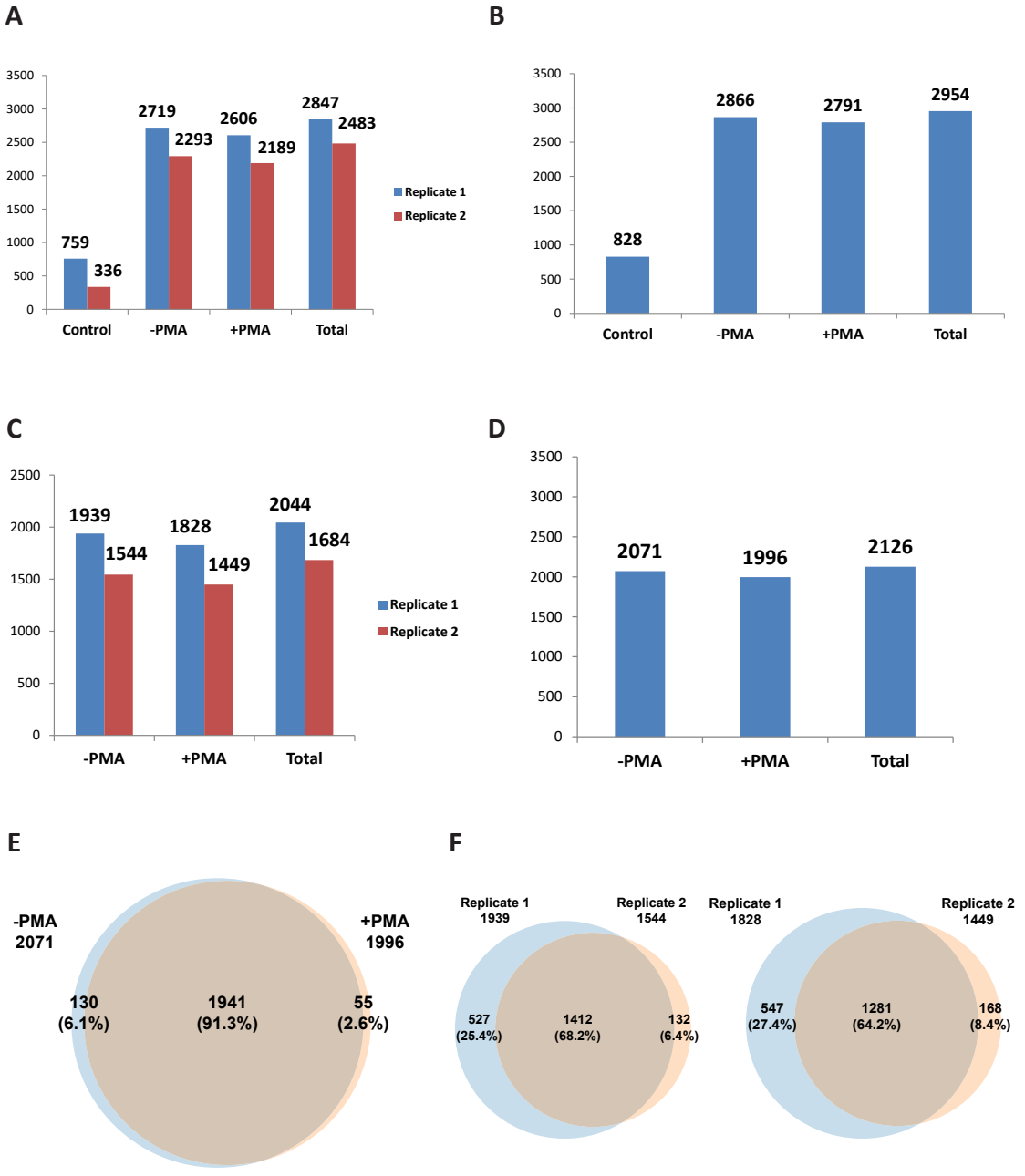

Figure 8: Shotgun analysis of Jurkat T cell surface proteins.
After performing treatments with PMA and the enrichment biotin process, we identified the proteins by mass spectrometry. **(A, B)** Almost 3000 proteins were detected in total by combining two replicates. **(C, D)** and about 2000 proteins after subtracting non-specific binding proteins identified in control. **(E, F)** Most of these proteins were shared between both treatments. This behavior was observed in both replicates as well as in the sum of both, although in the second replicate fewer proteins were identified. The proteins identified in each treatment were compared to check the reproducibility between replicates, obtaining an overlap of 65%.

exclusively to one of the two treatments. This data suggest that PMA treatment has minimal impact on global cell surfaceome, in we consider all the proteins identified.

1.3. GO representation of proteomic results

To corroborate the efficiency of enrichment of cell surface proteins following protein biotinylation, we analyzed the ontology annotations of the proteins identified and focused on their described cellular component category and predicted subcellular localization. For this purpose we used the protein annotations stored in the ontology of "cellular component" of Gene Ontology project (Ashburner et al., 2000). This tool permits to check whether a protein belongs to Gene Ontology categories related to plasma membrane and cell surface.

	Complete		Total		Common -+PMA		-PMA		+PMA	
NUCLEAR	2337	54%	941	44%	863	44%	54	42%	24	44%
CYTOPLASM	2365	54%	923	43%	837	43%	50	38%	36	65%
PLASMA MEMBRANE	922	21%	668	31%	613	32%	41	32%	14	25%
CELL SURFACE	148	3%	81	4%	74	4%	6	5%	1	2%
PERINUCLEAR	407	9%	161	8%	145	7%	10	8%	6	11%
GOLGI COMPLEX	250	6%	154	7%	144	7%	6	5%	4	7%
ENDOPLASMIC RETICULUM	383	9%	306	14%	277	14%	24	18%	5	9%
ENDOSOME	181	4%	97	5%	88	5%	6	5%	3	5%
MITOCHONDRIAL	741	17%	450	21%	422	22%	20	15%	7	13%
PEROXISOME	61	1%	51	2%	46	2%	2	2%	3	5%
CYTOSKELETON	355	8%	123	6%	112	6%	6	5%	5	9%
EXTRACELLULAR	1098	25%	504	24%	465	24%	29	22%	10	18%
	4359		2126		1941		130		55	

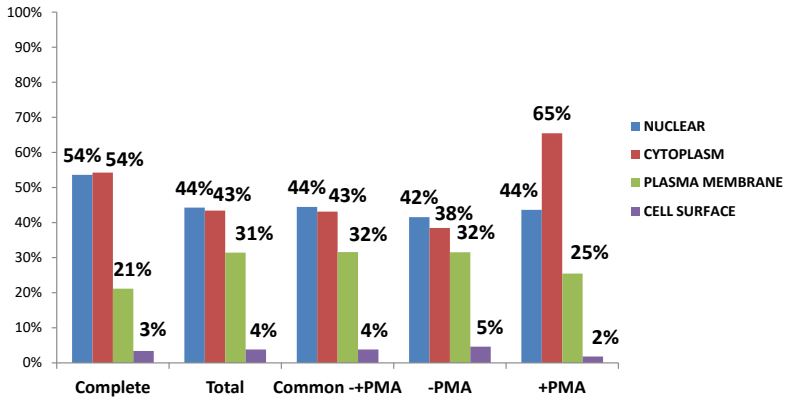

Figure 9: Subcellular protein distribution according to GO terms.
After shotgun analysis we studied the subcellular localization using annotations of cellular component from Gene Ontology. Unlike Jurkat complete cell lysate obtained with a commercial kit, a slight increase in the number of plasma membrane proteins was seen in enriched fractions by biotinylation. This represented a percentage above 30%. Furthermore, percentages of other contaminants fractions as nucleus or cytoplasm suffered consequent decreases. For proteins found only in one of the two PMA treatments, the percentage of membrane proteins was slightly lower.

By bioinformatic application PIKE (Medina-Aunon et al., 2010) it is possible to obtain the GO codes of these proteins automatically. The application uses this information to cluster proteins according to subcellular localization.

Our results showed an increased number of plasma membrane proteins if we compare to total cell lysates from Jurkat T cells (Figure 9) (Supplemental table 2). Biotinylation enrichment of cell surface proteins improved identification of plasma membrane proteins based on GO terms from 21% in general shotgun assays from total lysate extracts without membrane protein enrichment, to about 31%; although the absolute number of proteins was reduced from 922 to 668. This effect was accompanied with a decrease in proteins identified from other subcellular localizations such as nucleus and cytosol. We could also detect an increase in internal organelles, for instance in endoplasmic reticulum and mitochondria.

If we analyze jointly the protein content of plasma membrane in the treatments with PMA addition and without it, there were some differences. In the case of proteins shared in both treatments, the results were similar to the total. For these proteins present exclusively in one of the two treatments, the percentages of plasma membrane proteins were lower, and there were also decreases in other categories. Must be taken into account that in these cases the number of proteins was considerably lower and this may interfere with the distribution of percentages.

Direct observation of the results of subcellular localization percentages obtained revealed a redundancy between different clusters. There were proteins which were grouped into two or more categories, probably because effectively they were detected in different

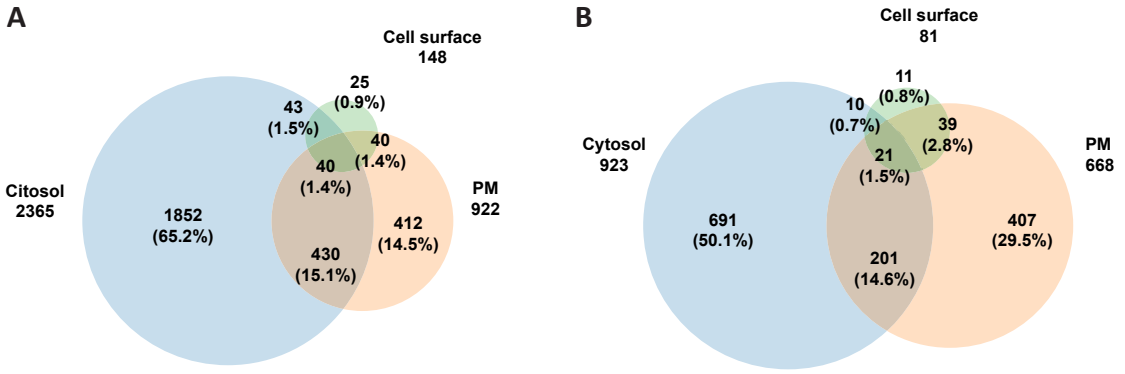

Figure 10: Plasma membrane, cell surface and cytosol clusters overlap.
Once the clustering according to the subcellular localization of proteins was performed, we analyzed the overlap among the categories of plasma membrane, cytosol and cell surface. We compared cases of proteins from total cell lysate **(A)** and those obtained by biotinylation **(B)**. Whereas the number of proteins of the three clusters was higher in the first case, in biotinylation the exclusive plasma membrane proteins reached a similar number in absolute terms, and represented a higher percentage of the total.

locations. To evaluate this, we analyzed the possible overlap between plasma membrane, cytosol and cell surface, comparing total cell lysate proteins and those enriched by biotinylation (Figure 10). The number of proteins is higher in all cases in the total lysate. However in the case of plasma membrane unique proteins the number was similar although the percentage was greater than in the case of proteins enriched by biotinylation.

1.4. High salt wash biotinylation

In an attempt to improve the percentage of enriched cell surface proteins, we modified biotinylation conditions to avoid contamination by non-specific protein binding. We increased the number of washes after the binding of the proteins to the neutravidin, as well as the salts concentration of the wash buffer to increase the ionic strength. We performed a shotgun analysis as in the previous experiment (Figure 11) (Supplemental table 3). When

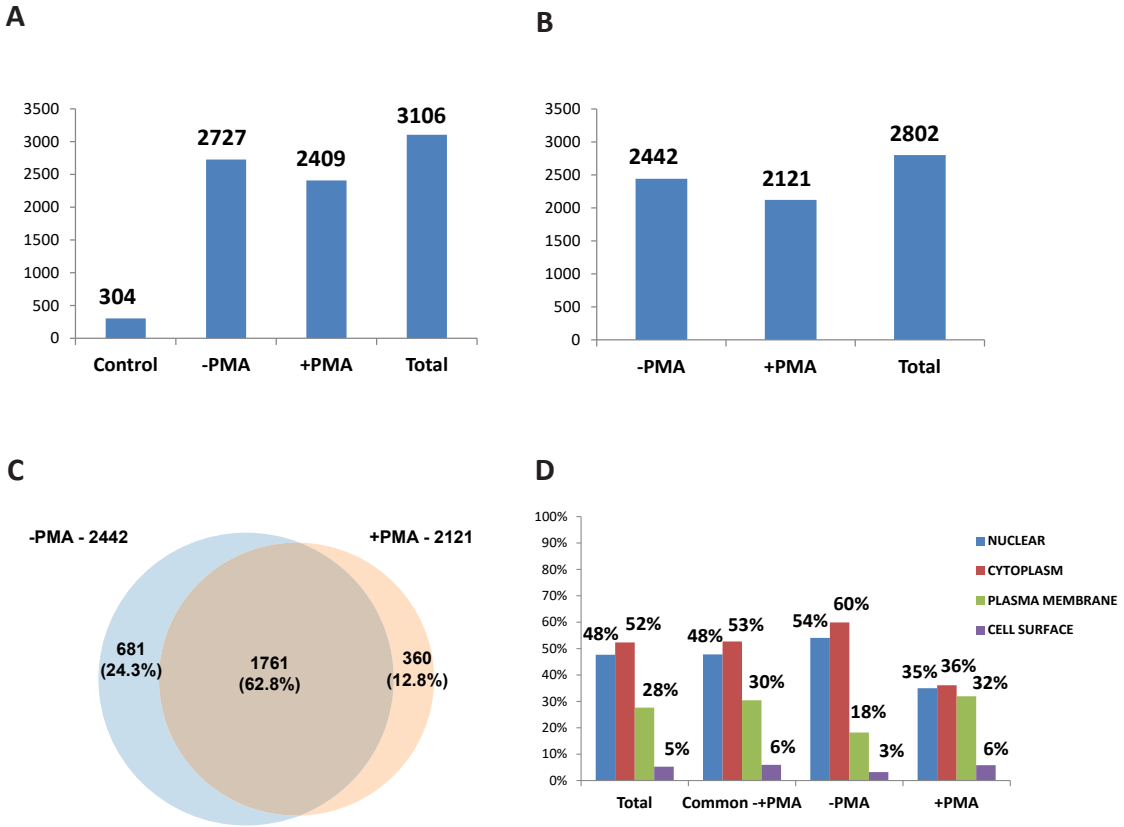

Figure 11: Shotgun and subcellular distribution analysis of biotinylation with high-salt wash method.
We performed a biotinylation with modified conditions to optimize plasma membrane proteins enrichment. **(A)** About 3000 proteins were identified combining both treatments. **(B)** After substracting proteins detected in control, the total number was about 2800. **(C)** Proteins shared by both treatments exceeded 60%. **(D)** Plasma membrane proteins percentages were around 30%.

analyzing the subcellular localization results by Gene Ontology, we did not see changes in the percentages of the proteins of the plasma membrane and of the cell surface. We concluded that no improvement was obtained following harsher purification conditions.

1.5. Optimization of biotinylation by using sulfo-NHS-SS-biotin

In order to improve the yield of biotinylation to obtain a greater number of cell surface proteins, we compared the performance of the biotin used in the previous work to a modified biotin reagent incorporating an internal disulfide bridge (Figure 12). This molecule, being more soluble, helps to avoid intracellular penetration, and also allows elimination of the biotin tag after labeling (Peirce et al., 2004). After comparing the efficacy of both reagents, we observed that in both cases the labeling of proteins with biotin was limited to the plasma membrane, so that contamination by labeling of internal proteins is low in any case. In spite of this, the recovery of membrane proteins such as the transferrin receptor was greater in the case of sulfo-NHS-SS-biotin. In the remaining subcellular localization markers there were no apparent changes, except for a lower PKCα contamination with sulfo-NHS-SS-Biotin.

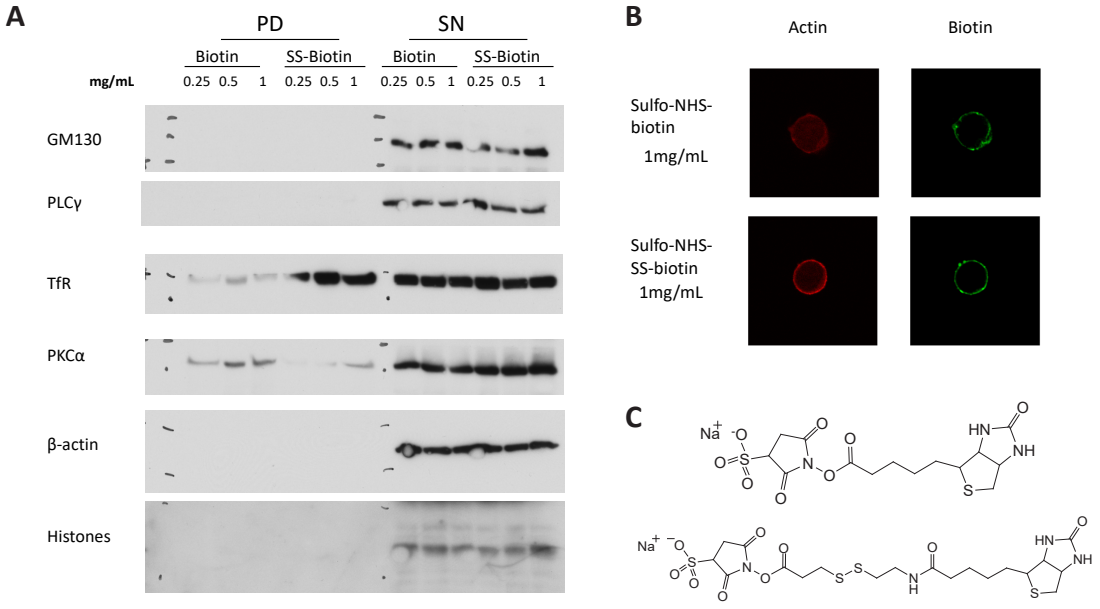

Figure 12: Comparison and titration of sulfo-NHS-biotin and sulfo-NHS-SS-biotin in Jurkat T cells.
(A) Western blot showing the expression of subcellular localization markers. Equimolar amounts of biotin were used for the titration of the biotin reagents, so the concentrations are referred to mg/mL sulfo-NHS-biotin in both cases. In the case of the transferrin receptor there was a higher yield with sulfo-NHS-SS-biotin. **(B)** Immunofluorescence in which the biotin of labeled proteins was detected to analyze its subcellular localization. In both cases the labeling was limited to the plasma membrane. **(C)** Structure of sulfo-NHS-biotin **(top)** and sulfo-NHS-SS-biotin **(bottom)**.

The existence of a disulfide bridge in the sulfo-NHS-SS-biotin molecule is conceived as a strategy to eliminate the biotin tag after the pull-down with neutravidin. Thus during the shotgun proteomic analysis the possibility of problems in the detection of biotinylated peptides was overcome. To optimize the procedure, we tested several elution conditions, verifying the presence of proteins in the pulldown by means of western blot (Figure 13). The largest recovery of proteins was observed when the biotinylated proteins bound to beads with neutravidin were boiled under reducing conditions. If only boiling or reducing conditions were applied, protein production was lower, which can be observed in the case of the membrane protein transferrin receptor.

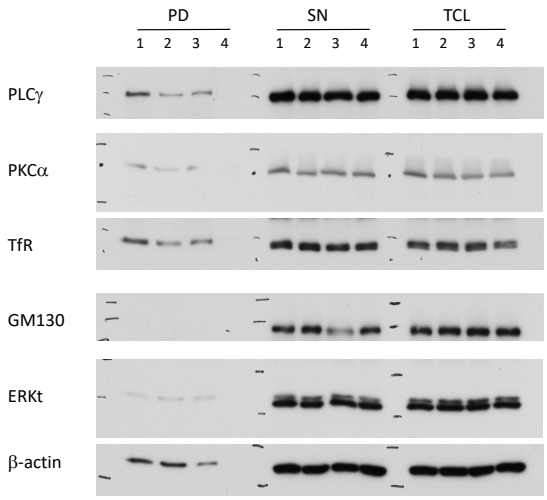

Figure 13: Evaluation of the elution of biotinylated proteins by sulfo-NHS-SS-biotin. The western blot showed that the treatment with larger protein recovery in the pull-down was boiling under reducing conditions. This recovery was greater than in the elution with only a reducing agent, or simply boiling. The integrity of sulfo-NHS-SS-biotin was maintained if these conditions were not applied, as we can see in the last case.

1.6. Enrichment of membrane proteins by subcellular fractionation

Performance enrichment using biotin based purification approaches were similar to those obtained in other studies (Weekes et al., 2010). We attempted alternative techniques to improve the percentage of plasma membrane proteins. As a new approach in our study we used a commercial subcellular fractionation kit to obtain cytosol, membranes and nucleus fractions. Thus, in addition to our membrane enriched fraction we can analyze the other fractions to search proteins from other locations.

For a first fractionation performance evaluation, we carried out a western blot from total lysates of the three fractions (Figure 14). We checked the expression of proteins that are normally found in a particular location in the cell, so they can serve as subcellular mark-

ers. For plasma membrane proteins we chose the transferrin receptor as reference, and Golgi protein GM130 for inner membranes. The blot showed how these proteins were detected preferably in the membrane fraction. In the cytosol fraction we observed a clear expression of tubulin, while the nucleus fraction included histones. In general, contamination between fractions was reduced.

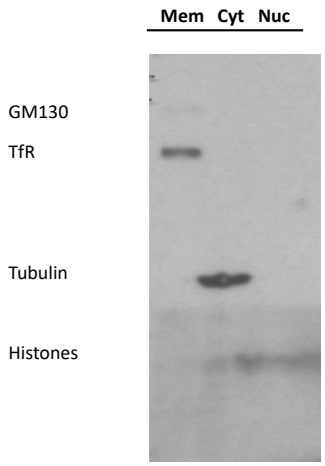

Figure 14: Subcellular fractionation from Jurkat T cells.
From a Jurkat T cell culture we carried out a subcellular fractionation using a commercial kit. To check the fractionation effectiveness we performed a western blot with cell lysates of the resulting fractions. It showed how the membrane fraction predominantly contained plasma membrane (transferrin receptor, TfR) and inner membrane proteins (GM130). Tubulin and histones appeared in the cytosol and nucleus fractions, respectively.

Shotgun proteomic analysis

The next step was to perform a shotgun proteomic analysis of the distinct fractions from cell lysates. This permitted us to identify the proteins present in each fraction, and actually evaluate the efficiency of the fractionating method. In our attempt to report the highest number of plasma membrane proteins, we used two different separation methods prior to the analysis by mass spectrometry. These were a protein separation by molecular mass by a one-dimensional SDS-PAGE gel, and a separation by hydrophobicity by reverse phase HPLC chromatography in basic pH. We wanted to check if the method used to reduce protein complexity can affect the number of plasma membrane proteins.

The proteomic analysis using the two separation methods indicated that in both cases a similar protein number was reached both for total and for each fraction (Figure 15) (Supplemental table 4A and B). However there was a slight advantage in the separation by RP-HPLC in basic pH. We detected near 6000 proteins, 4000 in cytosol and nucleus fractions, and almost 5000 in membrane fraction. The overlap between fractions was similar to biotinylation replicates. Within each experiment there was a significant overlap between cytosol, membrane and nucleus, so despite the results obtained by western blot there was contamination among fractions.

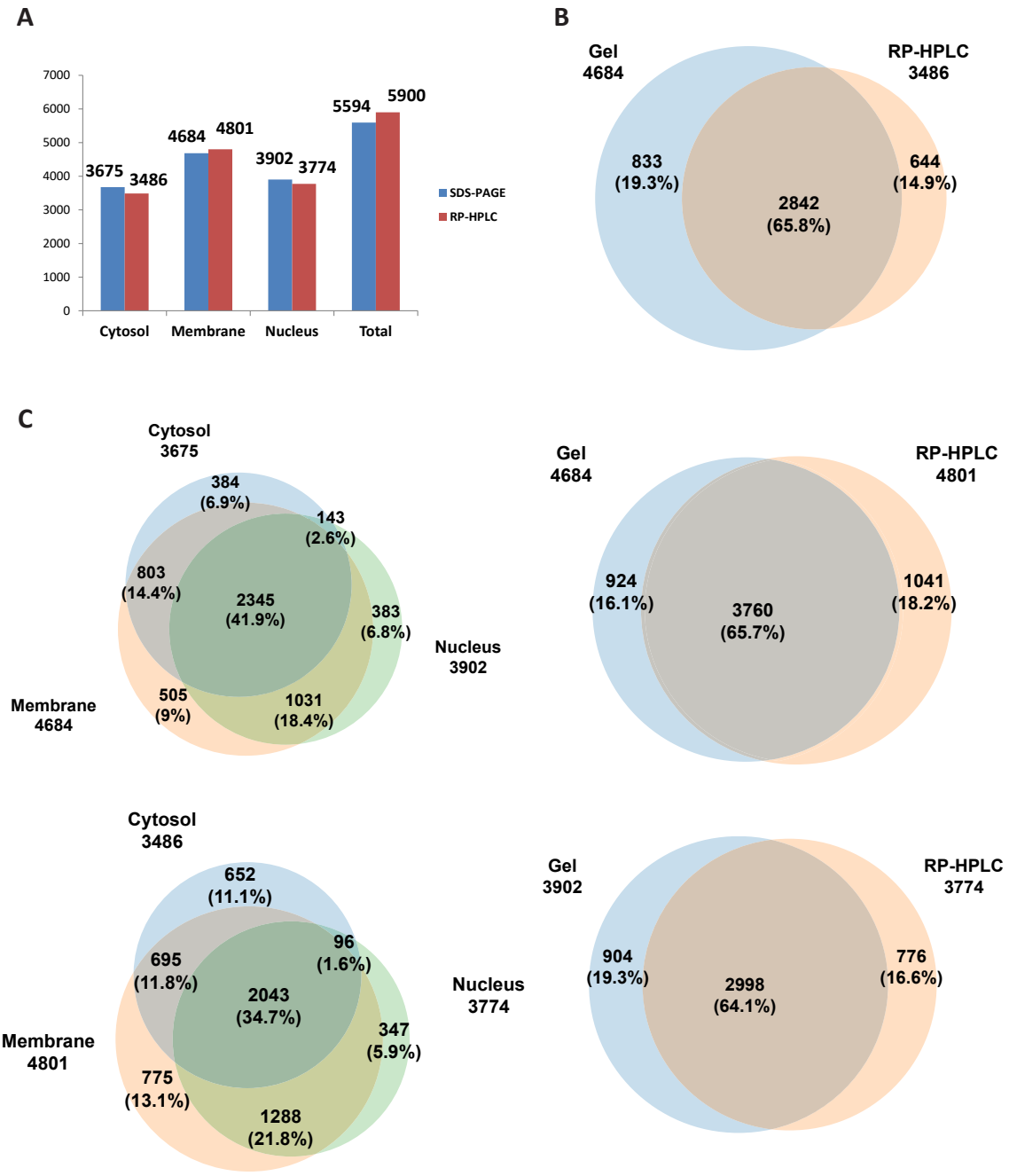

Figure 15: Results of Jurkat T cell fractionation shotgun analysis.
After making the subcellular fractionation, we analyzed by mass spectrometry the three fractions obtained. Previously we performed a separation to reduce the complexity of the sample by monodimensional SDS-PAGE or RP-HPLC in basic pH. **(A)** The amount of proteins detected in total and in each fraction was very similar with both methods. **(B)** Reproducibility was around 65% in cytosol **(top)**, membranes **(middle)** and nucleus **(bottom)** fractions. **(C)** The analysis of the overlap between the three fractions of SDS-PAGE **(top)** and RP-HPLC **(bottom)** showed that proteins common to the three fractions were the most abundant, indicating that the separation was not complete.

A

FRACTIONATION GEL	Total		Fract. Cytosol		Fract. Membrane		Fract. Nucleus	
NUCLEAR	2819	50%	2025	55%	2224	47%	2224	57%
CYTOPLASM	2900	52%	2410	66%	2415	52%	1969	50%
PLASMA MEMBRANE	1363	24%	701	19%	1269	27%	866	22%
CELL SURFACE	209	4%	143	4%	199	4%	138	4%
PERINUCLEAR	502	9%	416	11%	438	9%	361	9%
GOLGI COMPLEX	352	6%	220	6%	320	7%	221	6%
ENDOPLASMIC RETICULUM	532	10%	205	6%	521	11%	359	9%
ENDOSOME	237	4%	168	5%	228	5%	148	4%
MITOCHONDRIAL	844	15%	358	10%	799	17%	630	16%
PEROXISOME	74	1%	26	1%	74	2%	53	1%
CYTOSKELETON	463	8%	397	11%	393	8%	345	9%
EXTRACELLULAR	1272	23%	959	26%	1184	25%	902	23%
	5594		3675		4684		3902	

B

FRACTIONATION RP-HPLC	Total		Fract. Cytosol		Fract. Membrane		Fract. Nucleus	
NUCLEAR	2927	50%	1931	55%	2338	49%	2125	56%
CYTOPLASM	3018	51%	2333	67%	2400	50%	1826	48%
PLASMA MEMBRANE	1411	24%	597	17%	1255	26%	845	22%
CELL SURFACE	227	4%	125	4%	204	4%	133	4%
PERINUCLEAR	514	9%	385	11%	431	9%	330	9%
GOLGI COMPLEX	355	6%	201	6%	310	6%	200	5%
ENDOPLASMIC RETICULUM	542	9%	181	5%	506	11%	361	10%
ENDOSOME	248	4%	180	5%	224	5%	147	4%
MITOCHONDRIAL	977	17%	325	9%	919	19%	683	18%
PEROXISOME	80	1%	28	1%	78	2%	54	1%
CYTOSKELETON	456	8%	341	10%	364	8%	297	8%
EXTRACELLULAR	1374	23%	977	28%	1242	26%	877	23%
	5900		3486		4801		3774	

C

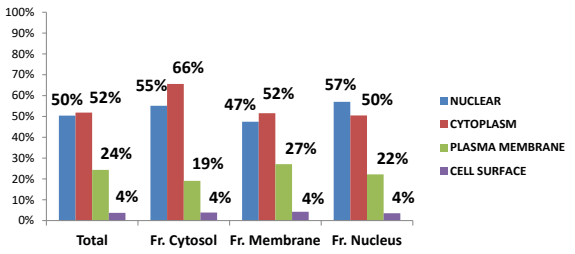

D

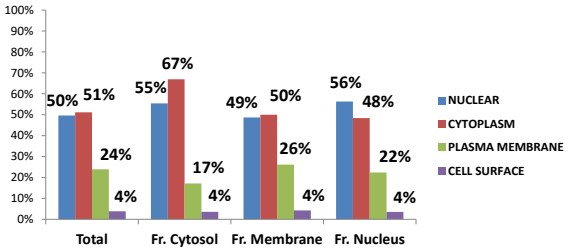

Figure 16: Fractionation subcellular protein distribution according to GO terms.

By both protein separation methods, SDS-PAGE **(A and C)** and RP-HPLC **(B and D)** we obtained similar results. In the case of the membrane fraction there was a slight enrichment in plasma membrane proteins and inner membranes, which however did not achieve the enrichment obtained by biotinylation. In cytosol and nucleus fractions there was also enrichment in these categories.

1.7. GO representation of proteomic results

The analysis by the Gene Ontology terms in each fraction confirmed enrichment in cytosol, plasma membrane and nucleus proteins with respect to total cell lysates (Figure 16). Enrichments nonetheless were moderate, especially in the case of membrane fraction where the enrichment was lower than that achieved by biotinylation. In this fraction there was also some enrichment in inner membranes. Only slight differences between the two separation methods prior proteomic analysis were observed. They were lower compared with the results of biotinylation enrichments.

To analyze the performance of the fractionation protocol to isolate cell surface proteins, we studied the presence of cluster of differentiation proteins or CD, cell surface proteins used to characterize the cell type by monoclonal antibodies (Bernard & Boumsell, 1984). In fractionation after gel separation all CD antigens were comprehended in membrane fraction, although some of them can be shared in the other fractions (Figure 17). Same situation was observed in fractionation carried out after RP-HPLC separation, except for one protein uniquely detected in cytosol fraction. This indicates that most characteristic cell surface proteins in immune cells were enriched in membrane fraction.

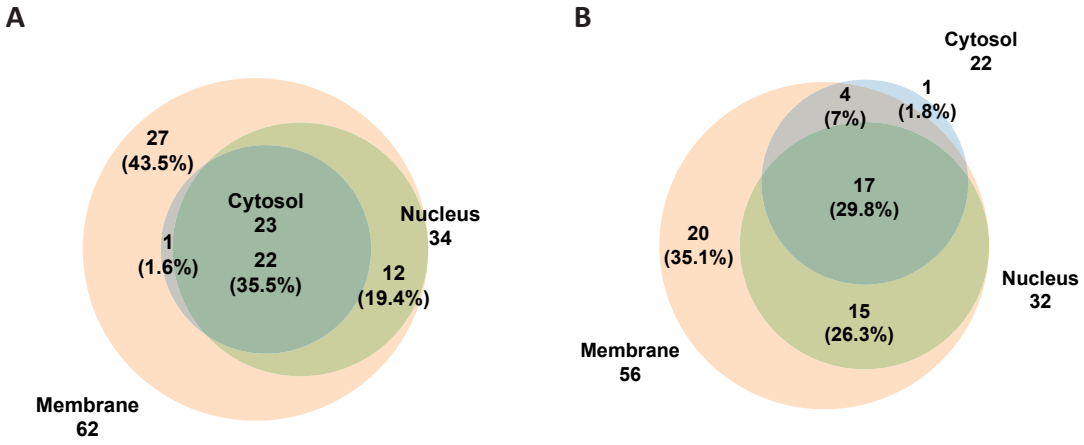

Figure 17: CD antigens distribution in fractions from Jurkat fractionations.
CD antigens were mostly detected in membrane fractions in SDS-PAGE **(A)** and RP-HPLC **(B)** fractionations. Some of them were part of cytosol and nucleus fractions, but shared with membrane. Only one protein in HPLC-RP fractionation was exclusively present in cytosol fraction.

1.8. Summary of membrane proteins recovery

After analyzing the results of the different enrichment techniques, we represented all the data together to determine the optimal approach we would use in the following experiments (Figure 18). When comparing the number of total proteins, this was smaller in the enrichment by biotinylation than in the fractionation. The same occurred in the case

of membrane proteins and cell surface. However the largest increase in the percentage of plasma membrane proteins occurred in the biotinylation approach. The cell surface percentage of protein remained equal in all cases, but not when analyzing the proteins classified as clusters of differentiation. In biotinylation and fractionation we reached a larger number of CD proteins than in the total cell lysate. For biotinylation the number was even greater if we consider CD antigens that were discarded because of they were also detected in the control treatment.

A

FRACTIONATION GEL	Complete		Jurkat biotinylation		Jurkat fractionation (Mem) Gel		Jurkat fractionation (Mem) RP	
NUCLEAR	4362		2126		4684		4801	
CYTOPLASM	922	21%	668	31%	1269	27%	1255	26%
PLASMA MEMBRANE	148	3%	81	4%	199	4%	204	4%
CELL SURFACE	34		39		62		56	

B

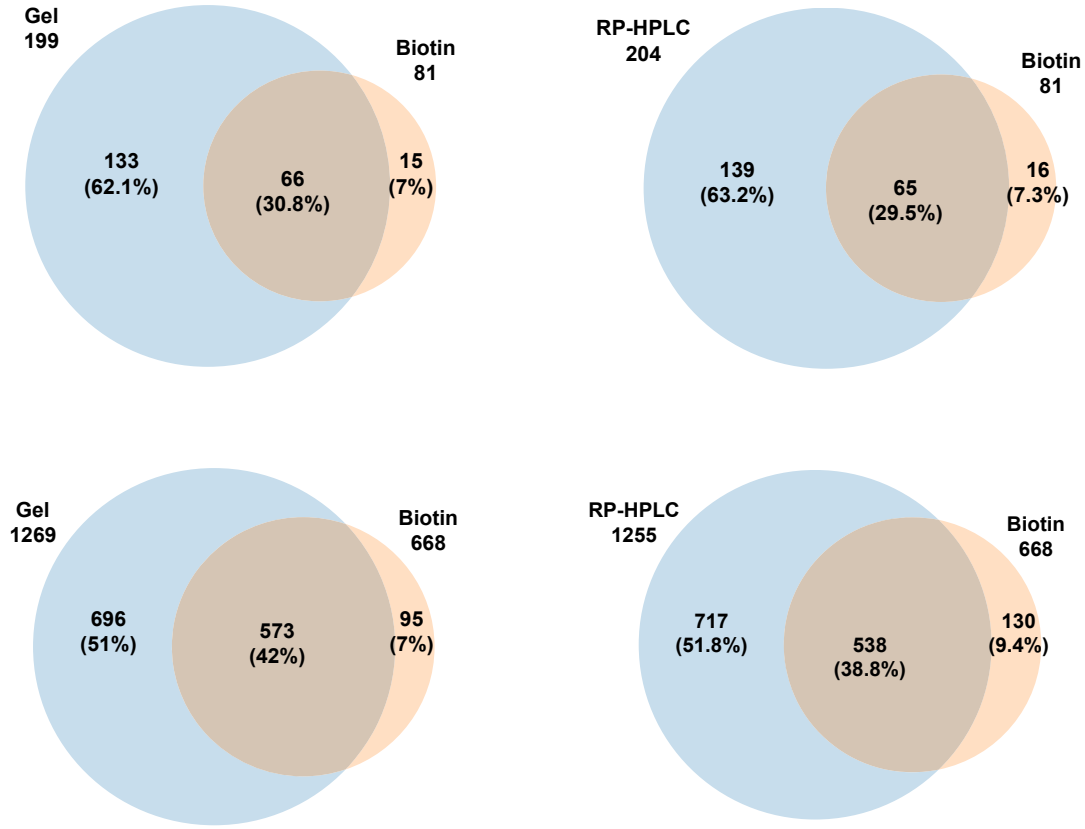

Figure 18: Summary report of plasma membrane proteins enrichment.
(A) In this table the amount of proteins of each enrichment approach was shown, and the percentage of Gene Ontology categories plasma membrane and cell surface proteins. The number of CD antigens is included too. **(B)** Graphs below represent the overlap in cell surface **(top)** and plasma membrane **(bottom)** proteins between biotinylation enrichment and membrane fractions, with SDS-PAGE on the **left** and RP-HPLC on the **right**.

We also compared the overlap between cell surface and plasma membrane GO clusters of Jurkat biotinylation enrichment and Jurkat fractionations. We expected more similarity in cell surface than in plasma membrane proteins, because biotinylation is theoretically more specific for cell surface proteins, while fractionation recovers all the membrane. However the coincidence is small, and even smaller in cell surface proteins.

2. Analysis of mouse T cell surfaceome

After optimizing cell surface protein enrichment techniques in the Jurkat T cell line, we moved to a mouse model where we could study the effects in a specific case of surfaceome changes. For this we focused on the OT-I model of CD8 T cells that allows the differentiation to cytotoxic T cells. OT-I mice express a TCR with the transgenic α (Vα2) and β (Vβ5) chains, capable of recognizing an ovalbumin peptide in the context of MHC class I H2-Kb (Hogquist et al., 1994). This model allows us to purify peripheral naïve CD8 T cells from the spleen or lymph nodes, activate them in culture with the agonist peptide, and expand them with several rounds of IL-2 to obtain a large number of CTL cells to perform shotgun proteomic studies. These mice were also crossed with DGKζ-deficient strain (Zhong et al., 2003), which allows us to analyze CTL with this phenotype.

2.1. Study of PMA on splenocytes

Prior to the study of mouse CTL, a relatively homogeneous population, we checked the expression of membrane proteins by biotinylation in activated splenocytes obtained from WT mice. These cells were extracted from spleen and stimulated with concanavalin A for 48h. After short treatment with PMA or control, we performed enrichment of cell surface proteins by biotinylation and neutravidin pull down, and we analyzed by shotgun

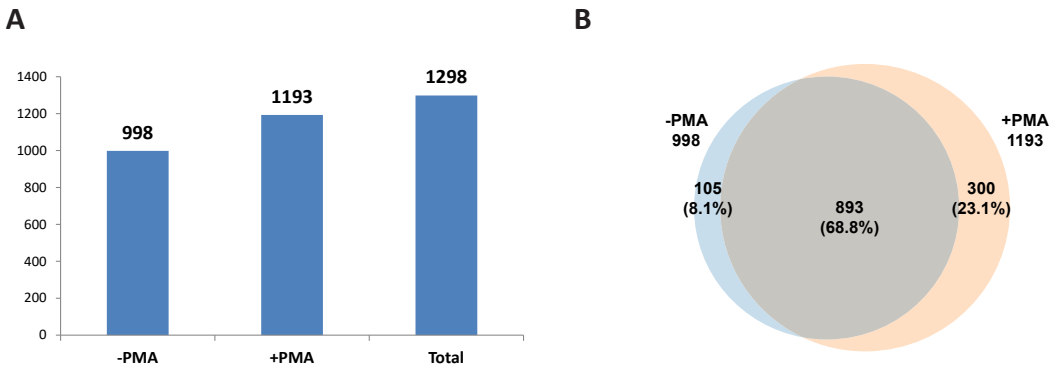

Figure 19: Shotgun analysis of splenocytes.
A) Number of proteins detected in each treatment and in total. **B)** Overlap between treatments with and without PMA. About 70% of the proteins were detected in both treatments. Most of the remaining proteins were detected in the treatment with PMA.

proteomics (Figure 19) (Supplemental table 5). We made only one replicate, so we obtained less total proteins than in the CTL experiment. Most proteins were detected both in the absence or presence of phorbol ester. Among those not common to both treatments, there was a greater expression of proteins in the treatment with PMA, probably because there were already more proteins in this treatment previously.

We also analyzed the protein distribution according to GO terms (Figure 20). With respect to CTL data there was an increase in cell surface proteins, and plasma membrane, although in general the number of proteins was similar. There was also a significant increase in extracellular proteins. The cell heterogeneity can be checked by analyzing the lists of proteins detected, which include B cell, CD4 T and CD8 markers among others.

	Total		Common -+PMA		-PMA		+PMA	
NUCLEAR	581	45%	419	47%	35	33%	127	42%
CYTOPLASM	564	43%	396	44%	44	42%	125	42%
PLASMA MEMBRANE	420	32%	288	32%	29	28%	103	34%
CELL SURFACE	107	8%	76	9%	11	10%	20	7%
PERINUCLEAR	116	9%	84	9%	9	9%	23	8%
GOLGI COMPLEX	83	6%	62	7%	5	5%	16	5%
ENDOPLASMIC RETICULUM	192	15%	145	16%	16	15%	31	10%
ENDOSOME	55	4%	32	4%	5	5%	18	6%
MITOCHONDRIAL	301	23%	228	26%	25	24%	48	16%
PEROXISOME	27	2%	20	2%	5	5%	2	1%
CYTOSKELETON	93	7%	58	6%	4	4%	31	10%
EXTRACELLULAR	537	41%	418	47%	30	29%	104	35%
	1298		893		105		300	

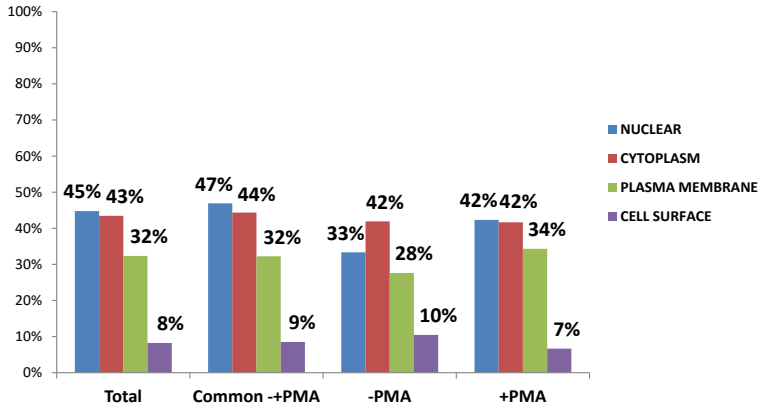

Figure 20: Subcellular protein distribution of mouse splenocytes according to GO terms.
The percentages of plasma membrane and cell surface proteins were slightly higher than in the CTL experiment. There was also a higher proportion of proteins classified as "extracellular".

2.2. Enrichment of membrane proteins by biotinylation in mouse CTL

Next we differentiated CTL WT or deficient in DGKζ and used a biotinylation protocol to enrich CTL lysates in cell surface proteins (Figure 21). After extracting lymph node cells from OT-I mice, we stimulated with OVA and expanded with IL-2. Then we re-stimulated with PMA, labeled with biotin, lysed, and performed a pull down with neutravidin. We analyzed by western blot the effect of activation with PMA and the subcellular localization markers that appeared in the pulldown. We observed that when PMA was added, ERK activation occurred in both WT and DGKζ$^{-/-}$ mice, with higher basal ERK activation in DGKζ$^{-/-}$ mice. Analysis of the pull down confirmed enrichment of transferrin receptor, that again was lost upon PMA treatment with stronger effect on DGKζ$^{-/-}$.

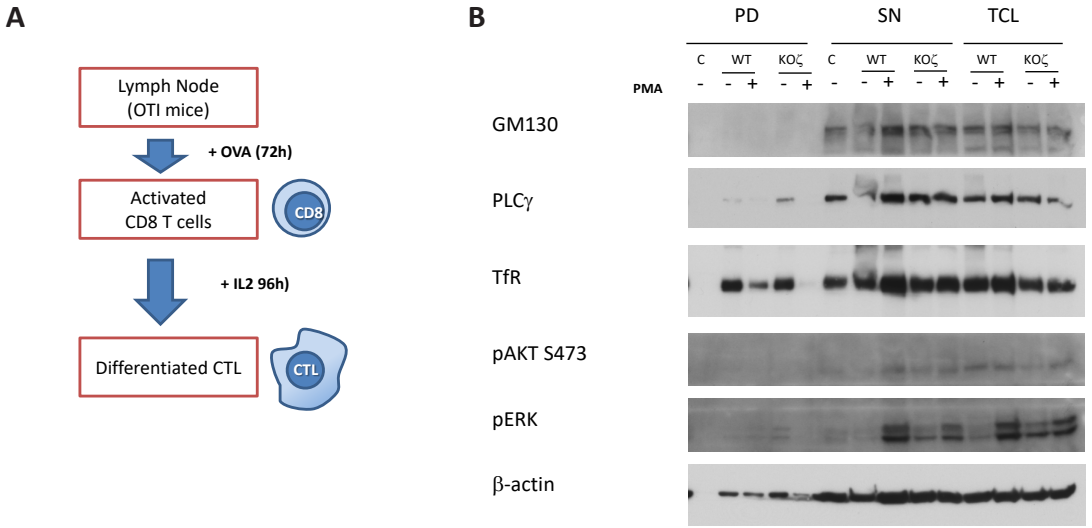

Figure 21: Cell surface protein enrichment by biotinylation in mouse CTL.
(A) Scheme depicting the procedure used to obtain CTL from lymph nodes of OT-I mice. **(B)** Western blot showing the activation of CTL with PMA and subcellular localization markers. In the pull down there was an enrichment in the case of the transferrin receptor, lower in the treatments with PMA.

2.3. Study of PMA on CTL: shotgun proteomic analysis

Following the same procedure that was used in Jurkat T cells, we performed a biotinylation experiment on CTL treated with or without PMA to enrich cell surface proteins, and subsequently analyzed by shotgun proteomics (Figure 22) (Supplemental table 6). The results showed a similar number of proteins between treatments with and without PMA, higher than 2000 proteins. Replicates had about 80% overlap, and were also similar in number of proteins.

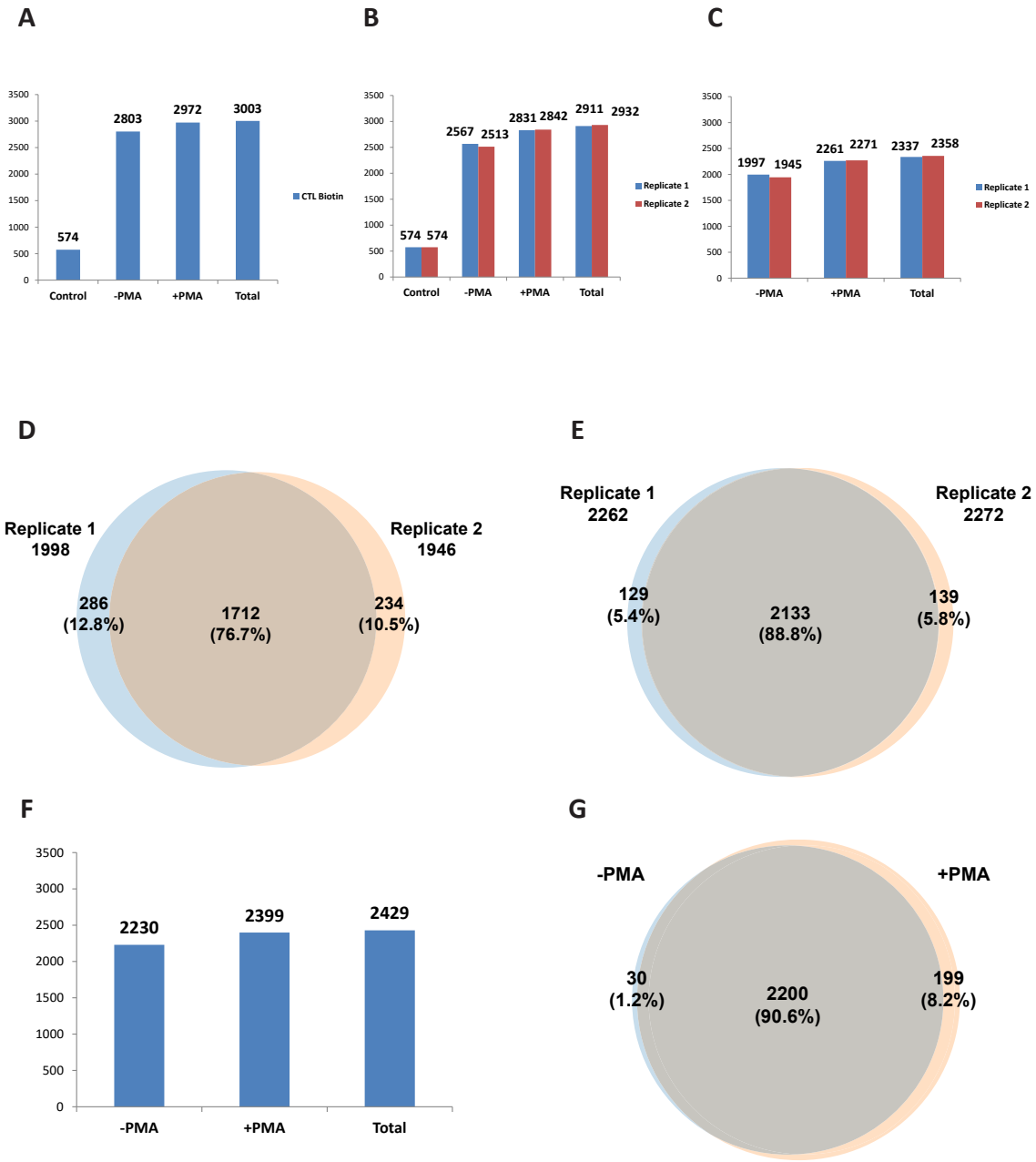

Figure 22: Results of shotgun analysis of mouse CTL.
(A) Total numbers of proteins per treatment, combining the two replicates. **(B)** Representation of the two replicates, the same control was used for both. **(C)** Treatments with the differentiated replicates, once the control proteins were subtracted. **(D)** Reproducibility between replicates. **(E)** Treatments without control proteins including both replicates. **(F)** Overlap between treatment with and without PMA.

2.4. Study of PMA on CTL: GO representation of proteomic results

Then we analyzed the distribution of the subcellular localization of the detected proteins by proteomics using the GO categories (Figure 23). Our results showed a proportion of cell surface proteins and plasma membrane similar to those obtained in Jurkat T cells,

although slightly with better results. There were no large differences between common proteins for both treatments and proteins that were only detected in the absence or presence of PMA. These differences could be explained by alterations due to the small number of proteins in these cases. We also expected some overlap between GO categories.

	Total		Common -+PMA		-PMA		+PMA	
NUCLEAR	1177	48%	1064	48%	14	47%	99	50%
CYTOPLASM	1098	45%	988	45%	18	60%	92	46%
PLASMA MEMBRANE	691	28%	632	29%	10	33%	49	25%
CELL SURFACE	145	6%	140	6%	1	3%	4	2%
PERINUCLEAR	208	9%	180	8%	6	20%	22	11%
GOLGI COMPLEX	150	6%	131	6%	2	7%	17	9%
ENDOPLASMIC RETICULUM	240	10%	226	10%	4	13%	10	5%
ENDOSOME	102	4%	92	4%	1	3%	9	5%
MITOCHONDRIAL	394	16%	349	16%	3	10%	42	21%
PEROXISOME	37	2%	32	1%	1	3%	4	2%
CYTOSKELETON	187	8%	165	8%	3	10%	19	10%
EXTRACELLULAR	559	23%	521	24%	7	23%	31	16%
	2429		2200		30		199	

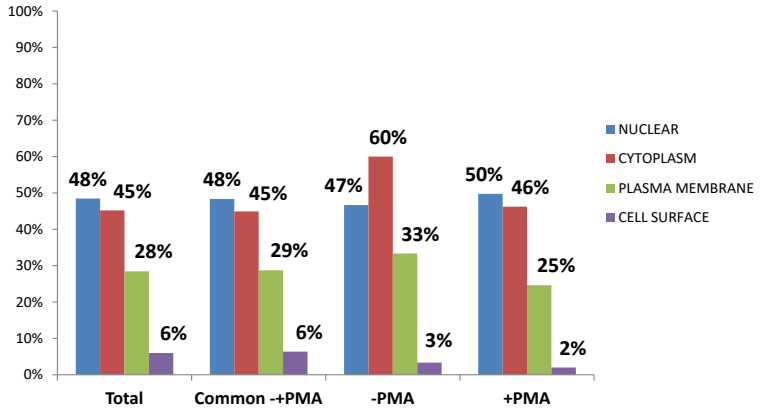

Figure 23: Subcellular protein distribution of mouse CTL according to GO terms.
The number of proteins and percentages associated with the main categories of GO of cellular component are represented. The percentages were similar to those obtained for Jurkat T cells. They also remained among proteins common in both treatments and those that were only detected in one of them.

2.5. PMA effect in CD proteins expression from mouse CTL

As we already did in experiments with Jurkat T cells, we checked the expression of proteins classified as cluster of differentiation, to evaluate the efficiency in the recovery of these surface molecules (Figure 24). We also obtained a snapshot of the expression of markers in membrane, to evaluate PMA-inducing changes. We could verify that the vast majority of markers were common in both replicates, including the expected CD8a and b, components of the TCR, costimulatory molecules like CD28 and activation markers like

CD44, CD69 or CD25. PMA dependent changes were not reproducible between the two replicates except for CD120b (TNFR2) that was found only in non-PMA treated samples. Changes in the replicates nonetheless identified TNF family of ligands or receptors as well as inhibitory checkpoints.

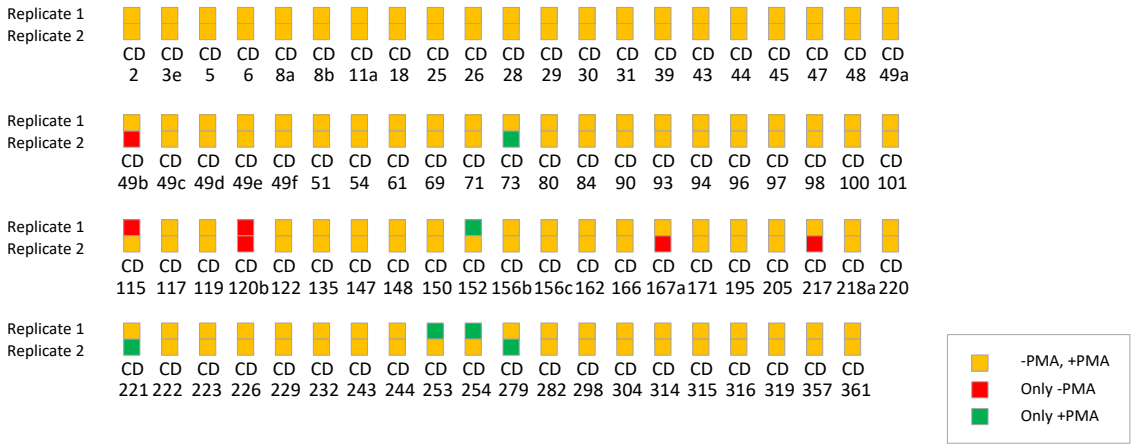

Figure 24: Identified CD proteins in mouse CTL biotinylation.
Drawing showing the expression in both replicates of the CD proteins. Orange indicates expression both in the presence and absence of PMA. In red are represented the proteins that would disappear when adding PMA, and in green those that would be expressed.

Study of CTL from DGKζ-deficient mice by biotinylation

In previous experiments we attempted to characterize changes in the CTL surfaceome in acute changes in DAG abundance, through the model of phorbol ester addition. These are rapid changes that may be due to phenomena such as the endocytosis/degradation of membrane proteins or shedding processes. The next step was to analyze changes in the CTL surfaceome from mice deficient in DGKζ, in which this deficit in DAG metabolism is sustained over time and may affect CTL differentiation. To this end, we used biotinylation to enrich cell surface proteins and proteomics to detect the expression of as many proteins as possible.

After following the same process to obtain differentiated CTL, we labeled with biotin, lysed and enriched through pull down with neutravidin. We analyzed the proteins present in the extract through shotgun proteomics (Figure 25) (Supplemental table 7). We detected in this case a greater amount of proteins in WT cells than in DGKζ deficient cells. This explains that the overlap between both treatments was less than other times, around 50%. Regarding the distribution of proteins according to the categories of GO, the percentage of proteins of plasma membrane and cell surface were slightly increased, and also an increase

A

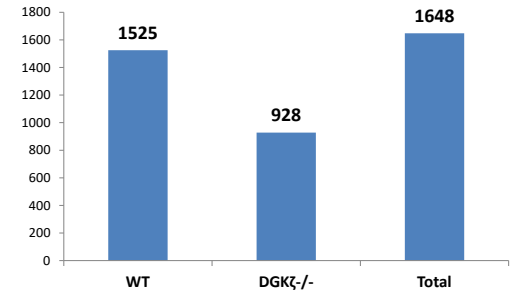

B

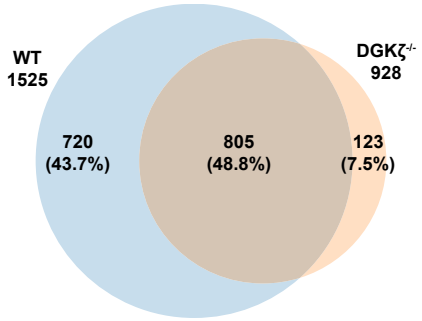

C

	Total		Common WT DGKζ$^{-/-}$		Only WT		Only DGKζ$^{-/-}$	
NUCLEAR	705	43%	368	46%	284	39%	53	43%
CYTOPLASM	794	48%	423	53%	295	41%	76	62%
PLASMA MEMBRANE	547	33%	274	34%	238	33%	35	28%
CELL SURFACE	139	8%	84	10%	48	7%	7	6%
PERINUCLEAR	150	9%	79	10%	52	7%	19	15%
GOLGI COMPLEX	113	7%	54	7%	49	7%	10	8%
ENDOPLASMIC RETICULUM	237	14%	107	13%	121	17%	9	7%
ENDOSOME	84	5%	38	5%	41	6%	5	4%
MITOCHONDRIAL	409	25%	188	23%	214	30%	7	6%
PEROXISOME	34	2%	9	1%	24	3%	1	1%
CYTOSKELETON	118	7%	60	7%	41	6%	17	14%
EXTRACELLULAR	689	42%	398	49%	262	36%	29	24%
	1648		805		720		123	

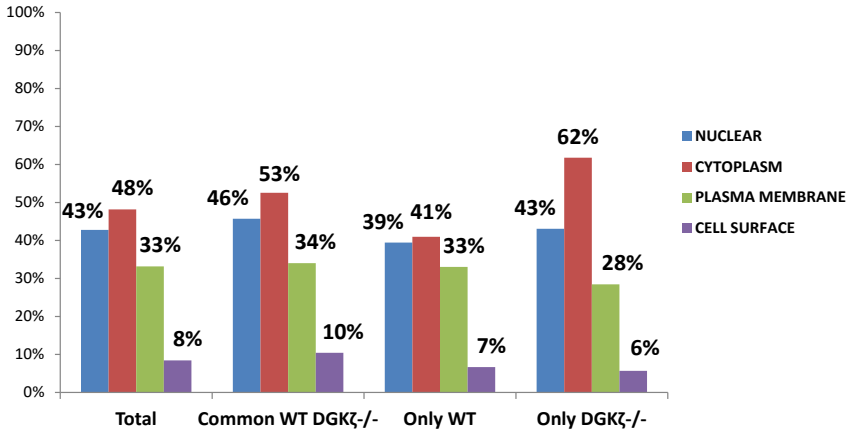

Figure 25: Shotgun analysis and subcellular protein distribution according to GO terms of mouse deficient in DGKζ

(A) Number of proteins detected in WT and DGKζ$^{-/-}$cells, as well as in total. **(B)** Overlap between the two cell types. **(C)** The distribution according to GO is shown below, in which the values of plasma membrane and cell surface were higher than in previous experiments.

in extracellular proteins can be observed.

Study of CTL from DGKζ-deficient mice by fractionation

To complete the biotinylation study we performed two fractionations comparing the WT and DGKζ$^{-/-}$ cells. Thus we analyzed mouse CTL with the other technique that we have tested in Jurkat T cells, and we amplified the knowledge about the surfaceome of these cells that we have. We differentiated in parallel the CTL of both mice and performed the frac-

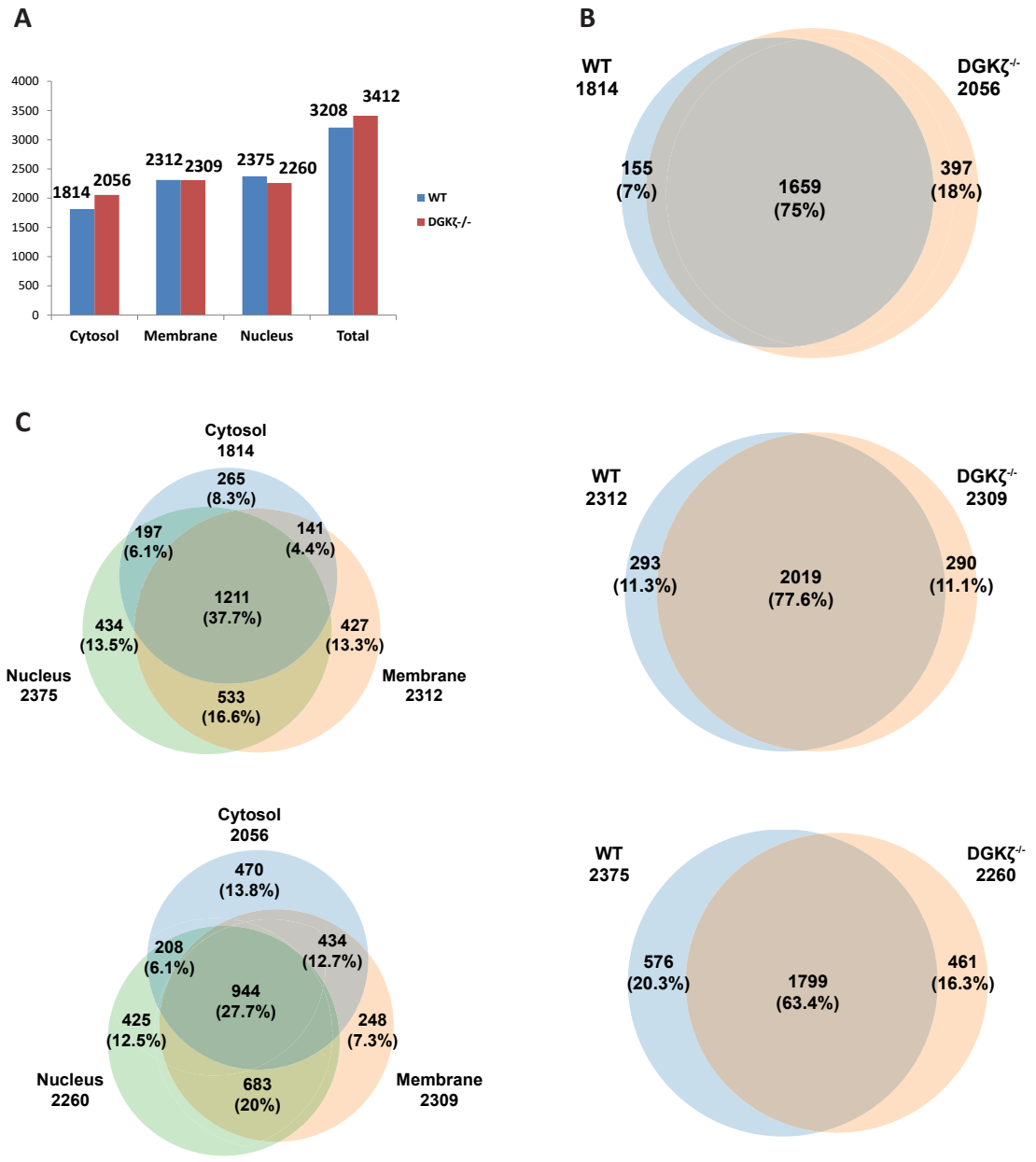

Figure 26: Shotgun analysis of fractionation of mouse deficient in DGKζ. **(A)** Number of proteins in total and in each fraction for WT and DGKζ$^{-/-}$ conditions. **(B)** Overlap of the three fractions between the two conditions, in cytosol **(top)**, membranes **(middle)** and nucleus **(bottom)** fractions. **(C)** Overlap within each condition between the three fractions, in WT **(top)** and in DGKζ$^{-/-}$ **(bottom)**.

tionation according to the instructions recommended by the manufacturer. We reserved a quantity of lysate from each fraction for proteomic analysis (Figure 26) (Supplemental

A

FRACTIONATION WT	Total		Fract. Cytosol		Fract. Membrane		Fract. Nucleus	
NUCLEAR	1571	49%	935	52%	992	43%	1305	55%
CYTOPLASM	1577	49%	1172	65%	1103	48%	1204	51%
PLASMA MEMBRANE	785	24%	370	20%	665	29%	514	22%
CELL SURFACE	158	5%	90	5%	138	6%	114	5%
PERINUCLEAR	288	9%	192	11%	214	9%	232	10%
GOLGI COMPLEX	199	6%	104	6%	163	7%	137	6%
ENDOPLASMIC RETICULUM	306	10%	106	6%	283	12%	201	8%
ENDOSOME	148	5%	95	5%	131	6%	94	4%
MITOCHONDRIAL	637	20%	227	13%	568	25%	411	17%
PEROXISOME	47	1%	20	1%	44	2%	31	1%
CYTOSKELETON	233	7%	164	9%	156	7%	190	8%
EXTRACELLULAR	1020	32%	766	42%	892	39%	806	34%
	3208		1814		2312		2375	

B

FRACTIONATION DGKζ$^{-/-}$	Total		Fract. Cytosol		Fract. Membrane		Fract. Nucleus	
NUCLEAR	1686	49%	1101	54%	1005	44%	1213	54%
CYTOPLASM	1666	49%	1291	63%	1093	47%	971	43%
PLASMA MEMBRANE	823	24%	375	18%	675	29%	544	24%
CELL SURFACE	163	5%	93	5%	144	6%	121	5%
PERINUCLEAR	311	9%	223	11%	217	9%	208	9%
GOLGI COMPLEX	211	6%	119	6%	161	7%	136	6%
ENDOPLASMIC RETICULUM	330	10%	117	6%	301	13%	235	10%
ENDOSOME	154	5%	108	5%	123	5%	89	4%
MITOCHONDRIAL	665	19%	229	11%	598	26%	465	21%
PEROXISOME	48	1%	16	1%	45	2%	30	1%
CYTOSKELETON	249	7%	179	9%	147	6%	189	8%
EXTRACELLULAR	1036	30%	778	38%	877	38%	647	29%
	3412	100%	2056	100%	2309	100%	2260	100%

C

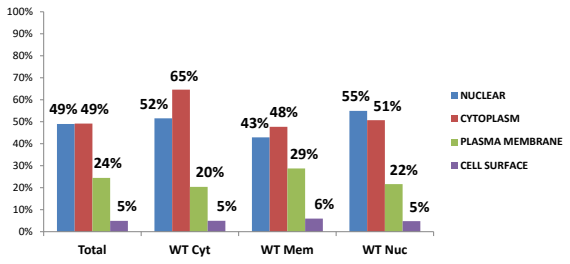

D

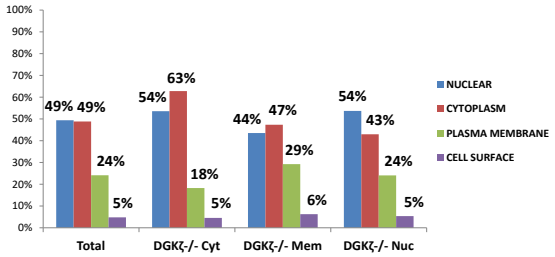

Figure 27: Subcellular protein distribution of WT and DGKζ$^{-/-}$ CTL fractionations according to GO terms.
(A and C) GO distribution of WT fractionation. **(B and D)** GO distribution of DGKζ$^{-/-}$ fractionation. In both cases the percentages were more similar to those obtained in Jurkat T cells, and were practically identical among them.

table 8). After the analysis we obtained more than 3000 proteins in total for each condition. In the case of the fraction of membranes we obtained more than 2000. If we compare between WT and DGKζ$^{-/-}$ for each fraction we found that the common proteins were mostly about 70%. Within each fractionation there was in turn a large overlap between fractions.

The distribution of GO terms was similar to that obtained during optimization with Jurkat T cells (Figure 27). The plasma membrane percentages in the membrane fraction were around 30%, while the cell surface fraction was 6%. More proteins were obtained in total, but the proportion of membrane proteins was lower.

We also verified the presence of CD antigens in WT and DGKζ$^{-/-}$ fractionations, as we did in Jurkat T cell (Figure 28). The membrane fraction collected again the majority of these proteins, although much of these were not exclusive, but overlap with other fractions.

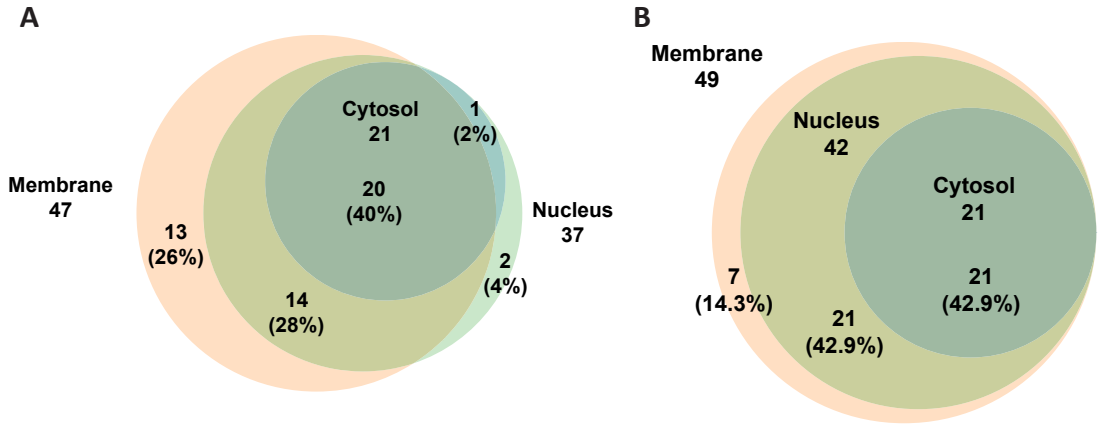

Figure 28: CD antigens overlapping in WT and DGKζ$^{-/-}$ fractionations.
Diagram depicting CD antigen overlap between different fractions, in WT **(A)** and DGKζ$^{-/-}$ **(B)**. Membrane fraction covered almost every CD antigen detected by proteomic analysis.

2.6. Summary of membrane proteins recovery in mouse cells

As we did when analyzing efficiency in Jurkat T cells, we collected in a table the results obtained from membrane proteins by fractionation and biotinylation in the different experiments with mouse cells (Table 4). The number of total proteins obtained was lower than in the case of Jurkat T cells. However in the case of biotinylation there was a similar number of membrane proteins, and higher of cell surface. The percentages of membrane and cell surface proteins were also higher in mouse, as well as the number of CD antigens. In the case of fractionation the total numbers were higher due to the large number of proteins detected, but the proportions were better in the case of the mouse cells.

Table 4: Summary report of plasma membrane proteins enrichment in mouse T cells. This table summarizes the number and percentages of proteins obtained in all the mouse experiments. The numbers of CD antigens in parentheses represent the total number of these proteins, rescuing those of the control treatment.

FRACTIONATION GEL	Complete		Jurkat biotinylation		Jurkat fractionation (membrane) Gel		Jurkat fractionation (membrane) RP	
NUCLEAR	4362		2126		4684		4801	
CYTOPLASM	922	21%	668	31%	1269	27%	1255	26%
PLASMA MEMBRANE	148	3%	81	4%	199	4%	204	4%
CELL SURFACE	34		39		62		56	

2.7. Expression of CD antigens in WT and DGKζ$^{-/-}$ CTL

We have previously studied the effect on rapid changes in DAG concentrations through the PMA addition model, without observing large differences in the expression of cell surface proteins. We next showed the expression of CD antigens obtained by prior enrichment by biotinylation or fractionation. In general a smaller number of them was detected, although the most characteristic CTL proteins are maintained. We detected some new proteins that we did not detect. There are divergences between both techniques, but comparing all the experiments we achieve a CD antigen expression profile that can give us an idea of the WT and DGKζ deficient CTL phenotypes (Figure 29).

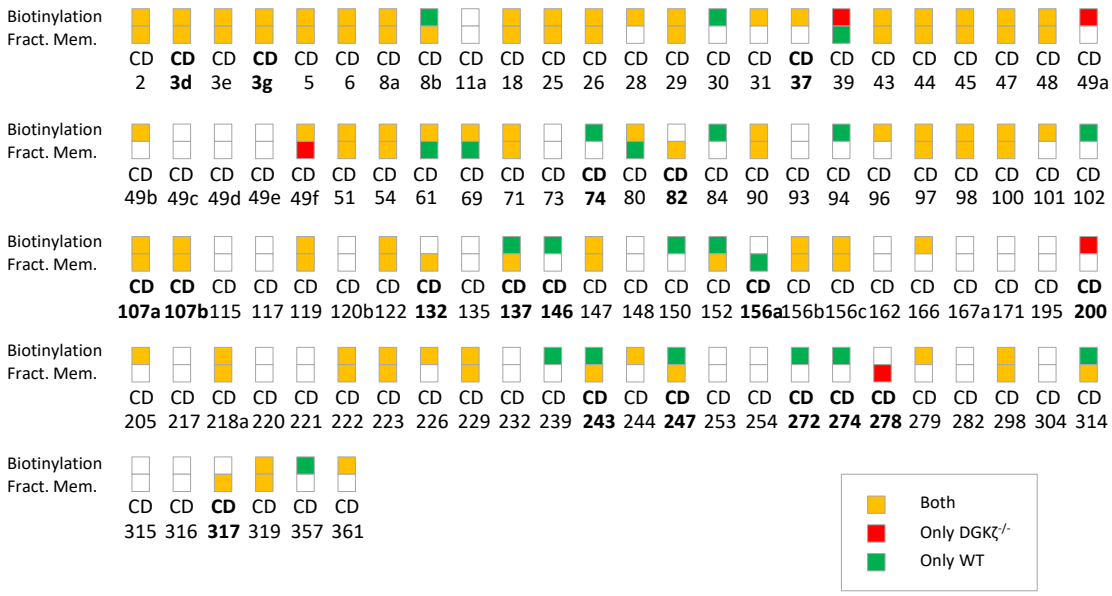

Figure 29: Identified CD antigens in mouse CTL WT and DGKζ$^{-/-}$.
The graphic depicts the CD antigen expression pattern in WT and DGKζ$^{-/-}$ cells. Orange indicates expression both in WT and DGKζ$^{-/-}$. Proteins detected only in WT and DGKζ$^{-/-}$ cells are represented in green and red, respectively.

2.8. Analysis of protein expression by flow cytometry

In the previous experiments we have analyzed by proteomics the global expression of cell surface proteins in CTL of mice deficient in DGKζ. Thanks to this, we have been able to perform an expression profile of CD antigens, checking which ones vary with respect to WT mice. These divergent proteins could explain the differences between the CTL of the two mouse strains. However, when proteomic analysis shows presence/absence of proteins, it is possible that the absence of expression may be a consequence of a detection problem (B. Zhang et al., 2006). To verify expression differences we validated our results by immunodetection of proteins by flow cytometry. We chose several markers of interest, which appear as differentially expressed in fractionation or biotinylation (Fig. 24). These were analyzed in differentiated CTL from OT-I mice in both WT and DGKζ$^{-/-}$. In addition, their expression was evaluated in DGKα$^{-/-}$ mice, which lack this other DGK isoform.

The results show that the expression profiles of the CD28, CD80 and PD-L1 proteins are very similar in both DGKζ$^{-/-}$ and DGKα$^{-/-}$ mice (Figure 30). The differences are very low both intra and interexperimentally, and when analyzing the differences in fluorescence emission statistically no significant differences were detected. In the case of the NKG2D and PD1 proteins (Figure 31), we observed there is more variation in percentages of cells expressing or not these markers, both within each treatment and between them. However, no significant differences were detected between WT, DGKα$^{-/-}$ and DGKζ$^{-/-}$ mice.

3. Quantitative proteomic analysis

3.1. Quantitative SILAC labeling

The different shotgun proteomic analyzes performed have allowed us to obtain an expression profile of the cell surface proteins of CTL from both WT and DGKζ deficient mice. However, when attempting to perform a comparative differential expression we have found limitations as lack of reproducibility in those proteins with less expression. It has also been shown that a study of absence/presence is not the best approximation to infer changes in expression between our two conditions, since apparent changes in expression have been found invaluable by other validation techniques. This is why a quantitative proteomic study was carried out to more accurately detect those proteins differentially expressed. The technique chosen was metabolic labeling by heavy isotope-labeled amino acids (SILAC) (Ong et al., 2002). In addition to detecting expression changes, the experimental variation is significantly reduced because of cells are marked during their expansion and are mixed before proteomic analysis.

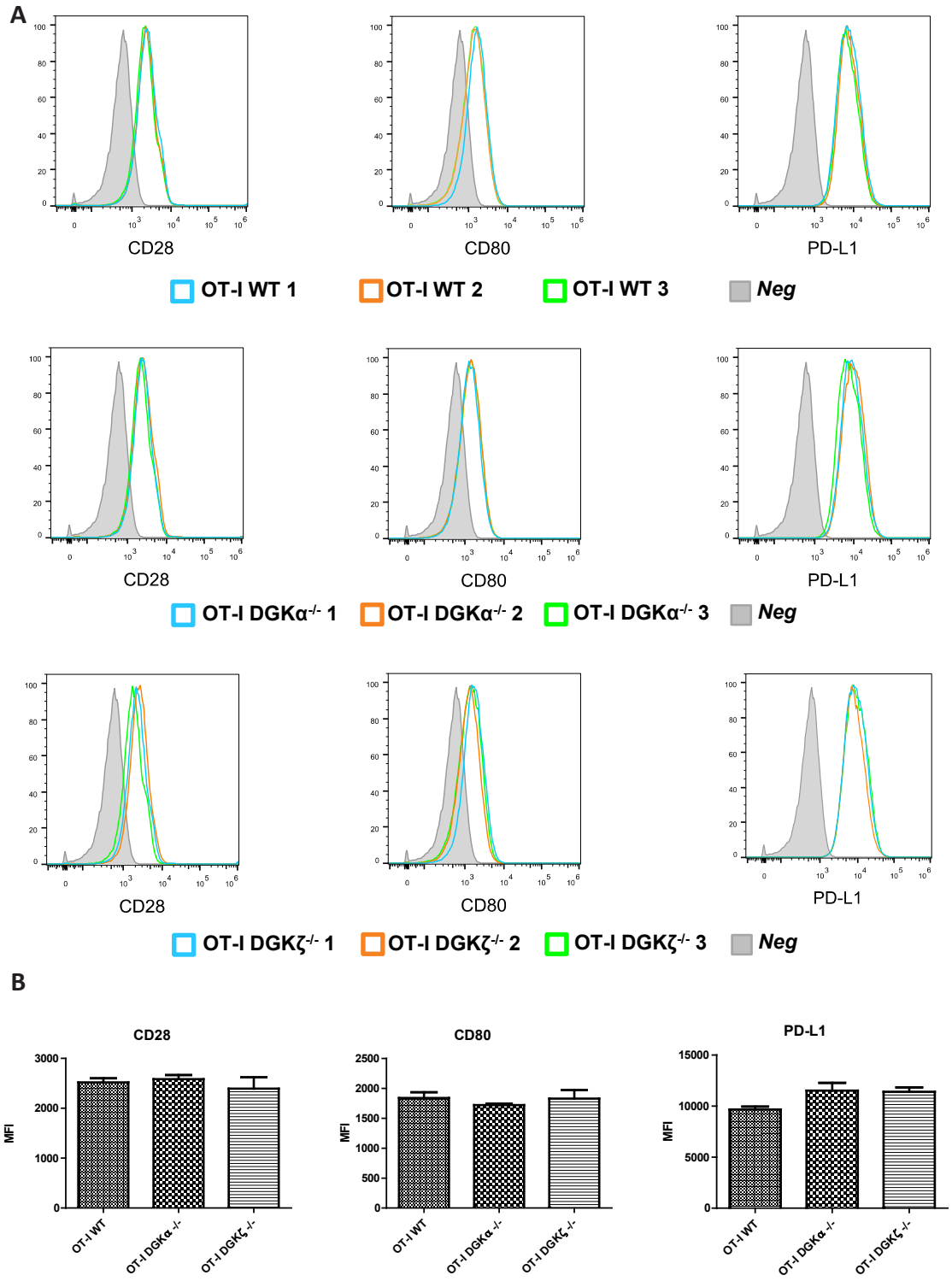

Figure 30: Validation of CD28, CD80 and PD-L1 expression in WT, DGKα$^{-/-}$ and DGKζ$^{-/-}$ mouse CTL by flow cytometry.
Cells extracted from OT-I WT, OT-I DGKα$^{-/-}$ and OT-I DGKζ$^{-/-}$ mouse lymph nodes were stimulated with OVA and differentiated in the presence of IL-2. **(A)** Expression profiles of CD28, CD80 and PD-L1. **(B)** Quantification of the MFI mean of the three experiments with SEM (n=3).

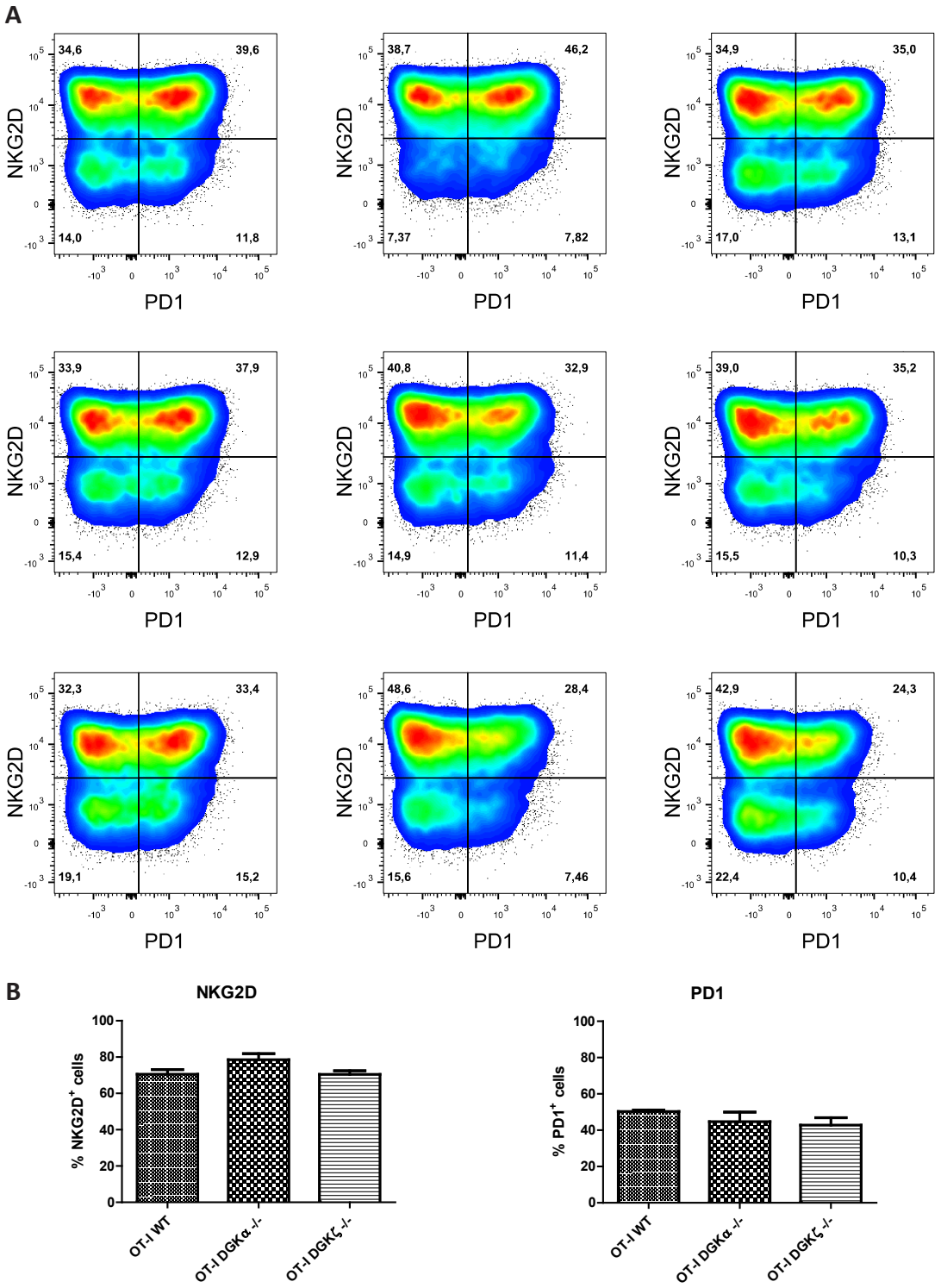

Figure 31: Validation of NKG2D and PD1 expression in WT, DGKα$^{-/-}$ and DGKζ$^{-/-}$ mouse CTL by flow cytometry.

As in the previous figure, mouse lymph node cells were extracted and then stimulated and differentiated with OVA and IL-2. A staining was used to compare the expression of both markers on cells of OT-I WT, OT-I DGKα$^{-/-}$ and OT-I DGKζ$^{-/-}$ mice. **(A)** Biparametric diagrams reflecting the percentages of simultaneous expression of NKG2D and PD1. **(B)** Quantification of mean percentages of NKG2D or PD1 expressing cells from the three experiments with SEM (n = 3).

For the SILAC analysis, CTL were differentiated from OT-I WT and DGKζ$^{-/-}$ mice. During differentiation, some cells from each mouse were cultured in normal medium and some in medium with SILAC-labeled amino acids (Figure 32A). At the end of the differentiation, WT and DGKζ$^{-/-}$ cells were mixed 1:1 with and without labeling, alternately to generate two replicates with labels exchanged for the two treatments. Once the cells were mixed, they were subcellularly fractionated as in previous experiments, and analyzed by mass spectrometry.

We evaluated the degree of labeling with heavy amino acids of Jurkat T cells over time (Figure 32B). We could assess that after the days of labeling in IL-2 almost all the proteins have exchanged their arginines and lysines for their heavy equivalents (R+6 and K+6). From day 4 the percentage of labeled spectra exceeded 95%, which ensures that CTL labeling is appropriate, since these cells undergo a very marked expansion phase in the presence of IL-2.

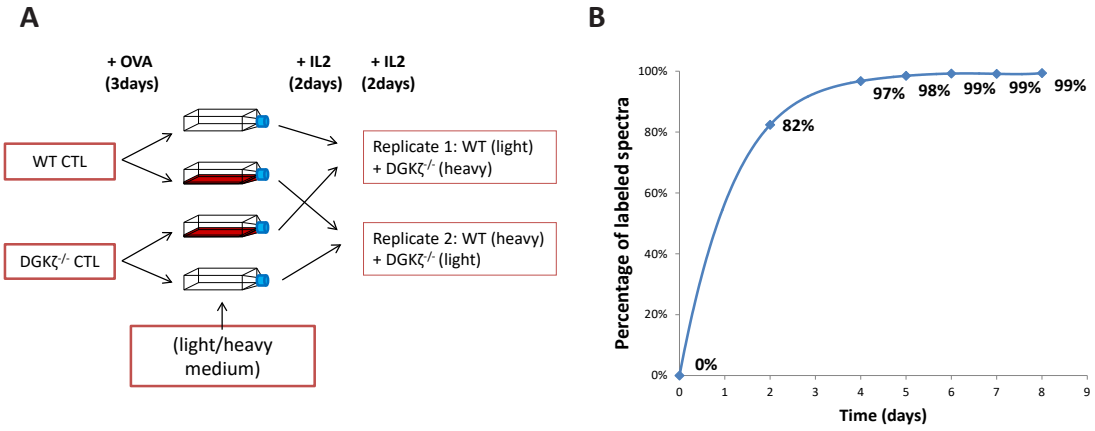

Figure 32: Experimental design for SILAC analysis of CTL WT KOζ fractionation.
(A) Scheme showing the experimental design for SILAC labeling. Cells extracted from mouse lymph nodes OT-I WT and OT-I DGKζ$^{-/-}$ were stimulated with OVA for 3 days and then cultured with IL-2 in the absence or presence of labeled amino acids (arginine and lysine). After this period, cells from alternative treatments were mixed in a 1:1 ratio and subcellular fractionation was performed as in previous analyzes. Cytosol, membrane and nuclear fractions were analyzed by LC-MS/MS. **(B)** Evolution of the labeling of Jurkat T cells when grown in medium with labeled arginine or lysine. The percentage of labeled spectra with at least one modification (K + 6 or R + 6) of all spectra exceeding a FDR <0.01 cutoff at the peptide level is plotted.

3.2. Shotgun proteomics and GO analysis of SILAC proteomic results

From the fractions obtained by subcellular fractionation of the two replicates we performed a study using LC-MS/MS similar to the previous ones. The results were quite sim-

ilar in terms of number of proteins and reproducibility with respect to CTL fractionation (Figure 33) (Supplemental table 9). The number of proteins detected was close to 3000 proteins and the overlap between the different fractions of the two replicates was around 70%.

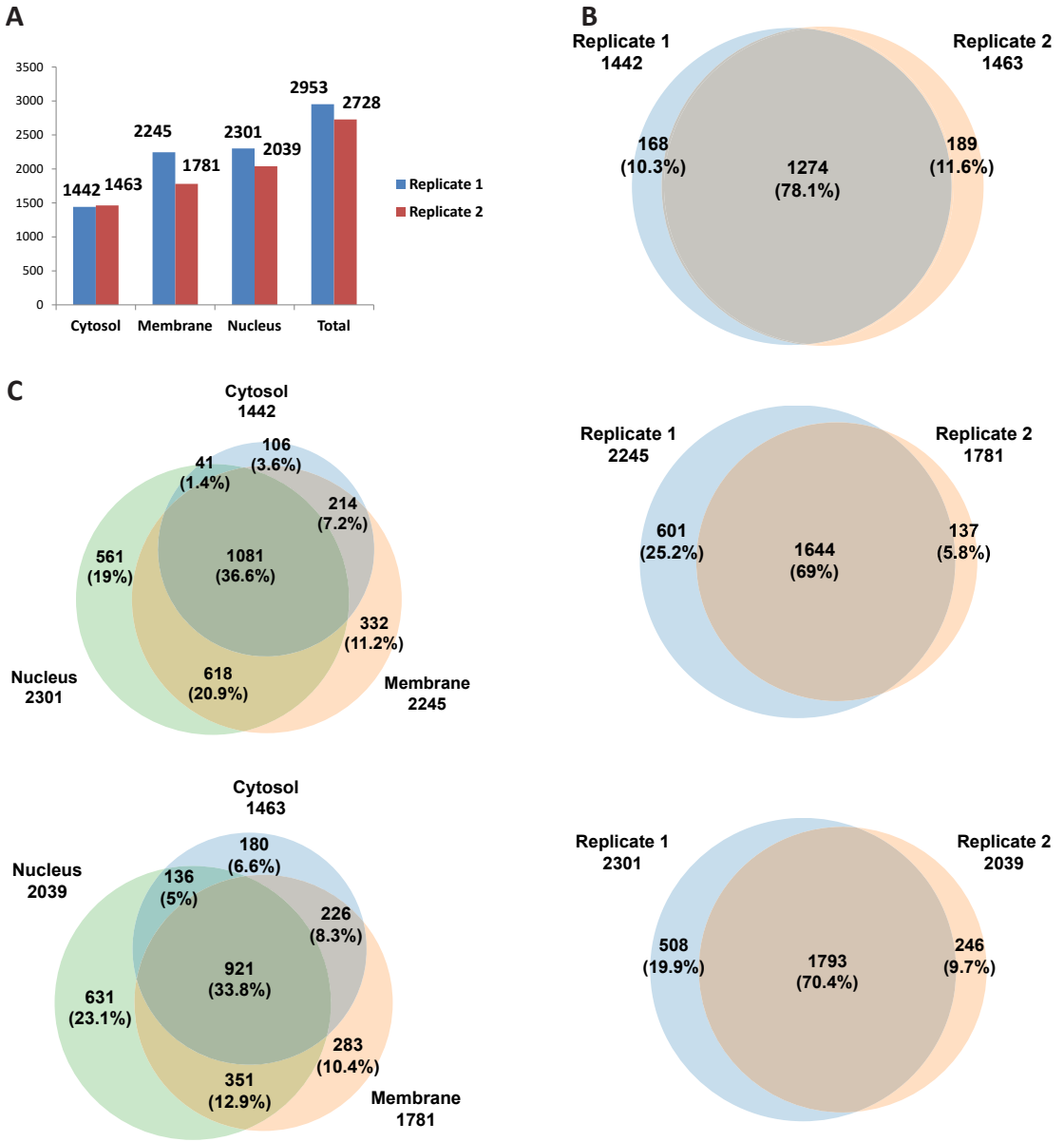

Figure 33: Shotgun proteomic of quantitative SILAC fractionation.
(A) Number of proteins in total and in each fraction for both SILAC replicates. **(B)** Overlap of the three fractions between the two conditions, in cytosol **(top)**, membranes **(middle)** and nucleus **(bottom)** fractions. **(C)** Overlap within replicate 1 **(top)** and replicate 2 **(bottom)** between the three fractions.

Regarding the distribution of proteins according to their classification by GO terms, the results are very similar again to the previous ones (Figure 34). The plasma membrane proteins represent a 28% in plasma membrane fraction, and 5-6% in the case of cell surface proteins.

A

	Total		Replicate 1 Cyt		Replicate 1 Mem		Replicate 1 Nuc	
NUCLEAR	1452	49%	753	52%	1025	46%	1207	52%
CYTOPLASM	1489	50%	972	67%	1183	53%	1145	50%
PLASMA MEMBRANE	751	25%	313	22%	623	28%	532	23%
CELL SURFACE	136	5%	84	6%	113	5%	95	4%
PERINUCLEAR	264	9%	158	11%	207	9%	211	9%
GOLGI COMPLEX	167	6%	74	5%	142	6%	119	5%
ENDOPLASMIC RETICULUM	313	11%	86	6%	279	12%	228	10%
ENDOSOME	135	5%	48	3%	113	5%	100	4%
MITOCHONDRIAL	559	19%	182	13%	457	20%	461	20%
PEROXISOME	44	1%	19	1%	40	2%	33	1%
CYTOSKELETON	235	8%	137	10%	163	7%	190	8%
EXTRACELLULAR	977	33%	698	48%	879	39%	784	34%
	2953		1442		2245		2301	

B

	Total		Replicate 2 Cyt		Replicate 2 Mem		Replicate 2 Nuc	
NUCLEAR	1377	50%	769	53%	861	48%	1119	55%
CYTOPLASM	1425	52%	985	67%	988	55%	1056	52%
PLASMA MEMBRANE	646	24%	309	21%	497	28%	411	20%
CELL SURFACE	123	5%	79	5%	101	6%	86	4%
PERINUCLEAR	261	10%	156	11%	187	10%	197	10%
GOLGI COMPLEX	150	5%	77	5%	118	7%	97	5%
ENDOPLASMIC RETICULUM	259	9%	84	6%	219	12%	159	8%
ENDOSOME	119	4%	51	3%	86	5%	80	4%
MITOCHONDRIAL	502	18%	176	12%	324	18%	404	20%
PEROXISOME	35	1%	17	1%	29	2%	25	1%
CYTOSKELETON	227	8%	138	9%	139	8%	183	9%
EXTRACELLULAR	934	34%	689	47%	738	41%	738	36%
	2728		1463		1781		2039	

C

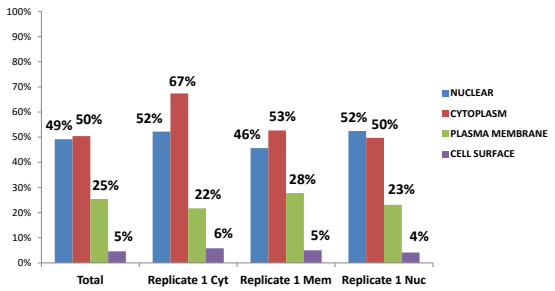

D

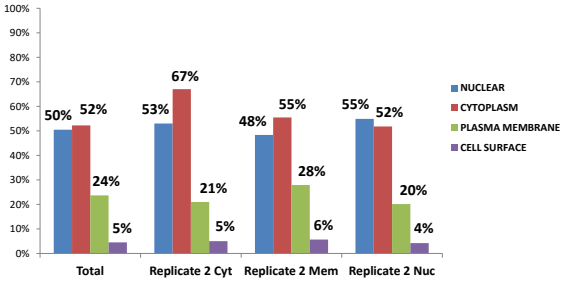

Figure 34: Subcellular protein distribution of WT and DGKζ$^{-/-}$ CTL SILAC fractionations according to GO terms.
Percentages of proteins classified according to GO terms, in replicate 1 **(A and C)** and replicate 2 **(B and D)**. The results were almost identical between both replicates.

3.3. Quantitative SILAC analysis

The bioinformatic quantitative analysis was carried out by Proteobotics S.L (Supplemental table 10). During this process from the data obtained through LC-MS/MS, searches were performed against databases using various search engines. The program algorithm was able to identify pairs of peaks for the same peptides with and without SILAC labeling, and to establish a quantitative relationship between them. Possible experimental alterations of the 1:1 ratio were avoided by normalizing the data obtained from the replicates for each fraction (Figure 35A). The quantitative results were represented according to their probability and the difference in expression between the WT and DGKζ$^{-/-}$ (Figure 35B, C). We observed that most of the proteins showed the same distribution in CTL from WT and the DGKζ$^{-/-}$ mice. We could however identify a signature of proteins with specific enrichment in the plasma membrane fraction of the DGKζ$^{-/-}$ CTL compared to WT, and the same situation occurs in nucleus fraction. Within the proteins that present a differential regulation, we focused our attention on the proteins that possessed the highest statistical confidence, both in the case of the membrane fraction (Table 5) and in the case of the nucleus fraction (Table 6).

Table 5: Proteins with confident up- or downregulation in membrane fraction. This table collects all the proteins that experienced up- and downregulation in the membranes fraction. The table shows the number of replicates in which they are detected, the number of peptides detected, the contrast performed and the type of differential regulation, the fold change in logarithmic scale, the FDR value, the protein ID and its description. Green and red colors indicate the DGKζ$^{-/-}$ upregulated and downregulated proteins, respectively.

Replicates	Peptides	Contrast	Diff. regulation	Log_2 Fold	p-value	FDR contrast	Inferred IDs	Description
2	7	DGKζ$^{-/-}$/WT	confident up	0.81	1.0e-006	0.00	P08882	Granzyme C
1	1	DGKζ$^{-/-}$/WT	confident up	6.87	1.0e-006	0.00	P11247	Myeloperoxidase
2	3	DGKζ$^{-/-}$/WT	confident up	0.66	1.0e-006	0.00	P18242	Cathepsin D
2	11	DGKζ$^{-/-}$/WT	confident up	0.86	1.0e-006	0.00	P04187	Granzyme B(G,H)
1	1	DGKζ$^{-/-}$/WT	confident up	1.12	4.1e-005	0.00	Q62418	Drebrin-like protein
2	5	DGKζ$^{-/-}$/WT	confident up	0.57	1.2e-004	0.01	P16110	Galectin-3
1	1	DGKζ$^{-/-}$/WT	confident up	1.75	2.0e-004	0.01	P11032	Granzyme A
1	1	DGKζ$^{-/-}$/WT	confident down	-11.55	1.0e-006	0.00	Q8R3C6	Probable RNA-binding protein 19
1	1	DGKζ$^{-/-}$/WT	confident down	-10.98	1.0e-006	0.00	Q61941	NAD(P) transhydrogenase, mitochondrial
1	1	DGKζ$^{-/-}$/WT	confident down	-4.07	1.0e-006	0.00	Q6PB44	Tyrosine-protein phosphatase non-receptor type 23
1	1	DGKζ$^{-/-}$/WT	confident down	-5.99	1.0e-006	0.00	O35929	GTP-binding protein REM 1
2	2	DGKζ$^{-/-}$/WT	confident down	-0.86	1.2e-004	0.01	Q9CYG7	Mitochondrial import receptor subunit TOM34
1	1	DGKζ$^{-/-}$/WT	confident down	-1.72	2.0e-004	0.01	P21995	Embigin

A

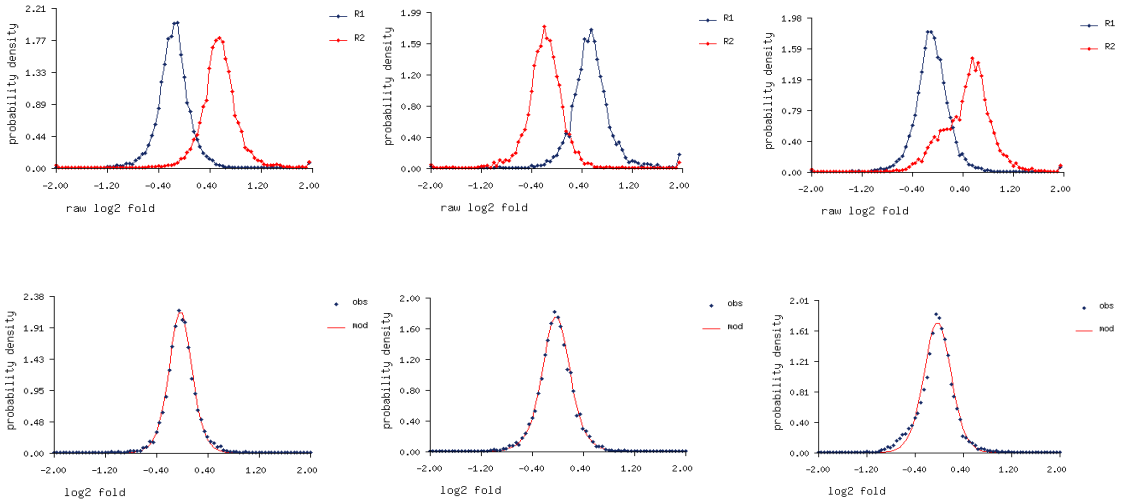

B

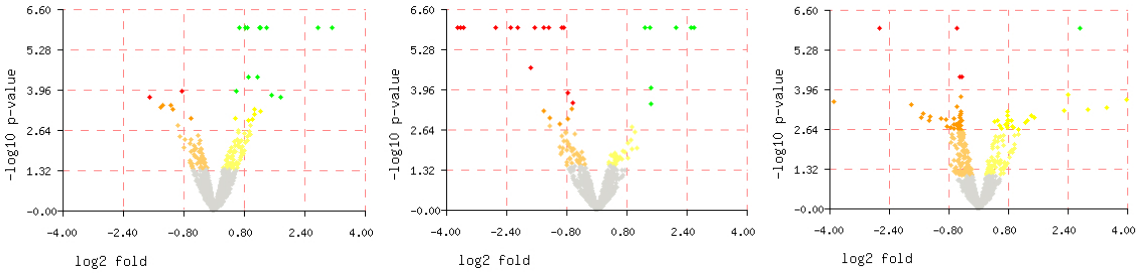

C

Differential regulation	DGKζ$^{-/-}$/ WT Membrane
Confident up	16
Likely up	6
Putative up	65
None	1689
Putative down	57
Likely down	5
Confident down	15
Total	1853

Differential regulation	DGKζ$^{-/-}$/ WT Nucleus
Confident up	14
Likely up	0
Putative up	27
None	1482
Putative down	40
Likely down	5
Confident down	26
Total	1594

Differential regulation	DGKζ$^{-/-}$/ WT Cytosol
Confident up	2
Likely up	26
Putative up	70
None	1273
Putative down	109
Likely down	36
Confident down	6
Total	1522

Figure 35: Quantitative SILAC analysis of subcellular fractions.
(A) The results obtained in membrane **(left)**, nucleus **(center)** and cytosol **(right)** fractions by analyzing the LC-MS/MS data were normalized to fit the probability model for a 1:1 ratio between the two treatments (WT and DGKζ$^{-/-}$) in every replicate. This normalization was applied to all fractions of the two inverse labeling replicates. **(B)** Volcano plots showing the differential expression between the WT and DGKζ$^{-/-}$ proteins for each of the fractions. The data were obtained from the two replicates of each fraction. The magnitude of the change in the expression is represented, as well as the probability that it is real. **(C)** Categorization of the total proteins detected by the analysis according to the probability of differential expression.

Table 6: Proteins with confident up- or downregulation in nuclear fraction. As in the previous table, here we collect all the proteins that experienced up- and downregulation in the nuclear fraction. The table shows the number of replicates in which they are detected, the number of peptides detected, the contrast performed and the type of differential regulation, the fold change in logarithmic scale, the FDR value, the protein ID and its description. Green and red colors indicate the DGKζ$^{-/-}$ upregulated and downregulated proteins, respectively.

Replicates	Peptides	Contrast	Diff. regulation	Log_2 Fold	p-value	FDR contrast	Inferred IDs	Description
1	1	DGKζ$^{-/-}$/WT	confident up	7.28	1.0e-006	0.00	J3QPY6	Protein Gm21957
1	1	DGKζ$^{-/-}$/WT	confident up	2.50	1.0e-006	0.00	P25976	Nucleolar transcription factor 1
1	1	DGKζ$^{-/-}$/WT	confident up	4.44	1.0e-006	0.00	P47968	Ribose-5-phosphate isomerase
2	5	DGKζ$^{-/-}$/WT	confident up	1.40	1.0e-006	0.00	Q00PI9	Heterogeneous nuclear RNP-U-like protein 2
1	1	DGKζ$^{-/-}$/WT	confident up	1.42	3.4e-004	0.01	Q61035	Histidine--tRNA ligase, cytoplasmic
1	1	DGKζ$^{-/-}$/WT	confident up	1.42	1.0e-004	0.00	Q8BQ30	Phostensin
1	2	DGKζ$^{-/-}$/WT	confident up	1.28	1.0e-006	0.00	Q8CIE6	Coatomer subunit alpha
1	4	DGKζ$^{-/-}$/WT	confident up	2.57	1.0e-006	0.00	Q99L45	Eukaryotic translation initiation factor 2 subunit 2
1	1	DGKζ$^{-/-}$/WT	confident up	5.88	1.0e-006	0.00	Q9QWR8	Alpha-N-acetylgalactosaminidase
1	1	DGKζ$^{-/-}$/WT	confident down	-3.56	1.0e-006	0.00	D3Z6Q9	Bridging integrator 2
1	1	DGKζ$^{-/-}$/WT	confident down	-4.39	1.0e-006	0.00	O08664	B-cell CLL/lymphoma 7 protein family member C
1	1	DGKζ$^{-/-}$/WT	confident down	-7.05	1.0e-006	0.00	O35929	GTP-binding protein REM 1
2	9	DGKζ$^{-/-}$/WT	confident down	-0.95	1.0e-006	0.00	P04187	Granzyme B(G,H)
2	4	DGKζ$^{-/-}$/WT	confident down	-1.67	1.0e-006	0.00	P11032	Granzyme A
2	3	DGKζ$^{-/-}$/WT	confident down	-0.66	3.0e-004	0.01	P16045	Galectin-1
1	2	DGKζ$^{-/-}$/WT	confident down	-3.72	1.0e-006	0.00	P18155	Bifunctional methylenetetrahydrofolate dehydrogenase/cyclohydrolase, mitochondrial
2	5	DGKζ$^{-/-}$/WT	confident down	-0.78	1.4e-004	0.01	P42225	Signal transducer and activator of transcription 1
2	1	DGKζ$^{-/-}$/WT	confident down	-1.43	1.0e-006	0.00	P53994	Ras-related protein Rab-2A
2	2	DGKζ$^{-/-}$/WT	confident down	-2.30	1.0e-006	0.00	P56395	Cytochrome b5
1	1	DGKζ$^{-/-}$/WT	confident down	-5.50	1.0e-006	0.00	P62748	Hippocalcin-like protein 1
2	2	DGKζ$^{-/-}$/WT	confident down	-1.28	1.0e-006	0.00	Q62351	Transferrin receptor protein 1
1	1	DGKζ$^{-/-}$/WT	confident down	-1.78	2.1e-005	0.00	Q8BJS4	SUN domain-containing protein 2
1	1	DGKζ$^{-/-}$/WT	confident down	-2.72	1.0e-006	0.00	Q9CZX9	ER membrane protein complex subunit 4
1	1	DGKζ$^{-/-}$/WT	confident down	-5.09	1.0e-006	0.00	Q9D4H7	LON peptidase N-terminal domain and RING finger protein 3
1	1	DGKζ$^{-/-}$/WT	confident down	-4.20	1.0e-006	0.00	Q9WV30	Nuclear factor of activated T-cells 5

To help understand the role of these proteins, we performed a functional study using DAVID (Huang et al., 2009b) and graphically represented it by EnrichmentMap plugging of Cytoscape (Merico et al., 2010) (Figure 36). There was a significant presence of lytic proteins related to cytotoxicity such as granzymes A, B and C and myeloperoxidase, as well as components of lysosomes such as cathepsins, drebrin-like protein, and regulators of apoptosis such as galectin. In the case of DGKζ$^{-/-}$ cells these proteins increased in the membrane fraction. Since many of these proteins are present in granules, this points to differences in degranulation processes between WT and DGKζ$^{-/-}$ cells.

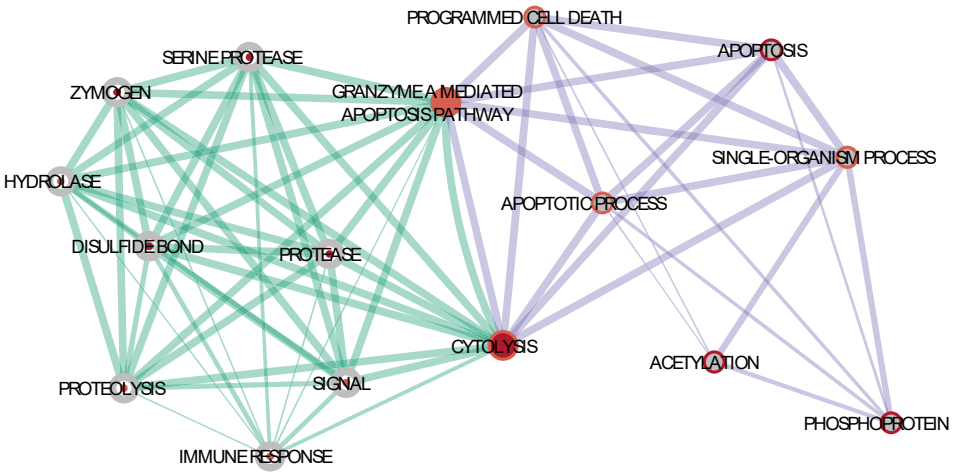

Figure 36: Functional analysis of SILAC subcellular fractions.
We performed a DAVID functional annotation analysis of confident regulated proteins for biological process from GO, pathways from Biocarta and keywords from Uniprot, with a p-value cutoff of 0.05, and represented it by Enrichment Map plug-in of Cytoscape. Bigger nodes indicate greater number of proteins assigned. The inner ring of each node refers to membrane fraction proteins, while the outer ring refers to the nucleus fraction. The more red color the nodes have, the more significant the enrichment for that category is. Thicker edges mean higher protein overlap between two categories. The edges are green or purple depending on if they bind proteins from the membrane or nucleus fractions, respectively. Results show an overrepresentation of proteins related with cytotoxicity.

When filtering by proteins of cluster of differentiation, we verified that the majority of these proteins did not present changes in the differential expression (Table 7). Only some of them presented changes, and they were not always included in the confident category of the analysis. For example, the transferrin receptor (CD71) was increased in the membrane fraction in DGKζ$^{-/-}$ cells. This can be interpreted as a lower internalization of this receptor. This situation corresponds to previously observed data on the transferrin receptor traffic in DGKζ deficient Jurkat T cells (Rincon et al., 2007), which provides solidity to our experimental model.

Table 7: CD proteins detected in SILAC analysis. The CD proteins detected in the membrane, cytosol and nucleus fractions are classified according to the confidence observed in their differential regulation (from major to minor, confident, likely, and putative). The proteins with the greatest expression in DGKζ$^{-/-}$ CTL versus WT are represented in green, and those whose expression is lower in red. CD proteins with no evidence of differential regulation are shown in gray.

	Membrane		Cytosol		Nucleus	
	CD	Description	CD	Description	CD	Description
Confident					CD71	Transferrin receptor protein 1
Likely	CD71	Transferrin receptor protein 1	CD8b	T-cell surface glycoprotein CD8 β chain		
			CD71	Transferrin receptor protein 1		
Putative	CD3e	T-cell surface glycoprotein CD3 ε chain	CD11a	Integrin α-L	CD3e	T-cell surface glycoprotein CD3 ε chain
	CD298	Sodium/potassium-transporting ATPase subunit β-3	CD18	Integrin β-2		
	CD43	Leukosialin	CD98	4F2 cell-surface antigen heavy chain		
	CD45	Receptor-type tyrosine-protein phosphatase C	CD223	Lymphocyte activation gene 3 protein		
			CD229	T-lymphocyte surface antigen Ly-9		
None	CD3d	T-cell surface glycoprotein CD3 δ chain	CD3d	T-cell surface glycoprotein CD3 δ chain	CD25	IL-2 receptor subunit α
	CD18	Integrin β-2	CD25	IL-2 receptor subunit α	CD45	Receptor-type tyrosine-protein phosphatase C
	CD25	IL-2 receptor subunit alpha	CD43	Leukosialin	CD90	Thy-1 membrane glycoprotein
	CD44	CD44 antigen	CD44	CD44 antigen	CD98	4F2 cell-surface antigen heavy chain
	CD45	Receptor-type tyrosine-protein phosphatase C	CD45	Receptor-type tyrosine-protein phosphatase C	CD222	Cation-independent mannose-6-phosphate receptor
	CD90	Thy-1 membrane glycoprotein	CD47	Leukocyte surface antigen CD47	CD223	Lymphocyte activation gene 3 protein
	CD98	4F2 cell-surface antigen heavy chain	CD48	CD48 antigen	CD229	T-lymphocyte surface antigen Ly-9
	CD100	Semaphorin-4D	CD51	Integrin α-V	CD247	T-cell surface glycoprotein CD3 ζ chain
	CD222	Cation-independent mannose-6-phosphate receptor	CD84	SLAM family member 5		
	CD223	Lymphocyte activation gene 3 protein	CD90	Thy-1 membrane glycoprotein		
			CD100	Semaphorin-4D		
			CD298	Sodium/potassium-transporting ATPase subunit β-3		

4. CTL CYTOLITIC GRANULES ANALYSIS

Our quantitative proteomics studies using SILAC have allowed us to find changes in protein expression between CTL obtained from DGKζ$^{-/-}$ and WT mice, including protein components of cytotoxic granules. These changes have been increased for DGKζ$^{-/-}$ CTL in the case of the fraction of membrane, which can point to differences in number of secretory lysosomes. To further explore this aspect, we carried out experiments with a probe that allows the monitoring of the lytic granules of cytotoxic cells. This probe, LTG, is a fluorescent molecule that is internalized in cellular compartments with acid pH as lysosomes (Chazotte, 2011). LTG has been used in previous studies to monitor cytotoxic granules of activated CD8+ cells (Shen et al., 2006). Thus, we can analyze the dynamics of these compartments and verify the existence of differences between our two conditions that may explain the data obtained by proteomics.

4.1. Titration of LTG

First, we performed an LTG titration to check different staining parameters. We used differentiated CTL using our standard protocol, and mixed cells from WT, DGKα$^{-/-}$ and DGKζ$^{-/-}$ mice to take into account the variability that might exist in the production of cytolytic granules under different conditions. We checked different concentrations of the probe, as well as the duration of the staining and if the staining medium was changed to PBS or it remained. The results showed that increasing concentration, time or keeping RPMI culture medium for staining yielded greater staining of cells (Figure 37A and Figure 37B). However, the largest differences were produced by the staining incubation medium. In the case we kept RPMI staining medium, the staining of the population was uniform and intense, while when we changed to PBS the variability reduced and the intensity of fluorescence increased.

To check the effect of LTG saturation on CTL labeling we performed a high and low LTG concentration in HBSS (similar to PBS) and in RPMI medium and analyzed by fluorescence microscopy (Figure 37E and Figure 37F). We can see how the saturation effect occurred mainly by incubation in RPMI medium, where there was staining not only of cytolytic granules but also of cytosol and other compartments such as Golgi. This saturation effect is not so marked when comparing high and low LTG concentration. We concluded that the best staining conditions were time of 2min, changing to PBS and concentration of 50nM LTG.

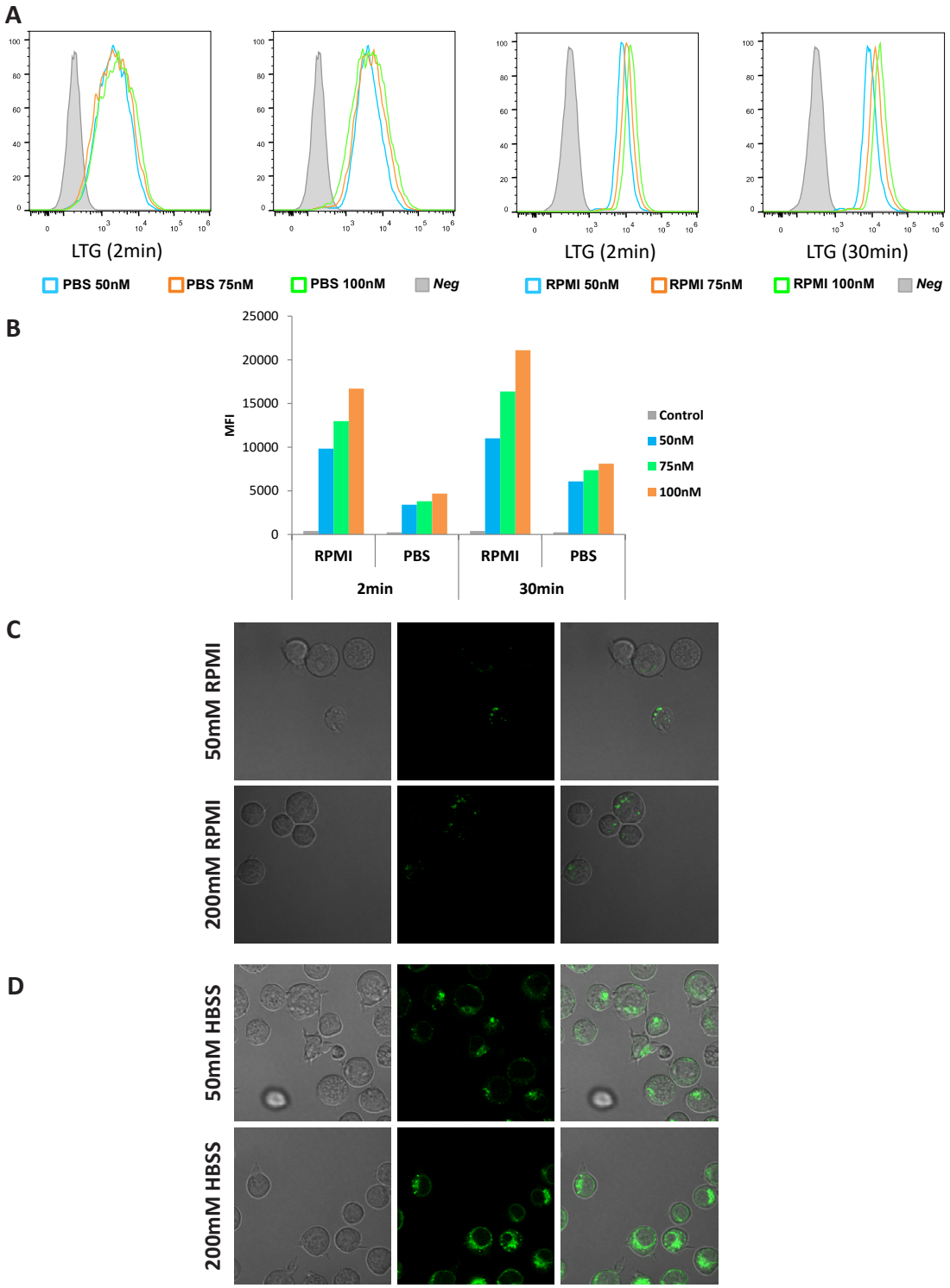

Figure 37: Lysotracker green titration in CTL.
(A) CTL stained with LTG were analyzed by flow cytometry to measure the fluorescence intensity of this dye. Differentiated CTL from mixed WT, DGKα$^{-/-}$ and DGKζ$^{-/-}$ mice were used for titration. Different staining conditions, such as time in the presence of dye (2 or 30min), and if the RPMI staining medium was changed to PBS or was kept, were evaluated. **(B)** Compilation of the MFI of the different titration experiments. **(C and D)** Confocal microscopy analysis of cytolytic granules staining of WT CTL, in RPMI medium **(C)** and HBSS **(D)**.

4.2. LTG labeling of CD4+ versus CD8+ cells

After optimizing the conditions for LTG staining, we studied the behavior of LTG over time for CD4+ and CD8+ cells obtained from mice deficient in DGKα or DGKζ, and stimulated with concanavalin A and IL-2. Thus, it is possible to check the formation of granules in CD8+ cells from activation to differentiation, with special interest in the effect of DGKα$^{-/-}$ and DGKζ$^{-/-}$ cells, as well as the behavior in CD4+, where generation of lysosomal granules has been reported (Shen et al., 2006). The results showed that at day 0 naïve cells remained with narrow LTG peaks, and that after three days of stimulation they had shifted, increasing the fluorescence intensity (Figure 38). However there were hardly any

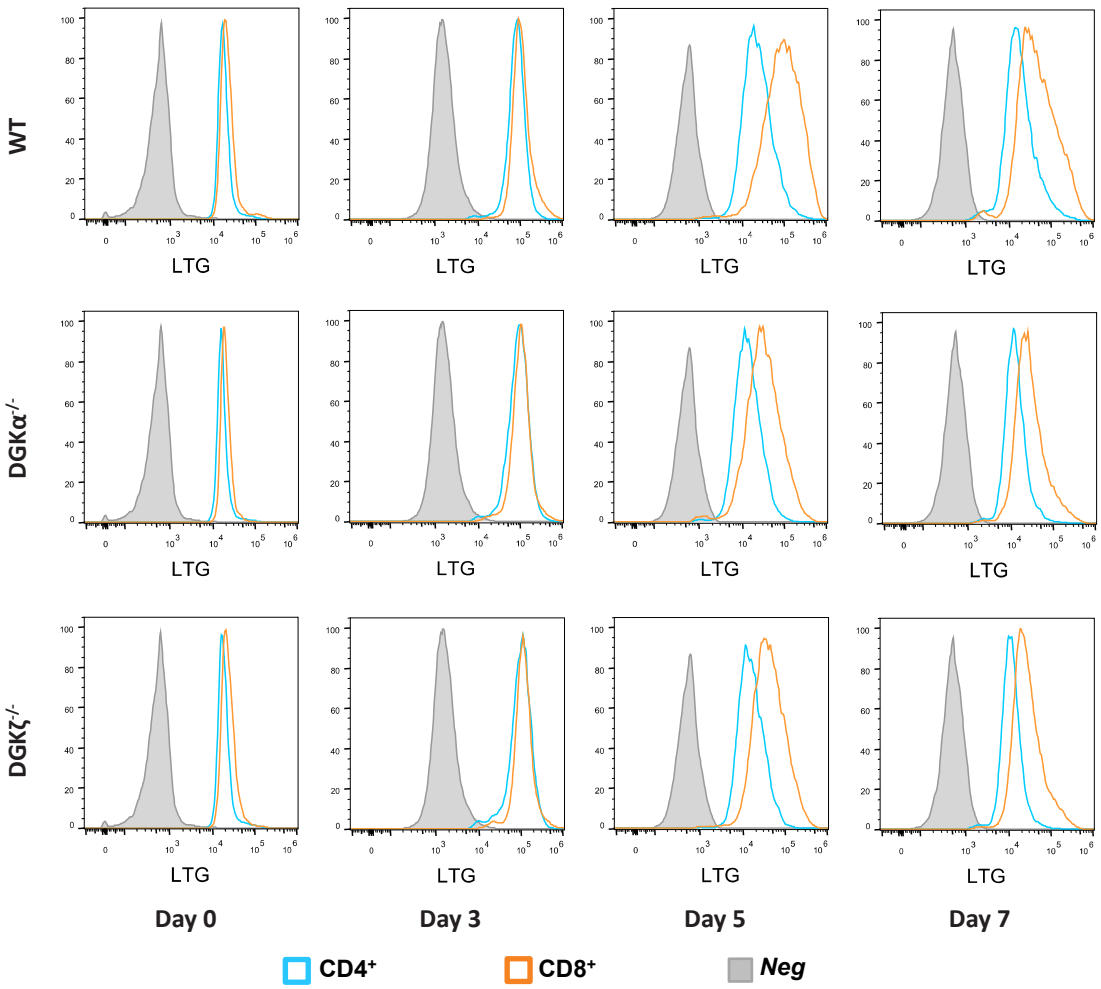

Figure 38: Evolution of LTG over time in CD4⁺ and CD8⁺ cells.
Splenocytes obtained from WT, DGKα$^{-/-}$ and DGKζ$^{-/-}$ mice were stimulated in vitro with concanavalin A for 48h, and then differentiated with IL-2. The cells were stained with anti-CD4 and CD8 antibodies, and then the fluorescence intensity of LTG was measured on cells stained in RPMI medium at 50nM and then transferred to PBS. When analyzing the results, we gated CD4 or CD8 populations of cells according to each case. For days 5 and 7 the acquisition protocol was modified, changing the voltage to avoid saturation of the signal for LTG.

differences between CD4+ and CD8+ cells. It is from day 5 when differentiation progressed and CD8+ cells showed greater intensity of LTG than CD4+ cells, differences that were already reduced to day 7. As in the titration we observed that WT cells had higher fluorescence intensity than in the case of DGKα$^{-/-}$ and DGKζ$^{-/-}$.

4.3. LTG labeling during CD8+ stimulation

In the previous experiment we analyzed the evolution of LTG labeling of CD4+ and CD8+ cells over time. Focusing on CD8+ cells, we observed that large changes in LTG expression occurred. For this reason, we analyzed in greater detail the changes in staining during secretory lysosomes development. From WT, DGKα$^{-/-}$ and DGKζ$^{-/-}$ cells obtained from OT-I mice we stimulated with the OVA peptide and monitored them during 8 days (Figure 39). The signal gradually increased until a large difference occurred on the third day, and then it grew gradually. When quantifying the fluorescence intensity, no significant differences were observed among WT, DGKα$^{-/-}$ and DGKζ$^{-/-}$.

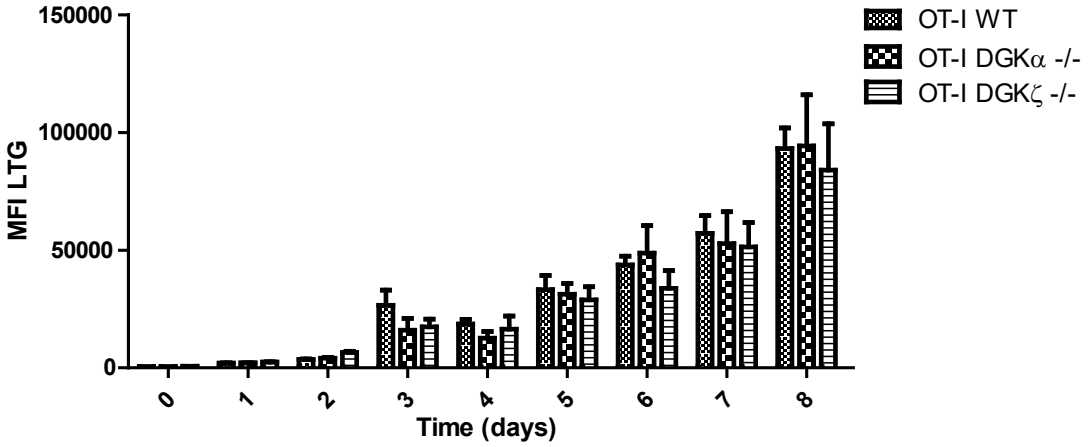

Figure 39: Evolution of LTG over time in CD8+ cells.
Cells extracted from lymph nodes of OT-I mice WT, DGKα$^{-/-}$ and DGKζ$^{-/-}$ were stimulated with the OVA peptide for 3 days, and then expanded with IL-2. LTG staining was performed every 24 hours to evaluate the development of cytolytic granules, according to the protocol used in previous experiments. A staining with anti-CD8 antibody was carried out to be able to gate the CD8+ population during first three days. The graph shows quantification of LTG mean fluorescence intensity of the three conditions (WT, DGKα$^{-/-}$ and DGKζ$^{-/-}$) with SEM (n = 3, two-way ANOVA).

DISCUSSION

Discussion

1. Optimization of plasma membrane protein enrichment methods

Characterization of the human proteome and the function of proteins was the next logical step after the determination of the human genome sequence (Kaiser, 2002). Currently, approximately 20,000 revised proteins are registered without considering isoforms (The UniProt Consortium, 2017). The enormous complexity of the proteome has made it necessary to subdivide it before its study in the case of strategies based on mass spectrometry. By following a targeted method for each subproteome it is possible to detect a larger number of proteins globally. In the case of membrane proteins using bioinformatic approaches it has been estimated that there are 4800 proteins with transmembrane domains, of which about 3700 belong to the cell surface; and 304 of the CD group are surface proteins, which represents an 85% (da Cunha et al., 2009). The combined study of several bioinformatics applications to predict transmembrane proteins retrieves about 5539 membrane proteins (Fagerberg et al., 2010). In Uniprot there are about 2300 proteins annotated as surface proteins (Bock et al., 2012), considering the total human proteome and not a particular cell lineage. With these limits in mind, we tried to determine as many of these proteins as possible in our study.

1.1. Biotinylation

To achieve our goal we must focus on studies on the CTL proteome (Hukelmann et al., 2016). In this work, a global analysis of the CTL proteome is performed with high resolution mass spectrometry. The number of protein groups obtained reaches 6800, from which there is a great difference in expression, since for example only 12 proteins represent 25% of the total proteome mass, with several orders of magnitude compared to the less frequent ones. In our study we obtained about 4359 by a single acquisition by mass spectrometry. By means of our biotinylation enrichment approach we were able to detect 2126 proteins, of which 668 were classified as plasma membrane proteins, which constitutes 31%. This represents a modest increase in plasma membrane proteins, as the total Jurkat lysate yielded 922 proteins, about 21%. In other words, despite the fact that contamination with other subcellular fractions is reduced, the number of plasma membrane proteins is lower than the total lysate, which indicates a loss of proteins in the enrichment process. The

number of proteins and the percentage reached in different studies varies according to the purification technique and the proteomic analysis. The most modest results are achieved with traditional proteomics techniques using two-dimensional gels and spot extraction, although the biotinylation enrichment process is similar (Peirce et al., 2004). In this work, the replacement of the gel isoelectric focusing by a solution allows to improve the results up to 74 membrane proteins out of 127 detected (58.3%). Among the shotgun proteomics works there is a great variety according to the enrichment strategy, from the use of sucrose gradient with about 220 plasma membrane proteins of 372 (59%) (Loyet et al., 2005), biotinylation with 48 of 391 (12.3%) (Ahram et al., 2005), or biocytin hydrazide with 81 of 87 splenocyte membrane proteins (93%) (Wollscheid et al., 2009). This last study was later improved by combining it with biotinylation, obtaining 538 membrane proteins from a total of 897 (60%) of acute myeloid leukemia cell lines (Hofmann et al., 2010). A number of studies in several cell lineages and purification methods yielded results of between 50% and 81% of plasma membrane proteins (Cordwell & Thingholm, 2010). In our case, we can affirm that although the number of plasma membrane proteins that we were able to detect is high, the proportion with respect to the total is lower than the studies cited. In the case of mouse T-lymphocytes this percentage remains similar in both splenocytes and CTL.

1.1.1. Alternative biotinylation approaches

In our study we implemented some strategies to improve the results obtained by biotinylation. These included the application of intensive high salt concentration washes to prevent the non-specific binding of proteins to complexes of biotinylated proteins and beads with neutravidine. While the application of additional washes may involve protein loss, it may improve plasma membrane protein percentages. However, the results obtained did not seem to differ. Similar results have been described with high salt washes, as well as with other strategies such as pleclearing, sucrose washing or Na2CO3 (Weekes et al., 2010), so we discarded this strategy.

Another optimization attempt was carried out by choosing a different biotin reagent including an internal disulfide bridge. This modification increases its molecular mass and favors the solubility of the molecule by reducing hydrophobicity, factors that hinder its ability to cross the plasma membrane and its internalization in the cytosol. Analysis of this undesired internalization of biotin by confocal microscopy showed no differences between two biotin molecules, although other studies have detected a reduction in permeability in the case of S-S-biotin with improved performance (Peirce et al., 2004). The use of this biotin does not ensure obtaining a great enrichment (Weekes et al., 2010). Although western blot analysis does seem to isolate a greater amount of a plasma membrane marker, the

transferrin receptor, the percentages of plasma membrane proteins are maintained in the following experiments in numbers similar to the original biotin. The use of S-S-biotin does not guarantee a good percentage of plasma membrane proteins. In addition, although the disulfide bridge could be used to recover proteins by a reduction treatment as indicated in the manufacturer's instructions, the highest yield is achieved by boiling the samples as in the original biotin. An advantage of the use of S-S-biotin, however, is that the loss of biotin moiety by the reduction of the disulfide bridge would avoid possible biotin interference in mass spectrometry detection, although part of the tag would still be present in the peptide (Markoutsa et al., 2014).

1.2. Fractionation

Another strategy developed in our study was to perform subcellular fractionation using a commercial kit from Calbiochem (Hwang & Han, 2013). With this tool it was possible to isolate cytosol, membrane and nuclear fractions. By means of western blot we verified how effectively each fraction was enriched with the proteins corresponding to each fraction. These results coincided with previous studies documenting a limited carry-over (Abdolzade-Bavil et al., 2004; Hwang & Han, 2013). However, the proteomic analysis showed a high level of overlap between the three fractions. This is possible, since although a protein belonging to a fraction is mostly retained in it, it can remains in other fractions in levels that can be detected by mass spectrometry. This phenomenon is observed when analyzing the presence of CD proteins. Although these proteins are detected in all three fractions, they are all contained in the membrane fraction, except in one case in RP-HPLC fractionation replicate. Likewise, limitations of the kit have been described when analyzing specific fractions, such as the case of the nuclear fraction (Murray et al., 2009).

By subcellular fractionation we obtained about 5594 proteins in Jurkat cells in SDS-PAGE replicate and about 5900 in RP-HPLC replicate. These data are close to but below 6800 proteins (Hukelmann et al., 2016), which may be partly due to the fact that the cytoskeleton fraction that allows the kit to be separated has not been analyzed. Within the membrane fraction the numbers obtained were 4684 and 4801 proteins in the two replicates respectively, of which 1269 and 1255 were included in plasma membrane proteins, representing 27% and 26%. The enrichment is slightly lower, possibly because this fraction is actually enriched not only in plasma membrane proteins, but also in other endomembrane proteins such as endoplasmic reticulum and Golgi apparatus. However, it is true that globally more plasma membrane proteins were detected than in the case of biotinylation, which was also the case with cell surface proteins and CD proteins. In the case of mouse T-cells, the proteins obtained were slightly less, about 3208 for WT and 3412 for deficient

mice at DGKζ. The corresponding membrane fractions included about 2312 and 2309 proteins, with a percentage of plasma membrane proteins of 29%. However, in this case fewer CD proteins were obtained than in the other biotinylation experiments. Both methodologies therefore have their advantages and can help us to obtain information about the plasma membrane proteome of our cells of interest.

As mentioned above, the proteins of the fractions obtained through the subcellular fractionation kit were separated by 1D-SDS-PAGE or RP-HPLC in basic medium. In this way, it was possible to verify which strategy could recover a greater number of plasma membrane proteins, which contain hydrophobic regions that can make solubilization difficult (Vit & Petrak, 2017). The number of plasma membrane proteins obtained in each method was similar, although higher in the case of chromatographic separation. However, when looking at the number of CD proteins, more were detected in gel separation. In view of these similar numbers, we opted for greater detection of these cell surface proteins, and therefore the following fractionations were carried out with gel separation.

1.3. Future strategies

In all the approaches we have carried out, problems of contamination with non membrane proteins have arisen. One of the possible causes would be the presence of cellular debris from dead cells or cell fragments that could have been marked with biotin, in spite of the abundant washing before and after the labeling (Weekes et al., 2010). Another cause could be certain degree of permeability of biotin, although it predominantly labels plasma membrane proteins (Peirce et al., 2004). In general, these causes will always be present and other aspects of the enrichment protocol should be improved. During this discussion, several studies have been cited that propose different strategies, which in some cases are contradictory to each other; some defend amino-oxy-biotin against sulfo-NHS-SS-biotin (Weekes et al., 2010), while others argue just the opposite (Hörmann et al., 2016). Perhaps an attractive solution would be an approach combining different strategies, such as biotinylation tagging and glycosylated protein isolation (Hofmann et al., 2010), although the difficulty of replicating this methodology by other laboratories has been recognized (Vit & Petrak, 2017). In short, there is probably no optimal methodology to replace the others, but each laboratory must carry out different complementary strategies whenever it reports an adequate number of plasma membrane proteins.

Another problem is the identification of the subcellular location of proteins by consulting the Gene Ontology database. In many cases the proteins are either not annotated or only incompletely annotated at the most general levels of abstraction. For example, proteins classified as membrane proteins but not as plasma membrane proteins (Weekes et al.,

2010). In our study we observed that when analyzing the overlap between GO terms, not all cell surface proteins were contained in plasma membrane proteins. Furthermore, while the overlap between cytosol and plasma membrane proteins may be plausible, it is more unlikely in the case of cytosol and cell surface proteins, as these are oriented towards the outer cell membrane. The ontological annotation of the databases should probably be improved. These inconsistencies may be due to the fact that much of the annotations have been inferred by electronic evidence and may be incorrect, and even though there is information in the scientific literature to complete the annotations, it is possible that they have not yet been completed, or have not pass through a curation process (Khatri & Draghici, 2005). An option for possible future studies could be the use of different softwares with access to other databases complementary to Gene Ontology, or with methods for predicting the subcellular location of proteins.

2. MOUSE SURFACEOME

All the effort made in the optimization of membrane protein enrichment has been applied in the characterization of the proteome in different physiological states of the cell. Our study has focused on the effect of DAG dependent signaling on T-cells. To analyze the role of DGK, experiments have been carried out with DAG analogs and mice deficient in DGKζ, a component of this enzyme family.

2.1. PMA

The PMA molecule is a phorbol ester that acts as a potent analog of DAG, and that has been used for the study of signaling (Kazanietz & Lorenzo, 2003). Its effectors include proteins with DAG binding domains, mainly PKC, as well as chimerins, Munc13, RasGRP, PKD and some DGK (Brose & Rosenmund, 2002). The DGK are responsible for the metabolism of the DAG (Mérida et al., 2008), so the addition of PMA can simulate a lack of activity, since the PMA is not consumed by the DGK.

To evaluate the importance of DGK in the expression of CTL membrane proteins, we carried out proteomics experiments in the absence and presence of PMA. One of the effects of PMA that particularly affects the expression of cell surface proteins is shedding. This phenomenon consists of the release of extracellular domains of membrane proteins due to the action of proteolytic enzymes known as sheddases. On the one hand, the expression of the target proteins is negatively regulated, since only the membrane and intracytosolic domains would remain unaltered. In addition, the soluble factors released may be involved in signaling processes (Hayashida et al., 2010). The fact that PMA can participate in shedding

has led to the discovery of the role of the PKCs in shedding. In fact, DGKζ has been associated with shedding regulation mediated by the action of PKCα (Gharbi et al., 2013). Like other studies, we conducted a proteomics approach to detect proteins whose expression might be affected by shedding (Ahram et al., 2005; Shirakabe et al., 2014).

In the analysis of cell surface proteins we focused on proteins classified as CD. The results showed that most of these surface proteins were common to both replicates, indicating acceptable reproducibility in experiments. In most cases, the same proteins were detected in both PMA and non PMA treatments. There is a case in both replicates where a protein was detected only in the PMA free treatment, which would indicate that it could have undergone a shedding process. This was CD120b, or tumor necrosis factor II receptor (TNFR-II). This molecule is described as a protein regulated by the action of shedding, which can be triggered by the addition of PMA (Porteu & Nathan, 1990). The role of TNF receptors has been associated with the activation of apoptosis pathways (Tseng et al., 2018), although in the case of TNFR-II a additional role as a co-stimulatory molecule during TCR activation has been demonstrated (Aspalter et al., 2003), so their elimination by shedding would act as a brake on the activation of these cells.

In other cases, loss of expression of membrane proteins was detected in only one of the replicates. This may be due to a very limited level of expression that may cause a protein not to be detected in all replicates. Among these cases were proteins such as CD49b or integrin α2, which acts as a subunit of the VLA-2 receptor (Hemler et al., 1985). Shedding processes have been described for integrins, also for α2 but in other cell types (Friedl et al., 1997), although in our proteomic analysis many other integrins were detected within CD49, so it is likely that their absence was due to a lack of adequate detection. A similar situation would occur in the case of the tyrosine kinase receptor CD167a, known as DDR1 (Epithelial discoidin domain-containing receptor 1), which also experiences shedding when binding to its collagen binding ligand (Vogel, 2002), and has been described as a T-cell coactivator (Dang et al., 2009). Also CD115, or CSF1R (macrophage colony-stimulating receptor factor), which undergoes shedding dependent on TACE/ADAM (Wilhelmsen & van der Geer, 2004). There is less information on evidence of shedding with CD217, the IL-17 receptor. To confirm the existence of shedding with all these molecules, a direct validation test must be used to measure protein expression under both conditions.

In the opposite situation would be those cell surface proteins detected only in PMA treatment. These proteins would not be present or with limited expression in the absence of treatment, while the addition of PMA would favor their expression or migration to the membrane. Again, this fact occurs in only one of the two replicates, so it could be due to insufficient sensitivity of the equipment. Within these proteins are the CTLA-4 (CD152)

and PD1 (CD279) receptors, involved in the negative regulation of T cell signaling after activation, which would be consistent with the expression pattern detected (Agata et al., 1996; Linsley et al., 1992). CD73 or 5'-nucleotidase, which converts AMP into adenosine, would also be expressed. This molecule has a role in the co-stimulation of T lymphocytes (Resta et al., 1998), and like the two previous proteins is considered a checkpoint for its ability to inactivate the T lymphocyte response (Chatterjee et al., 2014). Activation could lead to increased expression. In the case of CD253 or TRAIL (TNF-related apoptosis-inducing ligand), involved in apoptosis (Wiley et al., 1995), T-cell activation promotes its own expression (Mariani & Krammer, 1998). The addition of PMA would prevent TRAIL-mediated apoptosis mechanisms (Guo & Xu, 2001). Less clear is the case of CD254 or TRANCE (TNF-related activation-induced cytokine receptor), a molecule related to apoptosis and calcium regulation in bone (Akiyama et al., 2012). Although its expression in T cells is induced after activation (Josien et al., 1999), the addition of PMA would not be sufficient to trigger its increased expression (Wang et al., 2002). Something similar would happen with CD221 or IGF1R (insulin-like growth factor-1 receptor), a tyrosine kinase receptor that binds to IGF (insulin-like growth factor)-1 and 2 (Chitnis et al., 2008), where a decrease in expression by the addition of PMA has been described (Schillaci et al., 1998). This receptor would also have a negative effect on PMA-induced shedding (Li et al., 2009).

In addition to the possible problems mentioned above, variations not detected by this proteomic presence/absence technique may occur. When there is detection in both PMA and non PMA treatments, the protein in question would have detectable levels in both cases. However, this would not necessarily mean that the protein is expressed in exactly the same way, as there may also be variations. Therefore, the use of independent validation techniques is necessary to check the expression of the different candidates.

2.2. DGKζ-deficient mice

The other approach to study the role of DGKζ is the use of deficient mice in the expression of this enzyme. In this way the effects of an increase in the concentration of DAG can be observed, but also the effects of PA unlike the previous model, with different effects also on cell signaling (Krishna & Zhong, 2013). For this purpose we have used the biotinylation and subcellular fractionation techniques carried out on differentiated CTL cells from DGKζ$^{-/-}$ mice versus WT mice. The use of two different enrichment techniques has influenced the increase in variability, compared to the PMA study where two replicates of the same biotinylation technique were analyzed. Another challenge was the reduced expression of CD proteins despite the pre-enrichment process, which can hinder their detection during proteomic analysis (Bock et al., 2012). Several replicates of each of the two techniques would

be necessary to gain confidence through this presence/absence approach. Nonetheless, the comparison with the previous data provides us an overview of all the CD proteins detected in the different experiments, which allows us to establish a snapshot of the cell surface expression in CTL. 102 proteins have been detected considering all experiments, and in 95 of them at least one replicate has been detected in the two conditions studied, either minus/plus PMA or WT versus DGKζ$^{-/-}$ cells, depending on the case.

Although proteomic data are validated by statistical filters (Nesvizhskii et al., 2007), techniques such as detection through a specific antibody by western blot or flow cytometry, or techniques such as targeted proteomics (Picotti & Aebersold, 2012) can be used to check the effective change in expression between two conditions. In our case, we used immunocytometry techniques, where specific antibodies to these proteins can be used to measure their expression on the surface. We measured the expression of CD28, a molecule expressed in both conditions, and CD80, CD314 and CD274, which were expressed only in WT in some of the proteomics experiments. We extended the study to CD279 (PD1), the CD274 (PD-L1) receptor, already commented previously in the introduction. We also measured the expression of CD314 or NKG2D, a receptor activator of NK cells also present in CTL cells where it acts as a co-stimulatory molecule, and reinforces its cytotoxic action (Upshaw & Leibson, 2006). No differences were detected in any of these proteins. However, this does not mean that these molecules do not have an impact on cell phenotype DGKζ$^{-/-}$. It has been demonstrated that in the case of both NKG2D and PD1 there is an increase of around 1% in CD8+ CD44hi CD122hi cells (Andrada et al., 2017).

3. Quantitative study

After the results of the presence/absence proteomic studies, we changed our strategy towards a quantitative approach using SILAC metabolic labeling. By means of this technique we compared the expression of proteins that are present in different amount between two conditions. During its implementation, several experimental errors can occur. One of them is the arginine-to-proline conversion, which in our case we have solved by adding a higher concentration of proline to the culture medium. Another possible problem would be incomplete labeling with heavy amino acids, but their incorporation to cells was close to 100%. Finally, the possible error in the proportion of the two samples in a 1:1 ratio is compensated by a statistical correction, with a very good approximation in the case of the membrane fraction and the nuclear fraction. The experimental design with two replicates with reverse labeling also provides reliability to our study (Park et al., 2012).

Among the proteins with differential expression, we looked at those that have a high confidence in the membrane fraction. Instead of cell surface proteins, the more confident

changes were in proteins that are components of the lytic granules of CTL such as granzymes A, B and C and cathepsin D. There would also be an increase in the expression of galectin-3, a protein that increases its expression in activated T cells (Joo et al., 2001), which would correspond to a state of increased proliferation and activation due to the absence of DGKζ. This protein has a role in the initiation of apoptosis, so it may be used by tumors for immune evasion (Fukumori et al., 2003). On the other hand, tyrosine-protein phosphatase non-receptor type 23 (PTPN23) protein is related to the traffic of ubiquitinated proteins to multivesicular bodies (Doyotte et al., 2008). There are no CD proteins with a variation within the highest confidence range, but a single protein in the likely range: the transferrin receptor. As commented earlier in the results section, the lower expression of this receptor can be explained by an internalization of the receptor due to the absence of DGKζ (Rincon et al., 2007).

Within nuclear proteins we can highlight STAT1, a transcription factor activated by several cytokines, among which is IFNγ (Leonard & O'Shea, 1998), with a higher production in the case of mice DGKζ$^{-/-}$ (Wesley et al., 2018). The ubiquitination of STAT1 by a sustained ERK activation like occurs in DGKζ$^{-/-}$ mice may explain why they have lower STAT1 expression levels (Y. Zhang et al., 2018). Another transcription factor detected in one replicate, NFAT5, is activated in response to osmotic stress and helps to regulate lymphocyte activation (Go et al., 2004).

4. Analysis of CTL lytic granules

Once we have seen that there is more expression of granzymes and granule proteins, we wanted to check if this change was due to an increase in the number of secretory lysosomes. Alterations affecting the number and morphology of these granules are rare, generally affecting proteins related to vesicular traffic, as in the cases of Chediak-Higashi and Hermansky-Pudlak syndromes (Clark & Griffiths, 2003), so it would most likely be a difference in the rate of development and maturation of the granules in the CTL differentiation process. To check this we used a probe capable of labeling the acid compartments or lysosomes, which in the case of CTL correspond to the lytic granules (Blott & Griffiths, 2002). Titration gave us a guarantee that contamination of the cytosol was avoided, as verified by microscopy. On the other hand, flow cytometry measurement was able to detect the evolution of granules over time, which is greater in the case of CD8 cells than in CD4 cells. However, when analyzing the levels of lysotracker green in CTL of DGKα and DGKζ deficient mice no significant differences were observed compared to the WT, so we ruled out differences in secretory lysosomes, and therefore the differences in granzyme levels would only be due to changes in expression due to the absence of DGKζ.

Recently it has been described that the CTL deficiency in DGKζ expresses a greater amount of granzymes, both at the mRNA level (Andrada et al., 2017) and at the protein level (Wesley et al., 2018). In this way, the differences in granzyme expression detected by proteomics have been validated, leading the way for the rest of the proteins with differential expression. Our methodology based on quantitative proteomics has shown to be able to detect these candidate proteins. The data obtained helps to understand how DGKζ deficient CTL are more effective removing tumors (Riese et al., 2011), an enzyme that represents a target of interest for future immunotherapy approaches.

CONCLUSIONS

Conclusions

1. The techniques of biotinilation and subcellular fractionation allowed an enrichment from 20% to 30% of membrane proteins in both Jurkat cells and mouse lymphocytes. In the case of fractionation, more plasma membrane proteins were obtained than by biotinylation, although this technique recovered more CD proteins in mouse CTL.

2. In PMA experiments, 5 CD proteins were expressed only in the absence of PMA and 6 only in the presence of PMA, of a total amount of 83 CD proteins detected by CTL biotinylation, at least in some replicate. Among those CD proteins expressed only in the absence of PMA, proteins with possible shedding regulation such as CD49b, CD115, CD120b, CD167a and CD217 were included.

3. When comparing WT and DGKζ$^{-/-}$ CTL, 26 CD proteins showed differences in expression of a total amount of 77 CD proteins detected, in at least one of the replicates. However, when some of them were analysed by flow cytometry, no such changes in expression were detected.

4. Quantitative analysis showed an increase in the expression of granzyme proteins, cathepsin and galectin in CTL deficiency at DGKζ, responsible for cytotoxicity. These changes were not due to differences related to the development of cytotoxic CTL granules.

CONCLUSIONES

Conclusiones

1. Las técnicas de biotinilacion y fraccionamiento subcelular permiten un enriquecimiento de un 20% a un 30% de proteínas de membrana, tanto en células Jurkat como en linfocitos de ratón. En el caso del fraccionamiento se obtienen más proteínas de membrana plasmática que mediante biotinilación, aunque esta técnica recupera más proteínas CD en CTL de ratón.

2. En los experimentos con PMA, 5 proteínas CD se expresaron solo en ausencia de PMA y 6 solo en presencia de PMA de un total de 83 proteínas CD detectadas por biotinilación de CTL, al menos en alguna réplica. Dentro de las proteínas CD que solo se expresan en ausencia de PMA se hallan proteínas con posible regulación por *shedding* como CD49b, CD115, CD120b, CD167a y CD217.

3. Al comparar CTL WT y DGKζ$^{-/-}$, 26 proteínas CD mostraron diferencias en la expresión de un total de 77 proteínas CD detectadas, en al menos una de las réplicas. Sin embargo, al analizar su expresión mediante citometría de flujo no se detectaron cambios.

4. El análisis cuantitativo mostró un incremento de la expresión de proteínas de granzima, catepsina y galectina en CTL deficientes en DGKζ, responsables de los procesos de citotoxicidad. Estos cambios no se debieron a diferencias relacionadas con el desarrollo de gránulos citotóxicos en CTL.

REFERENCES

References

Abdolzade-Bavil, A., Hayes, S., Goretzki, L., Kröger, M., Anders, J., & Hendriks, R. (2004). Convenient and versatile subcellular extraction procedure, that facilitates classical protein expression profiling and functional protein analysis. *Proteomics*, *4*(5), 1397–1405.

Abraham, R. T., & Weiss, A. (2004). Jurkat T cells and development of the T-cell receptor signalling paradigm. *Nature Reviews. Immunology*, *4*(4), 301–308.

Aebersold, R., & Mann, M. (2016). Mass-spectrometric exploration of proteome structure and function. *Nature*, *537*(7620), 347–355.

Agata, Y., Kawasaki, A., Nishimura, H., Ishida, Y., Tsubata, T., Yagita, H., & Honjo, T. (1996). Expression of the PD-1 antigen on the surface of stimulated mouse T and B lymphocytes. *International Immunology*, *8*(5), 765–772.

Ahnadi, C. E., Giguère, P., Gravel, S., Gagné, D., Goulet, A. C., Fülöp, T., Payet, M., & Dupuis, G. (2000). Chronic PMA treatment of Jurkat T lymphocytes results in decreased protein tyrosine phosphorylation and inhibition of CD3- but not Ti-dependent antibody-triggered Ca2+ signaling. *Journal of Leukocyte Biology*, *68*(2), 293–300.

Ahram, M., Adkins, J. N., Auberry, D. L., Wunschel, D. S., & Springer, D. L. (2005). A proteomic approach to characterize protein shedding. *Proteomics*, *5*(1), 123–131.

Akiyama, T., Shinzawa, M., & Akiyama, N. (2012). RANKL-RANK interaction in immune regulatory systems. *World Journal of Orthopedics*, *3*(9), 142.

Alonso, R., Mazzeo, C., Rodriguez, M. C., Marsh, M., Fraile-Ramos, A., Calvo, V., Avila-Flores, A., Mérida, I., & Izquierdo, M. (2011). Diacylglycerol kinase α regulates the formation and polarisation of mature multivesicular bodies involved in the secretion of Fas ligand-containing exosomes in T lymphocytes. *Cell Death & Differentiation*, *18*(7), 1161–1173.

Andrada, E., Almena, M., de Guinoa, J. S., Merino-Cortes, S. V., Liebana, R., Arcos, R., Carrasco, S., Carrasco, Y. R., & Mérida, I. (2016). Diacylglycerol kinase limits the polarized recruitment of diacylglycerol-enriched organelles to the immune synapse in T cells. *Science Signaling*, *9*(459), ra127-ra127.

Andrada, E., Liébana, R., & Mérida, I. (2017). Diacylglycerol Kinase ζ Limits Cytokine-dependent Expansion of CD8 + T Cells with Broad Antitumor Capacity. *EBioMedicine*, *19*, 39–48.

Andrews, L. P., Marciscano, A. E., Drake, C. G., & Vignali, D. A. A. (2017). LAG3 (CD223) as a cancer immunotherapy target. *Immunological Reviews*, *276*(1), 80–96.

Andrin, C., Pinkoski, M. J., Burns, K., Atkinson, E. A., Krahenbuhl, O., Hudig, D., Fraser, S. A., Winkler, U., Tschopp, J., Opas, M., Bleackley, R. C., & Michalak, M. (1998). Interaction between a Ca $^{2+}$ -Binding Protein Calreticulin and Perforin, a Component of the Cytotoxic T-Cell Granules †. *Biochemistry*, *37*(29), 10386–10394.

Apweiler, R., Bairoch, A., Wu, C. H., Barker, W. C., Boeckmann, B., Ferro, S., Gasteiger, E., Huang, H., Lopez, R., Magrane, M., Martin, M. J., Natale, D. A., O'Donovan, C., Redaschi, N., & Yeh, L.-S. L. (2004). UniProt: the Universal Protein knowledgebase. *Nucleic Acids Research*, *32*(90001), 115D–119.

Artyomov, M. N., Lis, M., Devadas, S., Davis, M. M., & Chakraborty, A. K. (2010). CD4 and CD8 binding to MHC molecules primarily acts to enhance Lck delivery. *Proceedings of the National Academy of Sciences*, *107*(39), 16916–16921.

Ashburner, M., Ball, C. A., Blake, J. A., Botstein, D., Butler, H., Cherry, J. M., Davis, A. P., Dolinski, K., Dwight, S. S., Eppig, J. T., Harris, M. A., Hill, D. P., Issel-Tarver, L., Kasarskis, A., Lewis, S., Matese, J. C., Richardson, J. E., … Sherlock, G. (2000). Gene Ontology: tool for the unification of biology. *Nature Genetics*, *25*(1), 25–29.

Aspalter, R. M., Eibl, M. M., & Wolf, H. M. (2003). Regulation of TCR-mediated T cell activation by TNF-RII. *Journal of Leukocyte Biology*, *74*(4), 572–582.

Ávila-Flores, A., Arranz-Nicolás, J., Andrada, E., Soutar, D., & Mérida, I. (2017). Predominant contribution of DGKζ over DGKα in the control of PKC/PDK-1-regulated functions in T cells. *Immunology and Cell Biology*, *95*(6), 549–563.

Ávila-Flores, A., Santos, T., Rincón, E., & Mérida, I. (2005). Modulation of the Mammalian Target of Rapamycin Pathway by Diacylglycerol Kinase-produced Phosphatidic Acid. *Journal of Biological Chemistry*, *280*(11), 10091–10099.

Balaji, K. N., Schaschke, N., Machleidt, W., Catalfamo, M., & Henkart, P. A. (2002). Surface cathepsin B protects cytotoxic lymphocytes from self-destruction after degranulation. *The Journal of Experimental Medicine*, *196*(4), 493–503.

Balar, A. V., & Weber, J. S. (2017). PD-1 and PD-L1 antibodies in cancer: current status and future directions. *Cancer Immunology, Immunotherapy, 66*(5), 551–564.

Baldanzi, G., Cutrupi, S., Chianale, F., Gnocchi, V., Rainero, E., Porporato, P., Filigheddu, N., van Blitterswijk, W. J., Parolini, O., Bussolino, F., Sinigaglia, F., & Graziani, A. (2008). Diacylglycerol kinase-α phosphorylation by Src on Y335 is required for activation, membrane recruitment and Hgf-induced cell motility. *Oncogene*, *27*(7), 942–956.

Bantscheff, M., Lemeer, S., Savitski, M. M., & Kuster, B. (2012). Quantitative mass spectrometry in proteomics: critical review update from 2007 to the present. *Analytical and Bioanalytical Chemistry*, *404*(4), 939–965.

Barber, D. L., Wherry, E. J., Masopust, D., Zhu, B., Allison, J. P., Sharpe, A. H., Freeman, G. J., & Ahmed, R. (2006). Restoring function in exhausted CD8 T cells during chronic viral infection. *Nature*, *439*(7077), 682–687.

Bernard, A., & Boumsell, L. (1984). The clusters of differentiation (CD) defined by the First International Workshop on Human Leucocyte Differentiation Antigens. *Human Immunology*, *11*(1), 1–10.

Bindea, G., Galon, J., & Mlecnik, B. (2013). CluePedia Cytoscape plugin: pathway insights using integrated experimental and in silico data. *Bioinformatics*, *29*(5), 661–663.

Bindea, G., Mlecnik, B., Hackl, H., Charoentong, P., Tosolini, M., Kirilovsky, A., Fridman, W.-H., Pagès, F., Trajanoski, Z., & Galon, J. (2009). ClueGO: a Cytoscape plug-in to decipher functionally grouped gene ontology and pathway annotation networks. *Bioinformatics*, *25*(8), 1091–1093.

Blott, E. J., & Griffiths, G. M. (2002). Secretory lysosomes. *Nature Reviews Molecular Cell Biology*, *3*(2), 122–131.

Bock, T., Bausch-Fluck, D., Hofmann, A., & Wollscheid, B. (2012). CD proteome and beyond - technologies for targeting the immune cell surfaceome. *Frontiers in Bioscience (Landmark Edition)*, *17*, 1599–1612.

Bossi, G., Trambas, C., Booth, S., Clark, R., Stinchcombe, J., & Griffiths, G. M. (2002). The secretory synapse: the secrets of a serial killer. *Immunological Reviews*, *189*, 152–160.

Bovenschen, N., & Kummer, J. A. (2010). Orphan granzymes find a home. *Immunological Reviews*, *235*(1), 117–127.

Brose, N., & Rosenmund, C. (2002). Move over protein kinase C, you've got company: alternative cellular effectors of diacylglycerol and phorbol esters. *Journal of Cell Science*, *115*(Pt 23), 4399–4411.

Brunkow, M. E., Jeffery, E. W., Hjerrild, K. A., Paeper, B., Clark, L. B., Yasayko, S.-A., Wilkinson, J. E., Galas, D., Ziegler, S. F., & Ramsdell, F. (2001). Disruption of a new forkhead/winged-helix protein, scurfin, results in the fatal lymphoproliferative disorder of the scurfy mouse. *Nature Genetics*, *27*(1), 68–73.

Butte, M. J., Keir, M. E., Phamduy, T. B., Sharpe, A. H., & Freeman, G. J. (2007). Programmed Death-1 Ligand 1 Interacts Specifically with the B7-1 Costimulatory Molecule to Inhibit T Cell Responses. *Immunity*, *27*(1), 111–122.

Calderón-González, K. G., Hernández-Monge, J., Herrera-Aguirre, M. E., & Luna-Arias, J. P. (2016). Bioinformatics Tools for Proteomics Data Interpretation. In *Advances in experimental medicine and biology* (Vol. 919, pp. 281–341).

Carnielli, C. M., Winck, F. V., & Paes Leme, A. F. (2015). Functional annotation and biological interpretation of proteomics data. *Biochimica et Biophysica Acta (BBA) - Proteins and Proteomics*, *1854*(1), 46–54.

Chanmee, T., Ontong, P., Konno, K., & Itano, N. (2014). Tumor-Associated Macrophages as Major Players in the Tumor Microenvironment. *Cancers*, *6*(3), 1670–1690.

Chatterjee, S., Thyagarajan, K., Kesarwani, P., Song, J. H., Soloshchenko, M., Fu, J., Bailey, S. R., Vasu, C., Kraft, A. S., Paulos, C. M., Yu, X.-Z., & Mehrotra, S. (2014). Reducing CD73 Expression by IL1 -Programmed Th17 Cells Improves Immunotherapeutic Control of Tumors. *Cancer Research*, *74*(21), 6048–6059.

Chauveau, A., Le Floc'h, A., Bantilan, N. S., Koretzky, G. A., & Huse, M. (2014). Diacylglycerol kinase establishes T cell polarity by shaping diacylglycerol accumulation at the immunological synapse. *Science Signaling*, *7*(340), ra82-ra82.

Chazotte, B. (2011). Labeling lysosomes in live cells with lysotracker. *Cold Spring Harbor Protocols*, *6*(2).

Chen, W., Jin, W., Hardegen, N., Lei, K., Li, L., Marinos, N., McGrady, G., & Wahl, S. M. (2003). Conversion of Peripheral CD4 $^{+}$ CD25 $^{-}$ Naive T Cells to CD4 $^{+}$ CD25 $^{+}$ Regulatory T Cells by TGF-β Induction of Transcription Factor *Foxp3*. *The Journal of Experimental Medicine*, *198*(12), 1875–1886.

Chitnis, M. M., Yuen, J. S. P., Protheroe, A. S., Pollak, M., & Macaulay, V. M. (2008). The Type 1 Insulin-Like Growth Factor Receptor Pathway. *Clinical Cancer Research*, *14*(20), 6364–6370.

Clark, R., & Griffiths, G. M. (2003). Lytic granules, secretory lysosomes and disease. *Current Opinion in Immunology*, *15*(5), 516–521.

Cordwell, S. J., & Thingholm, T. E. (2010). Technologies for plasma membrane proteomics. *Proteomics*, *10*(4), 611–627.

Cullen, S. P., Adrain, C., Lüthi, A. U., Duriez, P. J., & Martin, S. J. (2007). Human and murine granzyme B exhibit divergent substrate preferences. *The Journal of Cell Biology*, *176*(4), 435–444.

da Cunha, J. P. C., Galante, P. A. F., de Souza, J. E., de Souza, R. F., Carvalho, P. M., Ohara, D. T., Moura, R. P., Oba-Shinja, S. M., Marie, S. K. N., Silva, W. A., Perez, R. O., Stransky, B., Pieprzyk, M., Moore, J., Caballero, O., Gama-Rodrigues, J., Habr-Gama, A., … de Souza, S. J. (2009). Bioinformatics construction of the human cell surfaceome. *Proceedings of the National Academy of Sciences*, *106*(39), 16752–16757.

Dang, N., Hu, J., Liu, X., Li, X., Ji, S., Zhang, W., Su, J., Lu, F., Yang, A., Han, H., Han, W., Jin, B., & Yao, L. (2009). CD167 Acts as a Novel Costimulatory Receptor in T-Cell Activation. *Journal of Immunotherapy*, *32*(8), 773–784.

de Saint Basile, G., Ménasché, G., & Fischer, A. (2010). Molecular mechanisms of biogenesis and exocytosis of cytotoxic granules. *Nature Reviews Immunology*, *10*(8), 568–579.

Deng, G. (2018). Tumor-infiltrating regulatory T cells: origins and features. *American Journal of Clinical and Experimental Immunology, 7*(5), 81–87.

Dennis, G., Sherman, B. T., Hosack, D. A., Yang, J., Gao, W., Lane, H. C., & Lempicki, R. A. (2003). DAVID: Database for Annotation, Visualization, and Integrated Discovery. *Genome Biology*, *4*(5), P3.

Dieckmann, N. M. G., Frazer, G. L., Asano, Y., Stinchcombe, J. C., & Griffiths, G. M. (2016). The cytotoxic T lymphocyte immune synapse at a glance. *Journal of Cell Science*, *129*(15), 2881–2886.

Domon, B., & Aebersold, R. (2006). Mass Spectrometry and Protein Analysis. *Science*, *312*(5771), 212–217.

Doyotte, A., Mironov, A., McKenzie, E., & Woodman, P. (2008). The Bro1-related protein HD-PTP/PTPN23 is required for endosomal cargo sorting and multivesicular body morphogenesis. *Proceedings of the National Academy of Sciences*, *105*(17), 6308–6313.

Dreger, M. (2003). Subcellular proteomics. *Mass Spectrometry Reviews*, *22*(1), 27–56.

Dunn, G. P., Bruce, A. T., Ikeda, H., Old, L. J., & Schreiber, R. D. (2002). Cancer immunoediting: from immunosurveillance to tumor escape. *Nature Immunology*, *3*(11), 991–998.

Ebinu, J. O., Bottorff, D. A., Chan, E. Y., Stang, S. L., Dunn, R. J., & Stone, J. C. (1998). RasGRP, a Ras guanyl nucleotide- releasing protein with calcium- and diacylglycerol-binding motifs. *Science (New York, N.Y.)*, *280*(5366), 1082–1086.

Egen, J. G., & Allison, J. P. (2002). Cytotoxic T lymphocyte antigen-4 accumulation in the immunological synapse is regulated by TCR signal strength. *Immunity*, *16*(1), 23–35.

Elia, G. (2008). Biotinylation reagents for the study of cell surface proteins. *Proteomics*, *8*(19), 4012–4024.

Elortza, F., Mohammed, S., Bunkenborg, J., Foster, L. J., Nühse, T. S., Brodbeck, U., Peck, S. C., & Jensen, O. N. (2006). Modification-Specific Proteomics of Plasma Membrane Proteins: Identification and Characterization of Glycosylphosphatidylinositol-Anchored Proteins Released upon Phospholipase D Treatment. *Journal of Proteome Research*, *5*(4), 935–943.

Fagerberg, L., Jonasson, K., von Heijne, G., Uhlén, M., & Berglund, L. (2010). Prediction of the human membrane proteome. *Proteomics*, *10*(6), 1141–1149.

Farkas, A. M., & Finn, O. J. (2010). Vaccines based on abnormal self-antigens as tumor-associated antigens: Immune regulation. *Seminars in Immunology*, *22*(3), 125–131.

Fenn, J. B., Mann, M., Meng, C. K., Wong, S. F., & Whitehouse, C. M. (1989). Electrospray ionization for mass spectrometry of large biomolecules. *Science (New York, N.Y.)*, *246*(4926), 64–71.

Francisco, L. M., Salinas, V. H., Brown, K. E., Vanguri, V. K., Freeman, G. J., Kuchroo, V. K., & Sharpe, A. H. (2009). PD-L1 regulates the development, maintenance, and function of induced regulatory T cells. *The Journal of Experimental Medicine*, *206*(13), 3015–3029.

Friedl, P., Maaser, K., Klein, C. E., Niggemann, B., Krohne, G., & Zänker, K. S. (1997). Migration of highly aggressive MV3 melanoma cells in 3-dimensional collagen lattices results in local matrix reorganization and shedding of alpha2 and beta1 integrins and CD44. *Cancer Research*, *57*(10), 2061–2070.

Fukumori, T., Takenaka, Y., Yoshii, T., Kim, H.-R. C., Hogan, V., Inohara, H., Kagawa, S., & Raz, A. (2003). CD29 and CD7 mediate galectin-3-induced type II T-cell apoptosis. *Cancer Research*, *63*(23), 8302–8311.

Galon, J., Costes, A., Sanchez-Cabo, F., Kirilovsky, A., Mlecnik, B., Lagorce-Pagès, C., Tosolini, M., Camus, M., Berger, A., Wind, P., Zinzindohoué, F., Bruneval, P., Cugnenc, P.-H., Trajanoski, Z., Fridman, W.-H., & Pagès, F. (2006). Type, Density, and Location of Immune Cells Within Human Colorectal Tumors Predict Clinical Outcome. *Science*, *313*(5795), 1960–1964.

Genot, E., & Cantrell, D. A. (2000). Ras regulation and function in lymphocytes. *Current Opinion in Immunology*, *12*(3), 289–294.

Gerasimenko, J. V, Tepikin, A. V, Petersen, O. H., & Gerasimenko, O. V. (1998). Calcium uptake via endocytosis with rapid release from acidifying endosomes. *Current Biology : CB*, *8*(24), 1335–1338.

Germain, R. N. (1994). MHC-dependent antigen processing and peptide presentation: providing ligands for T lymphocyte activation. *Cell*, *76*(2), 287–299.

Gharbi, S. I., Avila-Flores, A., Soutar, D., Orive, A., Koretzky, G. a, Albar, J. P., & Mérida, I. (2013). Transient PKCα shuttling to the immunological synapse is governed by DGKζ and regulates L-selectin shedding. *Journal of Cell Science*, *126*(10), 2176–2186.

Gharbi, S. I., Rincón, E., Avila-Flores, A., Torres-Ayuso, P., Almena, M., Cobos, M. A., Albar, J. P., & Mérida, I. (2011). Diacylglycerol kinase ζ controls diacylglycerol metabolism at the immunological synapse. *Molecular Biology of the Cell*, *22*(22), 4406–4414.

Glish, G. L., & Vachet, R. W. (2003). The basics of mass spectrometry in the twenty-first century. *Nature Reviews Drug Discovery*, *2*(2), 140–150.

Go, W. Y., Liu, X., Roti, M. A., Liu, F., & Ho, S. N. (2004). NFAT5/TonEBP mutant mice define osmotic stress as a critical feature of the lymphoid microenvironment. *Proceedings of the National Academy of Sciences*, *101*(29), 10673–10678.

Gooden, M. J. M., de Bock, G. H., Leffers, N., Daemen, T., & Nijman, H. W. (2011). The prognostic influence of tumour-infiltrating lymphocytes in cancer: a systematic review with meta-analysis. *British Journal of Cancer*, *105*(1), 93–103.

Goping, I. S., Barry, M., Liston, P., Sawchuk, T., Constantinescu, G., Michalak, K. M., Shostak, I., Roberts, D. L., Hunter, A. M., Korneluk, R., & Bleackley, R. C. (2003). Granzyme B-induced apoptosis requires both direct caspase activation and relief of caspase inhibition. *Immunity*, *18*(3), 355–365.

Gouw, J. W., Krijgsveld, J., & Heck, A. J. R. (2010). Quantitative Proteomics by Metabolic Labeling of Model Organisms. *Molecular & Cellular Proteomics*, *9*(1), 11–24.

Grohmann, U., Orabona, C., Fallarino, F., Vacca, C., Calcinaro, F., Falorni, A., Candeloro, P., Belladonna, M. L., Bianchi, R., Fioretti, M. C., & Puccetti, P. (2002). CTLA-4–Ig regulates tryptophan catabolism in vivo. *Nature Immunology*, *3*(11), 1097–1101.

Gstaiger, M., & Aebersold, R. (2009). Applying mass spectrometry-based proteomics to genetics, genomics and network biology. *Nature Reviews Genetics*, *10*(9), 617–627.

Guo, B. C., & Xu, Y. H. (2001). Bcl-2 over-expression and activation of protein kinase C suppress the Trail-induced apoptosis in Jurkat T cells. *Cell Research*, *11*(2), 101–106.

Gygi, S. P., Rist, B., Gerber, S. A., Turecek, F., Gelb, M. H., & Aebersold, R. (1999). Quantitative analysis of complex protein mixtures using isotope-coded affinity tags. *Nature Biotechnology*, *17*(10), 994–999.

Hadrup, S., Donia, M., & thor Straten, P. (2013). Effector CD4 and CD8 T Cells and Their Role in the Tumor Microenvironment. *Cancer Microenvironment*, *6*(2), 123–133.

Hanahan, D., & Weinberg, R. A. (2011). Hallmarks of Cancer: The Next Generation. *Cell*, *144*(5), 646–674.

Harlin, H., Meng, Y., Peterson, A. C., Zha, Y., Tretiakova, M., Slingluff, C., McKee, M., & Gajewski, T. F. (2009). Chemokine Expression in Melanoma Metastases Associated with CD8+ T-Cell Recruitment. *Cancer Research*, *69*(7), 3077–3085.

Hayashida, K., Bartlett, A. H., Chen, Y., & Park, P. W. (2010). Molecular and cellular mechanisms of ectodomain shedding. *Anatomical Record*, *293*(6), 925–937.

Hemler, M. E., Jacobson, J. G., & Strominger, J. L. (1985). Biochemical characterization of VLA-1 and VLA-2. Cell surface heterodimers on activated T cells. *The Journal of Biological Chemistry*, *260*(28), 15246–15252.

Hernandez, C., Huebener, P., & Schwabe, R. F. (2016). Damage-associated molecular patterns in cancer: a double-edged sword. *Oncogene*, *35*(46), 5931–5941.

Hodi, F. S., Mihm, M. C., Soiffer, R. J., Haluska, F. G., Butler, M., Seiden, M. V., Davis, T., Henry-Spires, R., MacRae, S., Willman, A., Padera, R., Jaklitsch, M. T., Shankar, S., Chen, T. C., Korman, A., Allison, J. P., & Dranoff, G. (2003). Biologic activity of cytotoxic T lymphocyte-associated antigen 4 antibody blockade in previously vaccinated metastatic melanoma and ovarian carcinoma patients. *Proceedings of the National Academy of Sciences*, *100*(8), 4712–4717.

Hoffmann, E. de, & Stroobant, V. (2007). Mass analyzers. In *Mass Spectrometry: Principles and Applications* (3rd Ed., pp. 85–173). Chichester: Wiley.

Hofmann, A., Gerrits, B., Schmidt, A., Bock, T., Bausch-Fluck, D., Aebersold, R., & Wollscheid, B. (2010). Proteomic cell surface phenotyping of differentiating acute myeloid leukemia cells. *Blood*, *116*(13), e26–e34.

Hogan, P. G., Chen, L., Nardone, J., & Rao, A. (2003). Transcriptional regulation by calcium, calcineurin, and NFAT. *Genes & Development*, *17*(18), 2205–2232.

Hogquist, K. A., Baldwin, T. A., & Jameson, S. C. (2005). Central tolerance: learning self-control in the thymus. *Nature Reviews Immunology*, *5*(10), 772–782.

Hogquist, K. A., Jameson, S. C., Heath, W. R., Howard, J. L., Bevan, M. J., & Carbone, F. R. (1994). T cell receptor antagonist peptides induce positive selection. *Cell*, *76*(1), 17–27.

Hörmann, K., Stukalov, A., Müller, A. C., Heinz, L. X., Superti-Furga, G., Colinge, J., & Bennett, K. L. (2016). A Surface Biotinylation Strategy for Reproducible Plasma Membrane Protein Purification and Tracking of Genetic and Drug-Induced Alterations. *Journal of Proteome Research*, *15*(2), 647–658.

Huang, D. W., Sherman, B. T., & Lempicki, R. A. (2009a). Bioinformatics enrichment tools: paths toward the comprehensive functional analysis of large gene lists. *Nucleic Acids Research*, *37*(1), 1–13.

Huang, D. W., Sherman, B. T., & Lempicki, R. A. (2009b). Systematic and integrative analysis of large gene lists using DAVID bioinformatics resources. *Nature Protocols*, *4*(1), 44–57.

Hukelmann, J. L., Anderson, K. E., Sinclair, L. V, Grzes, K. M., Murillo, A. B., Hawkins, P. T., Stephens, L. R., Lamond, A. I., & Cantrell, D. A. (2016). The cytotoxic T cell proteome and its shaping by the kinase mTOR. *Nature Immunology*, *17*(1), 104–112.

Huppa, J. B., & Davis, M. M. (2003). T-cell-antigen recognition and the immunological synapse. *Nature Reviews Immunology*, *3*(12), 973–983.

Hwang, S.-I., & Han, D. K. (2013). Subcellular Fractionation for Identification of Biomarkers: Serial Detergent Extraction by Subcellular Accessibility and Solubility. In *Methods in molecular biology (Clifton, N.J.)* (Vol. 1002, pp. 25–35).

Ishihama, Y., Sato, T., Tabata, T., Miyamoto, N., Sagane, K., Nagasu, T., & Oda, Y. (2005). Quantitative mouse brain proteomics using culture-derived isotope tags as internal standards. *Nature Biotechnology*, *23*(5), 617–621.

Joo, H. G., Goedegebuure, P. S., Sadanaga, N., Nagoshi, M., von Bernstorff, W., & Eberlein, T. J. (2001). Expression and function of galectin-3, a beta-galactoside-binding protein in activated T lymphocytes. *Journal of Leukocyte Biology*, *69*(4), 555–564.

Jordan, M. S., Singer, A. L., & Koretzky, G. A. (2003). Adaptors as central mediators of signal transduction in immune cells. *Nature Immunology*, *4*(2), 110–116.

Joshi, R. P., Schmidt, A. M., Das, J., Pytel, D., Riese, M. J., Lester, M., Diehl, J. A., Behrens, E. M., Kambayashi, T., & Koretzky, G. A. (2013). The Isoform of Diacylglycerol Kinase Plays a Predominant Role in Regulatory T Cell Development and TCR-Mediated Ras Signaling. *Science Signaling*, *6*(303), ra102-ra102.

Josien, R., Wong, B. R., Li, H. L., Steinman, R. M., & Choi, Y. (1999). TRANCE, a TNF family member, is differentially expressed on T cell subsets and induces cytokine production in dendritic cells. *Journal of Immunology (Baltimore, Md. : 1950)*, *162*(5), 2562–2568.

Juncker, A. S., Jensen, L. J., Pierleoni, A., Bernsel, A., Tress, M. L., Bork, P., von Heijne, G., Valencia, A., Ouzounis, C. A., Casadio, R., & Brunak, S. (2009). Sequence-based feature prediction and annotation of proteins. *Genome Biology*, *10*(2), 206.

Kägi, D., Ledermann, B., Bürki, K., Seiler, P., Odermatt, B., Olsen, K. J., Podack, E. R., Zinkernagel, R. M., & Hengartner, H. (1994). Cytotoxicity mediated by T cells and natural killer cells is greatly impaired in perforin-deficient mice. *Nature*, *369*(6475), 31–37.

Kaiser, J. (2002). PROTEOMICS: Public-Private Group Maps Out Initiatives. *Science*, *296*(5569), 827–827.

Kalos, M., & June, C. H. (2013). Adoptive T Cell Transfer for Cancer Immunotherapy in the Era of Synthetic Biology. *Immunity*, *39*(1), 49–60.

Kaplan, D. H., Shankaran, V., Dighe, A. S., Stockert, E., Aguet, M., Old, L. J., & Schreiber, R. D. (1998). Demonstration of an interferon gamma-dependent tumor surveillance system in immunocompetent mice. *Proceedings of the National Academy of Sciences of the United States of America*, *95*(13), 7556–7561.

Karas, M., & Hillenkamp, F. (1988). Laser desorption ionization of proteins with molecular masses exceeding 10,000 daltons. *Analytical Chemistry*, *60*(20), 2299–2301.

Kazanietz, M. G., & Lorenzo, P. S. (2003). Phorbol Esters as Probes for the Study of Protein Kinase C Function. In *Protein Kinase C Protocols* (Vol. 233, pp. 423–440). New Jersey: Humana Press.

Keir, M. E., Butte, M. J., Freeman, G. J., & Sharpe, A. H. (2008). PD-1 and its ligands in tolerance and immunity. *Annual Review of Immunology*, *26*, 677–704.

Khatri, P., & Draghici, S. (2005). Ontological analysis of gene expression data: current tools, limitations, and open problems. *Bioinformatics*, *21*(18), 3587–3595.

Klausner, R. D., Harford, J., & van Renswoude, J. (1984). Rapid internalization of the transferrin receptor in K562 cells is triggered by ligand binding or treatment with a phorbol ester. *Proceedings of the National Academy of Sciences of the United States of America*, *81*(10), 3005–3009.

Krammer, P. H., Arnold, R., & Lavrik, I. N. (2007). Life and death in peripheral T cells. *Nature Reviews Immunology*, *7*(7), 532–542.

Krensky, A. M., & Clayberger, C. (2009). Biology and clinical relevance of granulysin. *Tissue Antigens*, *73*(3), 193–198.

Krishna, S., & Zhong, X.-P. (2013). Regulation of lipid signaling by diacylglycerol kinases during T cell development and function. *Frontiers in Immunology*, *4*(JUL), 1–14.

Krogh, A., Larsson, B., von Heijne, G., & Sonnhammer, E. L. . (2001). Predicting transmembrane protein topology with a hidden markov model: application to complete genomes11Edited by F. Cohen. *Journal of Molecular Biology*, *305*(3), 567–580.

Laemmli, U. K. (1970). Cleavage of structural proteins during the assembly of the head of bacteriophage T4. *Nature*, *227*(5259), 680–685.

Lee, K.-H., Holdorf, A. D., Dustin, M. L., Chan, A. C., Allen, P. M., & Shaw, A. S. (2002). T Cell Receptor Signaling Precedes Immunological Synapse Formation. *Science*, *295*(5559), 1539–1542.

Legrain, P., Aebersold, R., Archakov, A., Bairoch, A., Bala, K., Beretta, L., Bergeron, J., Borchers, C. H., Corthals, G. L., Costello, C. E., Deutsch, E. W., Domon, B., Hancock, W., He, F., Hochstrasser, D. F., Marko-Varga, G., Salekdeh, G. H., … Omenn, G. S. (2011). The Human Proteome Project: Current State and Future Direction. *Molecular & Cellular Proteomics*, *10*(7), M111.009993.

Leonard, W. J., & O'Shea, J. J. (1998). JAKS AND STATS: Biological Implications. *Annual Review of Immunology*, *16*(1), 293–322.

Lescuyer, P., Hochstrasser, D. F., & Sanchez, J.-C. (2004). Comprehensive proteome analysis by chromatographic protein prefractionation. *ELECTROPHORESIS*, *25*(78), 1125–1135.

Li, S., Zhang, D., Yang, L., Burnier, J. V., Wang, N., Lin, R., Lee, E. R., Glazer, R. I., & Brodt, P. (2009). The IGF-I Receptor Can Alter the Matrix Metalloproteinase Repertoire of Tumor Cells through Transcriptional Regulation of PKC-α. *Molecular Endocrinology*, *23*(12), 2013–2025.

Lieberman, J. (2003). The ABCs of granule-mediated cytotoxicity: new weapons in the arsenal. *Nature Reviews Immunology*, *3*(5), 361–370.

Linsley, P. S., Greene, J. L., Brady, W., Bajorath, J., Ledbetter, J. A., & Peach, R. (1994). Human B7-1 (CD80) and B7-2 (CD86) bind with similar avidities but distinct kinetics to CD28 and CTLA-4 receptors. *Immunity*, *1*(9), 793–801.

Linsley, P. S., Greene, J. L., Tan, P., Bradshaw, J., Ledbetter, J. A., Anasetti, C., & Damle, N. K. (1992). Coexpression and functional cooperation of CTLA-4 and CD28 on activated T lymphocytes. *The Journal of Experimental Medicine*, *176*(6), 1595–1604.

Liu, K., Kunii, N., Sakuma, M., Yamaki, A., Mizuno, S., Sato, M., Sakai, H., Kado, S., Kumagai, K., Kojima, H., Okabe, T., Nagano, T., Shirai, Y., & Sakane, F. (2016). A novel diacylglycerol kinase α-selective inhibitor, CU-3, induces cancer cell apoptosis and enhances immune response. *Journal of Lipid Research*, *57*(3), 368–379.

Lopez, J. A., Susanto, O., Jenkins, M. R., Lukoyanova, N., Sutton, V. R., Law, R. H. P., Johnston, A., Bird, C. H., Bird, P. I., Whisstock, J. C., Trapani, J. A., Saibil, H. R., & Voskoboinik, I. (2013). Perforin forms transient pores on the target cell plasma membrane to facilitate rapid access of granzymes during killer cell attack. *Blood*, *121*(14), 2659–2668.

Loyet, K. M., Ouyang, W., Eaton, D. L., & Stults, J. T. (2005). Proteomic Profiling of Surface Proteins on Th1 and Th2 Cells. *Journal of Proteome Research*, *4*(2), 400–409.

Luo, B., Prescott, S. M., & Topham, M. K. (2003). Protein Kinase Cα Phosphorylates and Negatively Regulates Diacylglycerol Kinase ζ. *Journal of Biological Chemistry*, *278*(41), 39542–39547.

Macián, F., García-Cózar, F., Im, S. H., Horton, H. F., Byrne, M. C., & Rao, A. (2002). Transcriptional mechanisms underlying lymphocyte tolerance. *Cell*, *109*(6), 719–731.

Maere, S., Heymans, K., & Kuiper, M. (2005). BiNGO: a Cytoscape plugin to assess overrepresentation of Gene Ontology categories in Biological Networks. *Bioinformatics*, *21*(16), 3448–3449.

Malek, T. R. (2003). The main function of IL-2 is to promote the development of T regulatory cells. *Journal of Leukocyte Biology*, *74*(6), 961–965.

Mariani, S. M., & Krammer, P. H. (1998). Surface expression of TRAIL/Apo-2 ligand in activated mouse T and B cells. *European Journal of Immunology*, *28*(5), 1492–1498.

Markoutsa, S., Bahr, U., Papasotiriou, D. G., Häfner, A.-K., Karas, M., & Sorg, B. L. (2014). Sulfo-NHS-SS-biotin derivatization: A versatile tool for MALDI mass analysis of PTMs in lysine-rich proteins. *Proteomics*, *14*(6), 659–667.

Medina-Aunon, J. A., Paradela, A., Macht, M., Thiele, H., Corthals, G., & Albar, J. P. (2010). Protein Information and Knowledge Extractor: Discovering biological information from proteomics data. *Proteomics*, *10*(18), 3262–3271.

Meng, X. W., Heldebrant, M. P., Flatten, K. S., Loegering, D. A., Dai, H., Schneider, P. A., Gomez, T. S., Peterson, K. L., Trushin, S. A., Hess, A. D., Smith, B. D., Karp, J. E., Billadeau, D. D., & Kaufmann, S. H. (2010). Protein kinase Cbeta modulates ligand-induced cell surface death receptor accumulation: a mechanistic basis for enzastaurin-death ligand synergy. *The Journal of Biological Chemistry*, *285*(2), 888–902.

Merico, D., Isserlin, R., Stueker, O., Emili, A., & Bader, G. D. (2010). Enrichment Map: A Network-Based Method for Gene-Set Enrichment Visualization and Interpretation. *PLoS ONE*, *5*(11), e13984.

Mérida, I., Avila-Flores, A., & Merino, E. (2008). Diacylglycerol kinases: at the hub of cell signalling. *The Biochemical Journal*, *409*(1), 1–18.

Merino, E., Avila-Flores, A., Shirai, Y., Moraga, I., Saito, N., & Mérida, I. (2008). Lck-dependent tyrosine phosphorylation of diacylglycerol kinase alpha regulates its membrane association in T cells. *Journal of Immunology (Baltimore, Md. : 1950)*, *180*(9), 5805–5815.

Mingari, M. C., Pietra, G., & Moretta, L. (2005). Human cytolytic T lymphocytes expressing HLA class-I-specific inhibitory receptors. *Current Opinion in Immunology*, *17*(3), 312–319.

Monks, C. R. F., Freiberg, B. A., Kupfer, H., Sciaky, N., & Kupfer, A. (1998). Three-dimensional segregation of supramolecular activation clusters in T cells. *Nature*, *395*(6697), 82–86.

Monu, N. R., & Frey, A. B. (2012). Myeloid-Derived Suppressor Cells and anti-tumor T cells: a complex relationship. *Immunological Investigations*, *41*(6–7), 595–613.

Moon, E. K., Wang, L.-C., Dolfi, D. V., Wilson, C. B., Ranganathan, R., Sun, J., Kapoor, V., Scholler, J., Pure, E., Milone, M. C., June, C. H., Riley, J. L., Wherry, E. J., & Albelda, S. M. (2014). Multifactorial T-cell Hypofunction That Is Reversible Can Limit the Efficacy of Chimeric Antigen Receptor-Transduced Human T cells in Solid Tumors. *Clinical Cancer Research*, *20*(16), 4262–4273.

Moreno, M., Molling, J. W., von Mensdorff-Pouilly, S., Verheijen, R. H. M., Hooijberg, E., Kramer, D., Reurs, A. W., van den Eertwegh, A. J. M., von Blomberg, B. M. E., Scheper, R. J., & Bontkes, H. J. (2008). IFN-gamma-producing human invariant NKT cells promote tumor-associated antigen-specific cytotoxic T cell responses. *Journal of Immunology (Baltimore, Md. : 1950)*, *181*(4), 2446–2454.

Mortensen, P., Gouw, J. W., Olsen, J. V., Ong, S.-E., Rigbolt, K. T. G., Bunkenborg, J., Cox, J., Foster, L. J., Heck, A. J. R., Blagoev, B., Andersen, J. S., & Mann, M. (2010). MSQuant, an Open Source Platform for Mass Spectrometry-Based Quantitative Proteomics. *Journal of Proteome Research*, *9*(1), 393–403.

Motyka, B., Korbutt, G., Pinkoski, M. J., Heibein, J. A., Caputo, A., Hobman, M., Barry, M., Shostak, I., Sawchuk, T., Holmes, C. F., Gauldie, J., & Bleackley, R. C. (2000). Mannose 6-phosphate/insulin-like growth factor II receptor is a death receptor for granzyme B during cytotoxic T cell-induced apoptosis. *Cell*, *103*(3), 491–500.

Mueller, D. L. (2010). Mechanisms maintaining peripheral tolerance. *Nature Immunology*, *11*(1), 21–27.

Murphy, K., & Weaver, C. (2016). Basic concepts in immunology. In *Janeway's immunobiology* (pp. 1–36). New York: Garland Science.

Murray, C. I., Barrett, M., & Van Eyk, J. E. (2009). Assessment of ProteoExtract subcellular fractionation kit reveals limited and incomplete enrichment of nuclear subproteome from frozen liver and heart tissue. *Proteomics*, *9*(15), 3934–3938.

Nakajima, H., Park, H. L., & Henkart, P. A. (1995). Synergistic roles of granzymes A and B in mediating target cell death by rat basophilic leukemia mast cell tumors also expressing cytolysin/perforin. *The Journal of Experimental Medicine*, *181*(3), 1037–1046.

Neilson, K. A., Ali, N. A., Muralidharan, S., Mirzaei, M., Mariani, M., Assadourian, G., Lee, A., van Sluyter, S. C., & Haynes, P. A. (2011). Less label, more free: Approaches in label-free quantitative mass spectrometry. *Proteomics*, *11*(4), 535–553.

Nesvizhskii, A. I., Vitek, O., & Aebersold, R. (2007). Analysis and validation of proteomic data generated by tandem mass spectrometry. *Nature Methods*, *4*(10), 787–797.

Nishimura, H., Minato, N., Nakano, T., & Honjo, T. (1998). Immunological studies on PD-1 deficient mice: implication of PD-1 as a negative regulator for B cell responses. *International Immunology*, *10*(10), 1563–1572.

O'Farrell, P. H. (1975). High resolution two-dimensional electrophoresis of proteins. *The Journal of Biological Chemistry*, *250*(10), 4007–4021.

Olenchock, B. A., Guo, R., Carpenter, J. H., Jordan, M., Topham, M. K., Koretzky, G. a, & Zhong, X.-P. (2006). Disruption of diacylglycerol metabolism impairs the induction of T cell anergy. *Nature Immunology*, *7*(11), 1174–1181.

Ong, S.-E., Blagoev, B., Kratchmarova, I., Kristensen, D. B., Steen, H., Pandey, A., & Mann, M. (2002). Stable isotope labeling by amino acids in cell culture, SILAC, as a simple and accurate approach to expression proteomics. *Molecular & Cellular Proteomics : MCP*, *1*(5), 376–386.

Pan, S., Chen, R., Aebersold, R., & Brentnall, T. A. (2011). Mass Spectrometry Based Glycoproteomics—From a Proteomics Perspective. *Molecular & Cellular Proteomics*, *10*(1), R110.003251.

Pandiyan, P., Zheng, L., Ishihara, S., Reed, J., & Lenardo, M. J. (2007). CD4+CD25+-Foxp3+ regulatory T cells induce cytokine deprivation–mediated apoptosis of effector CD4+ T cells. *Nature Immunology*, *8*(12), 1353–1362.

Pappin, D. J., Hojrup, P., & Bleasby, A. J. (1993). Rapid identification of proteins by peptide-mass fingerprinting. *Current Biology : CB*, *3*(6), 327–332.

Pardoll, D. M. (2012). The blockade of immune checkpoints in cancer immunotherapy. *Nature Reviews Cancer*, *12*(4), 252–264.

Park, S.-S., Wu, W. W., Zhou, Y., Shen, R.-F., Martin, B., & Maudsley, S. (2012). Effective correction of experimental errors in quantitative proteomics using stable isotope labeling by amino acids in cell culture (SILAC). *Journal of Proteomics*, *75*(12), 3720–3732.

Parsa, A. T., Waldron, J. S., Panner, A., Crane, C. A., Parney, I. F., Barry, J. J., Cachola, K. E., Murray, J. C., Tihan, T., Jensen, M. C., Mischel, P. S., Stokoe, D., & Pieper, R. O. (2007). Loss of tumor suppressor PTEN function increases B7-H1 expression and immunoresistance in glioma. *Nature Medicine*, *13*(1), 84–88.

Pasero, C., & Olive, D. (2013). Interfering with coinhibitory molecules: BTLA/HVEM as new targets to enhance anti-tumor immunity. *Immunology Letters*, *151*(1–2), 71–75.

Pauken, K. E., & Wherry, E. J. (2015). Overcoming T cell exhaustion in infection and cancer. *Trends in Immunology*, *36*(4), 265–276.

Paul, S., & Schaefer, B. C. (2013). A new look at T cell receptor signaling to nuclear factor-κB. *Trends in Immunology*, *34*(6), 269–281.

Paul, W., & Steinwedel, H. (1953). Ein neues Massenspektrometer ohne Magnetfeld. *Zeitschrift Für Naturforschung A*, *8*(7), 448–450.

Peirce, M. J., Wait, R., Begum, S., Saklatvala, J., & Cope, A. P. (2004). Expression Profiling of Lymphocyte Plasma Membrane Proteins. *Molecular & Cellular Proteomics*, *3*(1), 56–65.

Peters, P. J., Borst, J., Oorschot, V., Fukuda, M., Krähenbühl, O., Tschopp, J., Slot, J. W., & Geuze, H. J. (1991). Cytotoxic T lymphocyte granules are secretory lysosomes, containing both perforin and granzymes. *The Journal of Experimental Medicine*, *173*(5), 1099–1109.

Picotti, P., & Aebersold, R. (2012). Selected reaction monitoring–based proteomics: workflows, potential, pitfalls and future directions. *Nature Methods*, *9*(6), 555–566.

Poetz, O., Schwenk, J. M., Kramer, S., Stoll, D., Templin, M. F., & Joos, T. O. (2005). Protein microarrays: catching the proteome. *Mechanisms of Ageing and Development*, *126*(1), 161–170.

Porteu, F., & Nathan, C. (1990). Shedding of Tumor-Necrosis-Factor Receptors by Activated Human Neutrophils. *Journal of Experimental Medicine*, *172*(2), 599–607.

Prinz, P. U., Mendler, A. N., Masouris, I., Durner, L., Oberneder, R., & Noessner, E. (2012). High DGK- and Disabled MAPK Pathways Cause Dysfunction of Human Tumor-Infiltrating CD8+ T Cells That Is Reversible by Pharmacologic Intervention. *The Journal of Immunology*, *188*(12), 5990–6000.

Quann, E. J., Liu, X., Altan-Bonnet, G., & Huse, M. (2011). A cascade of protein kinase C isozymes promotes cytoskeletal polarization in T cells. *Nature Immunology*, *12*(7), 647–654.

Quann, E. J., Merino, E., Furuta, T., & Huse, M. (2009). Localized diacylglycerol drives the polarization of the microtubule-organizing center in T cells. *Nature Immunology*, *10*(6), 627–635.

Rebholz-Schuhmann, D., Oellrich, A., & Hoehndorf, R. (2012). Text-mining solutions for biomedical research: enabling integrative biology. *Nature Reviews Genetics*, *13*(12), 829–839.

Resta, R., Yamashita, Y., & Thompson, L. F. (1998). Ecto-enzyme and signaling functions of lymphocyte CD73. *Immunological Reviews*, *161*, 95–109.

Riese, M. J., Grewal, J., Das, J., Zou, T., Patil, V., Chakraborty, A. K., & Koretzky, G. A. (2011). Decreased Diacylglycerol Metabolism Enhances ERK Activation and Augments CD8 + T Cell Functional Responses. *Journal of Biological Chemistry*, *286*(7), 5254–5265.

Riese, M. J., Wang, L.-C. S., Moon, E. K., Joshi, R. P., Ranganathan, A., June, C. H., Koretzky, G. A., & Albelda, S. M. (2013). Enhanced Effector Responses in Activated CD8+ T Cells Deficient in Diacylglycerol Kinases. *Cancer Research*, *73*(12), 3566–3577.

Rieux-Laucat, F., Le Deist, F., Hivroz, C., Roberts, I. A., Debatin, K. M., Fischer, A., & de Villartay, J. P. (1995). Mutations in Fas associated with human lymphoproliferative syndrome and autoimmunity. *Science (New York, N.Y.)*, *268*(5215), 1347–1349.

Rincon, E., Saez de Guinoa, J., Gharbi, S. I., Sorzano, C. O., Carrasco, Y. R., & Mérida, I. (2011). Translocation dynamics of sorting nexin 27 in activated T cells. *Journal of Cell Science*, *124*(5), 776–788.

Rincon, E., Santos, T., Avila-Flores, A., Albar, J. P., Lalioti, V., Lei, C., Hong, W., & Mérida, I. (2007). Proteomics Identification of Sorting Nexin 27 as a Diacylglycerol Kinase -associated Protein: New Diacylglycerol Kinase Roles in Endocytic Recycling. *Molecular & Cellular Proteomics*, *6*(6), 1073–1087.

Ross, P. L., Huang, Y. N., Marchese, J. N., Williamson, B., Parker, K., Hattan, S., Khainovski, N., Pillai, S., Dey, S., Daniels, S., Purkayastha, S., Juhasz, P., Martin, S., Bartlet-Jones, M., He, F., Jacobson, A., & Pappin, D. J. (2004). Multiplexed Protein Quantitation in *Saccharomyces cerevisiae* Using Amine-reactive Isobaric Tagging Reagents. *Molecular & Cellular Proteomics*, *3*(12), 1154–1169.

Sadlack, B., Löhler, J., Schorle, H., Klebb, G., Haber, H., Sickel, E., Noelle, R. J., & Horak, I. (1995). Generalized autoimmune disease in interleukin-2-deficient mice is triggered by an uncontrolled activation and proliferation of CD4+ T cells. *European Journal of Immunology*, *25*(11), 3053–3059.

Salmon, H., Franciszkiewicz, K., Damotte, D., Dieu-Nosjean, M.-C., Validire, P., Trautmann, A., Mami-Chouaib, F., & Donnadieu, E. (2012). Matrix architecture defines the preferential localization and migration of T cells into the stroma of human lung tumors. *Journal of Clinical Investigation*, *122*(3), 899–910.

Sanjuán, M. A., Jones, D. R., Izquierdo, M., & Mérida, I. (2001). Role of diacylglycerol kinase alpha in the attenuation of receptor signaling. *The Journal of Cell Biology*, *153*(1), 207–220.der.fcgi?artid=2185527&tool=pmcentrez&rendertype=abstract

Sanjuán, M. A., Pradet-Balade, B., Jones, D. R., Martínez-A, C., Stone, J. C., Garcia-Sanz, J. a, & Mérida, I. (2003). T cell activation in vivo targets diacylglycerol kinase alpha to the membrane: a novel mechanism for Ras attenuation. *Journal of Immunology (Baltimore, Md. : 1950)*, *170*(6), 2877–2883.

Santos, T., Carrasco, S., Jones, D. R., Mérida, I., & Eguinoa, A. (2002). Dynamics of Diacylglycerol Kinase ζ Translocation in Living T-cells. *Journal of Biological Chemistry*, *277*(33), 30300–30309.

Schaeffer, E. M., Debnath, J., Yap, G., McVicar, D., Liao, X. C., Littman, D. R., Sher, A., Varmus, H. E., Lenardo, M. J., & Schwartzberg, P. L. (1999). Requirement for Tec kinases Rlk and Itk in T cell receptor signaling and immunity. *Science (New York, N.Y.)*, *284*(5414), 638–641.

Schillaci, R., Brocardo, M. G., Galeano, A., & Roldán, A. (1998). Downregulation of Insulin-like Growth Factor-1 Receptor (IGF-1R) Expression in Human T Lymphocyte Activation. *Cellular Immunology*, *183*(2), 157–161.

Schmidt, A. M., Zou, T., Joshi, R. P., Leichner, T. M., Pimentel, M. A., Sommers, C. L., & Kambayashi, T. (2013). Diacylglycerol kinase ζ limits the generation of natural regulatory T cells. *Science Signaling*, *6*(303), ra101.

Schwanhäusser, B., Busse, D., Li, N., Dittmar, G., Schuchhardt, J., Wolf, J., Chen, W., & Selbach, M. (2011). Global quantification of mammalian gene expression control. *Nature*, *473*(7347), 337–342.

Schwartz, R. H. (2003). T cell anergy. *Annual Review of Immunology*, *21*(1), 305–334.

Shannon, P., Markiel, A., Ozier, O., Baliga, N. S., Wang, J. T., Ramage, D., Amin, N., Schwikowski, B., & Ideker, T. (2003). Cytoscape: A Software Environment for Integrated Models of Biomolecular Interaction Networks. *Genome Research*, *13*(11), 2498–2504.

Sharma, P., & Allison, J. P. (2015). The future of immune checkpoint therapy. *Science (New York, N.Y.)*, *348*(6230), 56–61.

Shen, D. T., Ma, J. S. Y., Mather, J., Vukmanovic, S., & Radoja, S. (2006). Activation of primary T lymphocytes results in lysosome development and polarized granule exocytosis in $CD4^+$ and $CD8^+$ subsets, whereas expression of lytic molecules confers cytotoxicity to $CD8^+$ T cells. *Journal of Leukocyte Biology*, *80*(4), 827–837.

Sheppard, K.-A., Fitz, L. J., Lee, J. M., Benander, C., George, J. A., Wooters, J., Qiu, Y., Jussif, J. M., Carter, L. L., Wood, C. R., & Chaudhary, D. (2004). PD-1 inhibits T-cell receptor induced phosphorylation of the ZAP70/CD3ζ signalosome and downstream signaling to PKCθ. *FEBS Letters*, *574*(1–3), 37–41.

Shi, L., Kraut, R. P., Aebersold, R., & Greenberg, A. H. (1992). A natural killer cell granule protein that induces DNA fragmentation and apoptosis. *The Journal of Experimental Medicine*, *175*(2), 553–566.

Shi, T., Song, E., Nie, S., Rodland, K. D., Liu, T., Qian, W.-J., & Smith, R. D. (2016). Advances in targeted proteomics and applications to biomedical research. *Proteomics*, *16*(15–16), 2160–2182.

Shirakabe, K., Shibagaki, Y., Yoshimura, A., Koyasu, S., & Hattori, S. (2014). A proteomic approach for the elucidation of the specificity of ectodomain shedding. *Journal of Proteomics*, *98*, 233–243.

Shiratori, T., Miyatake, S., Ohno, H., Nakaseko, C., Isono, K., Bonifacino, J. S., & Saito, T. (1997). Tyrosine phosphorylation controls internalization of CTLA-4 by regulating its interaction with clathrin-associated adaptor complex AP-2. *Immunity*, *6*(5), 583–589.

Silva-Santos, B., Serre, K., & Norell, H. (2015). γδ T cells in cancer. *Nature Reviews Immunology*, *15*(11), 683–691.

Smith-Garvin, J. E., Koretzky, G. A., & Jordan, M. S. (2009). T cell activation. *Annual Review of Immunology*, *27*, 591–619.

Speers, A. E., Blackler, A. R., & Wu, C. C. (2007). Shotgun Analysis of Integral Membrane Proteins Facilitated by Elevated Temperature. *Analytical Chemistry*, *79*(12), 4613–4620.

Stinchcombe, J. C., Bossi, G., Booth, S., & Griffiths, G. M. (2001). The immunological synapse of CTL contains a secretory domain and membrane bridges. *Immunity*, *15*(5), 751–761.

Stinchcombe, J. C., Majorovits, E., Bossi, G., Fuller, S., & Griffiths, G. M. (2006). Centrosome polarization delivers secretory granules to the immunological synapse. *Nature*, *443*(7110), 462–465.

Subramanian, A., Tamayo, P., Mootha, V. K., Mukherjee, S., Ebert, B. L., Gillette, M. A., Paulovich, A., Pomeroy, S. L., Golub, T. R., Lander, E. S., & Mesirov, J. P. (2005). Gene set enrichment analysis: A knowledge-based approach for interpreting genome-wide expression profiles. *Proceedings of the National Academy of Sciences*, *102*(43), 15545–15550.

Sun, J., Bird, C. H., Sutton, V., McDonald, L., Coughlin, P. B., De Jong, T. A., Trapani, J. A., & Bird, P. I. (1996). A cytosolic granzyme B inhibitor related to the viral apoptotic regulator cytokine response modifier A is present in cytotoxic lymphocytes. *The Journal of Biological Chemistry*, *271*(44), 27802–27809.

Sutton, V. R., Davis, J. E., Cancilla, M., Johnstone, R. W., Ruefli, A. A., Sedelies, K., Browne, K. A., & Trapani, J. A. (2000). Initiation of apoptosis by granzyme B requires direct cleavage of bid, but not direct granzyme B-mediated caspase activation. *The Journal of Experimental Medicine*, *192*(10), 1403–1414.

Takeishi, K., Taketomi, A., Shirabe, K., Toshima, T., Motomura, T., Ikegami, T., Yoshizumi, T., Sakane, F., & Maehara, Y. (2012). Diacylglycerol kinase alpha enhances hepatocellular carcinoma progression by activation of Ras–Raf–MEK–ERK pathway. *Journal of Hepatology*, *57*(1), 77–83.

Taube, J. M., Anders, R. A., Young, G. D., Xu, H., Sharma, R., McMiller, T. L., Chen, S., Klein, A. P., Pardoll, D. M., Topalian, S. L., & Chen, L. (2012). Colocalization of Inflammatory Response with B7-H1 Expression in Human Melanocytic Lesions Supports an Adaptive Resistance Mechanism of Immune Escape. *Science Translational Medicine*, *4*(127), 127ra37-127ra37.

Taylor, G. (1964). Disintegration of Water Drops in an Electric Field. *Proceedings of the Royal Society A: Mathematical, Physical and Engineering Sciences*, *280*(1382), 383–397.

The UniProt Consortium. (2017). UniProt: the universal protein knowledgebase. *Nucleic Acids Research*, *45*(D1), D158–D169.

Thompson, A., Schäfer, J., Kuhn, K., Kienle, S., Schwarz, J., Schmidt, G., Neumann, T., Johnstone, R., Mohammed, A. K. A., & Hamon, C. (2003). Tandem mass tags: a novel quantification strategy for comparative analysis of complex protein mixtures by MS/MS. *Analytical Chemistry*, *75*(8), 1895–1904.

Torres-Ayuso, P., Daza-Martín, M., Martín-Pérez, J., Ávila-Flores, A., & Mérida, I. (2014). Diacylglycerol kinase α promotes 3D cancer cell growth and limits drug sensitivity through functional interaction with Src. *Oncotarget*, *5*(20), 9710–9726.

Torres-Ayuso, P., Tello-Lafoz, M., Mérida, I., & Ávila-Flores, A. (2015). Diacylglycerol kinase-ζ regulates mTORC1 and lipogenic metabolism in cancer cells through SREBP-1. *Oncogenesis*, *4*(8), e164–e164.

Tschopp, J., Masson, D., & Stanley, K. K. (1986). Structural/functional similarity between proteins involved in complement- and cytotoxic T-lymphocyte-mediated cytolysis. *Nature*, *322*(6082), 831–834.

Tseng, W.-Y., Huang, Y.-S., Lin, H.-H., Luo, S.-F., McCann, F., McNamee, K., Clanchy, F., & Williams, R. (2018). TNFR signalling and its clinical implications. *Cytokine*, *101*, 19–25.

Tzouros, M., Golling, S., Avila, D., Lamerz, J., Berrera, M., Ebeling, M., Langen, H., & Augustin, A. (2013). Development of a 5-plex SILAC Method Tuned for the Quantitation of Tyrosine Phosphorylation Dynamics. *Molecular & Cellular Proteomics*, *12*(11), 3339–3349.

Ünlü, M., Morgan, M. E., & Minden, J. S. (1997). Difference gel electrophoresis. A single gel method for detecting changes in protein extracts. *Electrophoresis*, *18*(11), 2071–2077.

Upshaw, J. L., & Leibson, P. J. (2006). NKG2D-mediated activation of cytotoxic lymphocytes: Unique signaling pathways and distinct functional outcomes. *Seminars in Immunology*, *18*(3), 167–175.

Vigneron, N. (2015). Human Tumor Antigens and Cancer Immunotherapy. *BioMed Research International*, *2015*, 1–17.

Vit, O., & Petrak, J. (2017). Integral membrane proteins in proteomics. How to break open the black box? *Journal of Proteomics*, *153*, 8–20.

Vogel, W. F. (2002). Ligand-induced shedding of discoidin domain receptor 1. *FEBS Letters*, *514*(2–3), 175–180.

Waldhauer, I., & Steinle, A. (2008). NK cells and cancer immunosurveillance. *Oncogene*, *27*(45), 5932–5943.

Walker, L. S. K., & Sansom, D. M. (2015). Confusing signals: Recent progress in CTLA-4 biology. *Trends in Immunology*, *36*(2), 63–70.

Wang, R., Zhang, L., Zhang, X., Moreno, J., Celluzzi, C., Tondravi, M., & Shi, Y. (2002). Regulation of activation-induced receptor activator of NF-κB ligand (RANKL) expression in T cells. *European Journal of Immunology*, *32*(4), 1090–1098.

Waterhouse, N. J., Sedelies, K. A., & Trapani, J. A. (2006). Role of Bid-induced mitochondrial outer membrane permeabilization in granzyme B-induced apoptosis. *Immunology and Cell Biology*, *84*(1), 72–78.

Waterhouse, P., Penninger, J. M., Timms, E., Wakeham, A., Shahinian, A., Lee, K. P., Thompson, C. B., Griesser, H., & Mak, T. W. (1995). Lymphoproliferative disorders with early lethality in mice deficient in Ctla-4. *Science (New York, N.Y.)*, *270*(5238), 985–988.

Weekes, M. P., Antrobus, R., Lill, J. R., Duncan, L. M., Hör, S., & Lehner, P. J. (2010). Comparative analysis of techniques to purify plasma membrane proteins. *Journal of Biomolecular Techniques : JBT*, *21*(3), 108–115.

Weickhardt, C., Moritz, F., & Grotemeyer, J. (1996). Time-of-flight mass spectrometry: State-of the-art in chemical analysis and molecular science. *Mass Spectrometry Reviews*, *15*(3), 139–162.

Wesley, E. M., Xin, G., McAllister, D., Malarkannan, S., Newman, D. K., Dwinell, M. B., Cui, W., Johnson, B. D., & Riese, M. J. (2018). Diacylglycerol Kinase ζ (DGKζ) and Casitas b-Lineage Proto-Oncogene b–Deficient Mice Have Similar Functional Outcomes in T Cells but DGKζ-Deficient Mice Have Increased T Cell Activation and Tumor Clearance. *ImmunoHorizons*, *2*(4), 107–118.

Wiley, S. R., Schooley, K., Smolak, P. J., Din, W. S., Huang, C. P., Nicholl, J. K., Sutherland, G. R., Smith, T. D., Rauch, C., & Smith, C. A. (1995). Identification and characterization of a new member of the TNF family that induces apoptosis. *Immunity*, *3*(6), 673–682.

Wilhelmsen, K., & van der Geer, P. (2004). Phorbol 12-myristate 13-acetate-induced release of the colony-stimulating factor 1 receptor cytoplasmic domain into the cytosol involves two separate cleavage events. *Molecular and Cellular Biology*, *24*(1), 454–464.

Wilkins, M. (2009). Proteomics data mining. *Expert Review of Proteomics*, *6*(6), 599–603.

Wing, K., Onishi, Y., Prieto-Martin, P., Yamaguchi, T., Miyara, M., Fehervari, Z., Nomura, T., & Sakaguchi, S. (2008). CTLA-4 Control over Foxp3+ Regulatory T Cell Function. *Science*, *322*(5899), 271–275.

Wollscheid, B., Bausch-Fluck, D., Henderson, C., O'Brien, R., Bibel, M., Schiess, R., Aebersold, R., & Watts, J. D. (2009). Mass-spectrometric identification and relative quantification of N-linked cell surface glycoproteins. *Nature Biotechnology*, *27*(4), 378–386.

Yang, J., Zhang, P., Krishna, S., Wang, J., Lin, X., Huang, H., Xie, D., Gorentla, B., Huang, R., Gao, J., Li, Q.-J., & Zhong, X.-P. (2016). Unexpected positive control of NFκB and miR-155 by DGKα and ζ ensures effector and memory CD8+ T cell differentiation. *Oncotarget*, *7*(23), 33744–33764.

Yates, J. R. (2013). The Revolution and Evolution of Shotgun Proteomics for Large-Scale Proteome Analysis. *Journal of the American Chemical Society, 135*(5), 1629–1640.

Yates, J. R., Ruse, C. I., & Nakorchevsky, A. (2009). Proteomics by Mass Spectrometry: Approaches, Advances, and Applications. *Annual Review of Biomedical Engineering*, *11*(1), 49–79.

Zhang, B., VerBerkmoes, N. C., Langston, M. A., Uberbacher, E., Hettich, R. L., & Samatova, N. F. (2006). Detecting differential and correlated protein expression in label-free shotgun proteomics. *Journal of Proteome Research*, *5*(11), 2909–2918.

Zhang, L., Xie, J., Wang, X., Liu, X., Tang, X., Cao, R., Hu, W., Nie, S., Fan, C., & Liang, S. (2005). Proteomic analysis of mouse liver plasma membrane: use of differential extraction to enrich hydrophobic membrane proteins. *Proteomics*, *5*(17), 4510–4524.

Zhang, Y., Chen, Y., Liu, Z., & Lai, R. (2018). ERK is a negative feedback regulator for IFN-γ/STAT1 signaling by promoting STAT1 ubiquitination. *BMC Cancer*, *18*(1), 613.

Zheng, Y., Zha, Y., & Gajewski, T. F. (2008). Molecular regulation of T-cell anergy. *EMBO Reports*, *9*(1), 50–55.

Zhong, X.-P., Guo, R., Zhou, H., Liu, C., & Wan, C.-K. (2008). Diacylglycerol kinases in immune cell function and self-tolerance. *Immunological Reviews*, *224*, 249–264.

Zhong, X.-P., Hainey, E. A., Olenchock, B. A., Jordan, M. S., Maltzman, J. S., Nichols, K. E., Shen, H., & Koretzky, G. A. (2003). Enhanced T cell responses due to diacylglycerol kinase zeta deficiency. *Nature Immunology*, *4*(9), 882–890.

Zhong, X.-P., Hainey, E. A., Olenchock, B. A., Zhao, H., Topham, M. K., & Koretzky, G. A. (2002). Regulation of T Cell Receptor-induced Activation of the Ras-ERK Pathway by Diacylglycerol Kinase ζ. *Journal of Biological Chemistry*, *277*(34), 31089–31098.

Zhu, C., Anderson, A. C., Schubart, A., Xiong, H., Imitola, J., Khoury, S. J., Zheng, X. X., Strom, T. B., & Kuchroo, V. K. (2005). The Tim-3 ligand galectin-9 negatively regulates T helper type 1 immunity. *Nature Immunology*, *6*(12), 1245–1252.

AGRADECIMIENTOS

Agradecimientos

Si alguien se merece reconocimiento por el trabajo presentado en esta tesis, son todas aquellas personas que me han acompañado a lo largo de estos años, y que me han ofrecido su guía y su apoyo; no solo para la realización del trabajo científico, sino también para recorrer esta etapa, una de las más excitantes, felices y a la vez desafiantes de mi vida.

Muchas gracias Juan Pablo por confiar en mí, y darme la oportunidad de formar parte de tu laboratorio. Siempre pensamos en la vida como una serie de elecciones, pero muchas veces es ella la que nos elige. En cierta manera me has seguido acompañando hasta el día de hoy. Gracias Isabel por todo el apoyo que me has prestado este tiempo, sin el cual no habría podido llegar a la meta. De ti he aprendido a dar los primeros pasos en ciencia: planificar experimentos, interpretar resultados, descubrir que al intentar resolver un interrogante surgen otros cien más... y sobre todo a sentir pasión y disfrutar un camino tan exigente como este. Severine, podría decir que me has enseñado prácticamente todo lo que sé de proteómica, a ser meticuloso con los experimentos, con el orden, y a trabajar en equipo con el resto del laboratorio. Pero por encima de eso te tengo que dar las gracias por ser tan buena persona conmigo y preocuparte tanto por mí estos años. Eso vale más que cualquier conocimiento del mundo.

Es imprescindible para mí recordar a toda la gente del 414 que me ha ayudado siempre. Denise, a veces las cosas aparentemente más pequeñas son las más grandes. Aprender a cultivar células, hacer un lisado, un *western blot*, una tinción de citometría... La energía y entusiasmo que irradiabas era el mejor reclamo para empezar esta aventura. Admiramos a los grandes sabios, pero a los maestros nunca se les olvida. Gracias por cuidar tanto de mí. Pedro, has sido siempre un ejemplo a seguir en ciencia, pero además me demostraste que podías darlo todo por ayudarme. Tu apoyo y compañía ha sido fundamental. Gracias también a Rosa y Raquel, que no solo me han dado su magnífico trabajo y saber hacer, sino que además lo han hecho siempre con total disposición y una sonrisa. María, Elena, Cris, Javi, mis compañeros de tesis, jamás dudasteis un segundo en ayudarme cuando lo necesité. Gracias también a Toñi, Mónica y María por vuestra ayuda y consejos desde la experiencia, y a todos los que coincidieron en este laboratorio de una forma u otra.

Si he sobrevivido al reto de la proteómica ha sido por todo el respaldo que siempre me ha regalado la gran familia del B1. A Alberto, Rosana, Sergio, Silvia, Gema, Inés, toda la gente del servicio que ha estado siempre dispuesta a la hora de lidiar con los equipos de la unidad, y de resolver cualquier duda que tuviera. Gracias también a los informáticos:

Alberto, Antonio, Salva y Migue, sin los cuales no habría podido enfrentarme a verdaderas montañas de datos en el Tolkien. A Carmen y Adán que me han ayudado siempre que he estado perdido recién llegado desde la cuarta planta. A Lola, Vir, Miguel, Manuel, Maricarmen, Ana, Marisol, que me han prestado su ayuda en todo momento. Gracias a todos por acogerme como uno más pese a estar tanto tiempo fuera del labo, y por todos los buenos ratos pasados en celebraciones, jamonadas, congresos; y por el calor y la compañía en los momentos duros como en la pérdida de Juan Pablo. Ojalá conservéis siempre esa unidad y fraternidad que me habéis demostrado todos estos años.

No puedo olvidar tampoco a toda la gente del DIO, en especial a todos aquellos que después de un día de trabajo quedábamos a tomar algo los miércoles por la tarde para seguir hablando de ciencia y de lo que se terciara. Eva, gracias por toda la ayuda y el cariño que me has dado desde la poyata del fondo. A veces desde fuera se ven las cosas desde otra perspectiva, y tus consejos me han ayudado a seguir adelante. Sheila, tú también me has echado una mano en todo momento, y sobre todo has sido alguien en quien poder confiar. Jesús, gracias por recibirme con cariño en el 413, para solucionar cualquier duda o hablar de lo que fuese, o animarme saliendo por la noche. Araceli, un placer compartir todas esas cañas con una miembro fundadora, y también los consejos de alguien con experiencia. Gema, la teniente Rooney, por todas esas tardes ensayando donde no solo pude conocer a una gran actriz, sino a una gran persona. Amaia, por esos buenos ratos, incluyendo las conversaciones en alemán de la escuela de idiomas. Violeta y Sara, las chicas del Zeiss, voy a echar de menos entrar sigilosamente en vuestro pasillo. Jorge, que además de ser un buen científico es una persona increíble. Carla y Rachele, mis italianas favoritas, gracias por esos ratos en el departamento y en las casas rurales. A mi paisana Lorena, siempre con una sonrisa cuando más lo necesitas. Míriam, gracias por esas conversaciones sobre la tesis que tanta fuerza me han dado. A la vieja guardia, Vicen, Dimitri, Rubén, Laura, Javi, Ángeles, Albert… y a los nuevos, Manu, Lidia, Jesús, Alejandra, Miguel… Me llevo cada momento que he pasado con todos vosotros, en el DIO o fuera de él, porque habéis formado una parte importante de mi vida en todos estos años.

No quiero dejar de mencionar a todos los servicios, científicos o no, del DIO y del CNB, incluyendo citometría con Maricarmen y Sara, microscopía con Anabel y cocinas. Y a todos los investigadores del CNB que han compartido su conocimiento y sus ideas, y que tanto me han hecho crecer.

Al grupo de Ignacio Rubio, que me acogió estupendamente en el CMB de Jena. Gracias por enseñarme todo lo que necesité y ayudarme en todo lo posible. También a todo su grupo y la gente del departamento, que me hicieron sentir integrado desde el primer momento: Ledia, Govind, Caroline, Kristin, Martina, Trim, Odeta. *Vielen Dank für deine*

Hilfe!

Al grupo de teatro del CNB Nokaut, por esas comidas y tardes de ensayos e improvisaciones, que han sacado de mí una faceta totalmente desconocida y me han ayudado a conocerme mejor. Aunque no siempre era fácil conciliar, los momentos divertidos compensaban con creces, sin ninguna duda. Inolvidable nuestra primera obra, un elenco maravilloso. ¡Al asalto!

También quería agradecer a toda la gente que desde fuera del CNB ha estado conmigo en toda esta etapa. Adrián, espero que ahora pueda compensar de alguna forma todas tus buenas palabras en tus balances anuales. Durante la carrera siempre me ayudaste con las prácticas, los apuntes, y en mi vida personal por si fuera poco. El que me encuentre ahora en este momento ha sido en parte gracias a ti. La vida es cuestión de prioridades me decías, gracias por incluirme en ellas. Lucía, con tu dulzura y desparpajo le diste un cambio a mi vida en los años de facultad. Aunque ahora estés lejos, sigues estando muy presente. Gracias por acompañarme en este camino. Ana, de ti he aprendido que hay que tomar la vida con decisión y luchar por lo que se quiere en vez de quejarse. Gracias por los buenos momentos que hemos compartido.

Carlos, tú has sido y sigues siendo otro de mis grandes apoyos. Desde que te conocí no has dejado de darme ánimos para conseguir todo lo que me proponía. Y sobre todo me has hecho sentir muy querido y me has hecho saber que siempre podré confiar en ti. Jota, has sabido sacarme una sonrisa cuando lo he necesitado, discreto pero siempre has estado ahí. Vanesa, tú fuiste también un gran descubrimiento, imposible de olvidar esas conversaciones en la facultad. Vanessa, aunque te conocí más tarde te has convertido en una persona fundamental. Bajo esa apariencia seria se esconde un corazón enorme. Gracias por todos los ánimos que me has dado con la tesis (tenías razón). Nerea, gracias por arrancar tantas risas en todos los momentos de cumpleaños, casas rurales y quedadas. Estefanía, mi bailarina favorita, si de alguien he aprendido a sonreírle a la vida es de ti. María Victoria, espero que sigamos viéndonos en esas visitas al sur, al igual que la doctora Marta ahora ya estás más cerca. Gracias también a Marga, Ángel, Álvaro y Tone por estar en los momentos clave. Y a Ana y David, cuando nos vemos parece que no haya pasado el tiempo.

A todo el grupo de mostoleños, que siempre han intentado entender mis preocupaciones científicas y me han levantado el ánimo con una buena cerveza. Jorge, siempre has sido una buenísima persona, si ahora te va todo tan bien es sin duda por eso. Kevin, cada vez que regresas por aquí traes siempre la alegría. Ya sabes que hay un pandemic esperándote. Fionn y Eva, por tantas noches de partidas, pero sobre todo de buen rollo y conversaciones interminables. Ian y Carmen, inolvidables esas nocheviejas en vuestra casa,

seguid siendo como sois. Luismi y Miguel, los ingenieros expatriados, cuento los días para la próxima visita. Pérez y Escudero, siempre aportando esa locura y caos, imprescindibles.

A mi familia, que me ha apoyado de manera incondicional todos estos años, aunque todo lo que les contase les sonase extraño. A mi abuela que siempre me pregunta cómo voy con lo mío. A mis otros abuelos que pese a que ya no están aquí sin duda se sentirían orgullosos. A mis tíos, y a mi primo Alejandro, que desde mucho antes de empezar ya sabía que podía contar con ellos para todo. A todos los Gozalo y Rodríguez, que me han adoptado como uno más y siempre se preocupan por mí. A mi hermana Elena, por su paciencia para escucharme hablándole de linfocitos y células diana, por quererme a pesar de todas mis rarezas, y por regalarme su arte. A mis padres, Tomás y Matilde, que siempre lo han dado todo por mí y me han apoyado en las decisiones que he ido tomando a lo largo de mi vida. Por todo su esfuerzo y todas sus enseñanzas soy lo que soy, y he podido llegar al final de este camino.

A María, mi compañera de viaje. Por aguantar mis cambios de humor y mi ansiedad, y las horas que he estado ausente por mi trabajo. Porque siempre has creído en mí, y te alegras más que yo por haber llegado a la meta. Por los sueños que hemos cumplido y los que están por venir. Si este es mi momento, lo es contigo, lo es gracias a ti.

APPENDICES

Appendices

1. Appendix I: Supplemental tables

Supplemental table 1

Proteins identified in a shotgun analysis of Jurkat T cells treated with PMA, enriched in membrane proteins by a biotinylation strategy and neutravidin pulldown. See attached Excel file “SuppTable1” on CD.

Supplemental table 2

Proteins identified by a shotgun analysis of Jurkat T cells with PMA, after optimization of biotinylation process by applying high salt washes after pull down. See attached Excel file “SuppTable2” on CD.

Supplemental table 3

Protein identifications after a shotgun analysis of Jurkat T cell complete cell lysate, performed with a commercial kit. See attached Excel file “SuppTable3” on CD.

Supplemental table 4

Proteins identified in a shotgun analysis of Jurkat T cells after subcellular fractionation with a commercial kit. See attached Excel files “SuppTable4a” and "SuppTable4b" on CD.

Supplemental table 5

Proteins identified in a shotgun analysis of mouse splenocytes, after a biotinylation enrichment of membrane proteins. See attached Excel file “SuppTable5” on CD.

Supplemental table 6

Proteins identified in a shotgun analysis of mouse CTL treated with PMA, and enriched in membrane proteins after biotinylation and neutravidin pull down. See attached Excel file “SuppTable6” on CD.

Supplemental table 7

Proteins identified in a shotgun analysis of DGKζ$^{-/-}$ mouse CTL enriched in membrane proteins after neutravidin pull down. See attached Excel file “SuppTable7” on CD.

Supplemental table 8

Proteins identified in a shotgun analysis of DGKζ$^{-/-}$ mouse CTL after subcellular frac-

tionation with a commercial kit. See attached Excel file “SuppTable8” on CD.

Supplemental table 9

Proteins identified in a shotgun analysis of DGKζ$^{-/-}$ mouse CTL labeled with SILAC after subcellular fractionation with a commercial kit. See attached Excel file “SuppTable9” on CD.

Supplemental table 10

Quantitative analysis by Proteobotics S.L. of DGKζ$^{-/-}$ mouse CTL labeled with SILAC after subcellular fractionation with a commercial kit. See attached Excel file “SuppTable10” on CD.

2. Appendix II: Articles published

Tello-Lafoz, M., **Martínez-Martínez, G.**, Rodríguez-Rodríguez, C., Albar, J. P., Huse, M., Gharbi, S., & Merida, I. (2017). Sorting nexin 27 interactome in T-lymphocytes identifies zona occludens-2 dynamic redistribution at the immune synapse. *Traffic*, *18*(8), 491–504.